University of Southern Queensland

Faculty of Engineering and Surveying

Best percentage by weight of micro-spheres as fillers in phenolic resins, with fracture toughness as a benchmark

A dissertation submitted by

Robert James Davey

in fulfilment of the requirements of

Courses ENG4111 and 4112 Research Project

towards the degree of

Bachelor of Engineering (Mechanical)

Submitted: November, 2006

Abstract

Phenol formaldehyde was filled with Envirospheres slg to increase the strength and fracture toughness of the composite for structural applications by the Centre of Excellence in Engineered Fiber Composites (CEEFC), University of Southern Queensland (USQ). In order to reduce costs, the Centre wishes to fill as much slg as possible subject to maintaining sufficient impact toughness of the composites in structural applications. This project varies the percentage by weight of the slg in the composites which are then subjected to fracture toughness tests. The results show that composite with 20 % by weight of the slg produces the highest impact values combined with a reasonable fluidity for casting.

University of Southern Queensland

Faculty of Engineering and Surveying

Certification

I certify that the ideas, designs and experimental work, results, analyses and conclusions set out in this dissertation are entirely my own effort, except where otherwise indicated and acknowledged.

I further certify that the work is original and has not been previously submitted for assessment in any other course or institution, except where specifically stated.

Robert James Davey

Student Number: 0050010155

_____
                        Signature

_____
                        Date

Acknowledgements

Contents

List of Figures

List of Tables

Nomenclature

FCDD   Fibre Composite Design and Development

CEEFC   Centre of Excellence in Engineered Fiber Composites

PMC   Polymer Matrix Composites

MMC   Metal Matrix Composites

CMC   Ceramic Matrix Composites

PVC   Poly-Vinyl Chloride

LEFM   Linear Elastic Fracture Mechanics

SENB   Single Edge Notch Bend

OHT   Over-Head Transparency

Chapter 1

Introduction

1.1   Introduction

Phenolic resin is a thermosetting, polymer based, particulate composite and is commonly used in a wide variety of applications in aerospace, marine, transportation and civil engineering. Phenolics are currently most widely used in insulation and for electrical purposes as well as for adhesives as they are the best for joining metals.

Composites are produced when two or more materials or phases are combined to give a flexible combination of mechanical properties that cannot be obtained otherwise. Composites are extremely versatile and are being increasingly used in a wide range of applications such as aerospace, marine, transportation, mechanical and civil engineering. In order to reduce the costs of composites a wide range of fillers are being used and resulting properties explored.

Composites can generally be place into three major categories depending on their geometry:

- Particulate – Composites like concrete which is a mixture of cement and gravel to form a tough material.

- Fibre – fibreglass is an example of fibre composite as it contains an array of glass fibres arranged to give a lightweight, thin but strong material.

- Laminar – Plywood contains layers of wood veneer positioned for increased strength and versatility.

Particulate composites can further be broke down into many more groups. The groups of interest are polymer thermosets and thermoplastics. Phenolic resin is a type of thermoset as once cured it can not once again become a liquid unlike thermoplastics.

Phenolics were the first thermoset material to be synthesized under the name of Bakelite^{TM} by Leo Bakeland in 1907 (Strong 2000). Therefore the ideas about commercialising composites and their application have been around for about a century. However, it is only quite recently that a lot of research effort has gone into understanding the properties of composites as their application has dramatically increased and become widely accepted by engineers and consumers.

1.1.2   Project Aims

The project aims to explore and evaluate the best percentage by weight of micro-spheres as fillers in phenolic resin composites in relation to fracture toughness therefore increasing the understanding of polymer reinforced composites and leading to an increased application in the engineering field.

1.1.3   Specific Objectives

Fracture toughness analysis will be done by the production of a range of phenolic resin specimens with different percentage by weight of filler. Specimens will then be post-cured in an oven for ten hours. Viscosity tests will be conducted to ensure there are no fluidity problems. Fracture toughness will be evaluated by the means of short bar

tests. Findings can then be analysed in detail to establish behavioural trends and formulas that can be used to theoretically predict filled polymer behaviour.

1.2   Risk Assessment

There are many risks involved in this project in the manufacture of both the mould itself, in handling the composite materials, and in the fracture testing processes.

During the design of the mould the safety of the machine operators had to be considered and therefore this simplifies the mould to basic manufacturing techniques. All workers working in the workshop environment are required to wear the appropriate safety clothing, these include, fully covered shoes, protective clothing as needed, protective eye ware or even a face mask if needed.

The moulding of specimens is done in a safe controlled environment with ventilation and access to cleansers and water readily available. There are three components in making the phenolic resins that could potentially cause bodily harm if not protected against correctly. The three components are the filler, which is extremely fine micro-spheres of aluminium silicate that could possibly be breather in or cause skin irritation. The phenol formaldehyde resin solution J-2027L, and the phenolic resin hardener catalyst both of which are hazardous.

The following information has been extracted from the Chemwatch Material Safety Data Sheet for both resin and hardener.

1.2.1   Hexion Cellobond J2027L Resin

Statement of Hazardous Nature: Hazardous substance, non-dangerous goods.

Poison Schedule: S6

Risk:

Toxic by inhalation, in contact with skin and if swallowed.

Causes burns.

Risk of damage to eyes.

Risk of serious damage to eyes.

Risk of irreversible effects.

Safety:

Keep locked up.

Keep container in well ventilated space

Avoid exposure – obtain special instruction before use.

Clean with water and detergent.

Keep container closed tightly.

Dispose of material and container in a safe way.

In case of contact with eyes, rinse with plenty of water and contact doctor or poison information centre.

If you feel unwell contact doctor or poisons information centre.

In case of accident by inhalation: remove casualty to fresh air and keep at rest.

Further information can be obtained from the CHEMWATCH 4601-85 information sheet.

1.2.2 Hexion Phencat 15 Hardener

Statement of Hazardous Nature: Hazardous substance, Dangerous goods.

Poison Schedule: None

Risk:

Harmful by inhalation and if swallowed.

Causes burns.

Risk of serious damage to eyes.

Possible cancer causing agent.

Safety:

Keep locked up.

Keep container in well ventilated space

Avoid exposure – obtain special instruction before use.

Clean with water.

Keep container closed tightly.

Take off immediately all contaminated clothing.

If you feel unwell contact doctor or poisons information centre.

Further information can be obtained from the CHEMWATCH 4601-93 information sheet.

The above chemicals require caution when handling and personal protective equipment to be worn at all times, this includes safety goggles, a respirator, gloves, covered footwear and a long sleeve shirt.

Risks associated with the tensile testing of specimens involve flying particles, loose clothing being caught, material dropping hazards, and fingers being jammed. Caution should be exercised when fastening the test piece and whilst releasing to ensure no bodily harm occurs. Personal protective equipment includes covered footwear and safety goggles and also aid and initial briefing by a qualified operator.

1.3   Overview of Dissertation

This dissertation is organised as follows:

Chapter 2 is a brief discussion of polymer reinforced fibre composites and explains everything involved to a molecular level. Fibre composites, currently used polymers, resin matrices, phenolics and fillers are some of the topics covered.

Chapter 3 is about fracture mechanics and it explains the fracture toughness property of materials and also the importance involved in understanding how materials fail in order to be able to design improved components and give materials a wider field of application.

Chapter 4 outlines standard and non-standard fracture toughness test that are commonly used today. The limitations involved with some of the tests and their specimen geometries are discussed.

Chapter 5 gives details about the short rod/short bar fracture toughness test, that will be use to evaluate fracture toughness in this project. This chapter goes into great detail about the development, specimen geometries, tolerances and the calibrations and mathematical equations used to calculate fracture toughness.

Chapter 6 is the experimental methodology that was followed throughout the project. The processes of specimen and mould creation are discussed as well as the post curing and finishing techniques used to prepare the specimens for testing.

Chapter 7 is about the testing apparatus and methods. It outline the requirements of a good test in relation to the short bar specimen geometry and evaluates a few tests methods that were designed specifically for testing the short bar specimen. The MTS 810 Material Testing System is also described as it is used in this project for conducting the tests.

Chapter 8 is the results and discussion chapter where the data from the previous chapters is evaluated and discussed.

Chapter 9 is the conclusion.

Appendix A is the Project Specification.

Appendix B is the short bar specimen dimensions that were used in this project.

Appendix C is the design of the mould that was used for construction.

Appendix D contains the composite mixing tables for the mixing of the composites.

Appendix E is the MTS 810 Material Testing System results.

Appendix F is the specimen dimensions measured using callipers after testing.

Appendix G contains a table with the fracture toughness results.

Chapter 2

Fibre Reinforced Polymer Composites

2.1   Introduction to Fibre Composites

Composites have been used for thousands of years and are not a new concept. Early man reinforced mud with twigs, the Romans used a primitive form of concrete in order to build structures, some of which are still standing to this day. There are many forms of naturally occurring composites like abalone shell, wood, bone and teeth (Askeland 2003).

A composite is a material which is comprised of two or more different phases. The phases are combined to create a product with a desired set of properties that otherwise would not be attainable. Fibre reinforced composites are a two-phase material in which one phase acts to reinforce the second phase. The second phase is called the matrix.

The fibres in a composite are the primary load bearing elements and the surrounding matrix ensures the fibres remain in the desired position and orientation. The matrix transfers external loads evenly throughout the fibres, and also helps to protect them from the environment. The second phase or matrix material in fibre composites can be

polymers, metals, or ceramics. Composite materials are generally classified by the matrix material. Polymer matrix composites are (PMCs), metal matrix composites (MMCs), and ceramic matrix composites (CMCs) (Mallick 1997).

2.2   Introduction to Polymers

Polymers are materials composed of molecules of very high molecular weight, which are generally referred to as macromolecules. The molecular structure of polymers gives them unique material properties and great versatility in processing methods. Polymers, or plastics (polymers with additives) are the most sought after material today and this is attributed to their ease of manufacture and processing. Traditional materials such as metals and wood are a lot harder to work and form. Polymers, however, have a low density and can be shaped and moulded at relatively low temperatures. Components that have normally been made from wood, metal, ceramics, and glass are now constantly being redesigned using polymers (Osswald & Menges 1996). Figure 2.1 is an definition of the types of plastics.
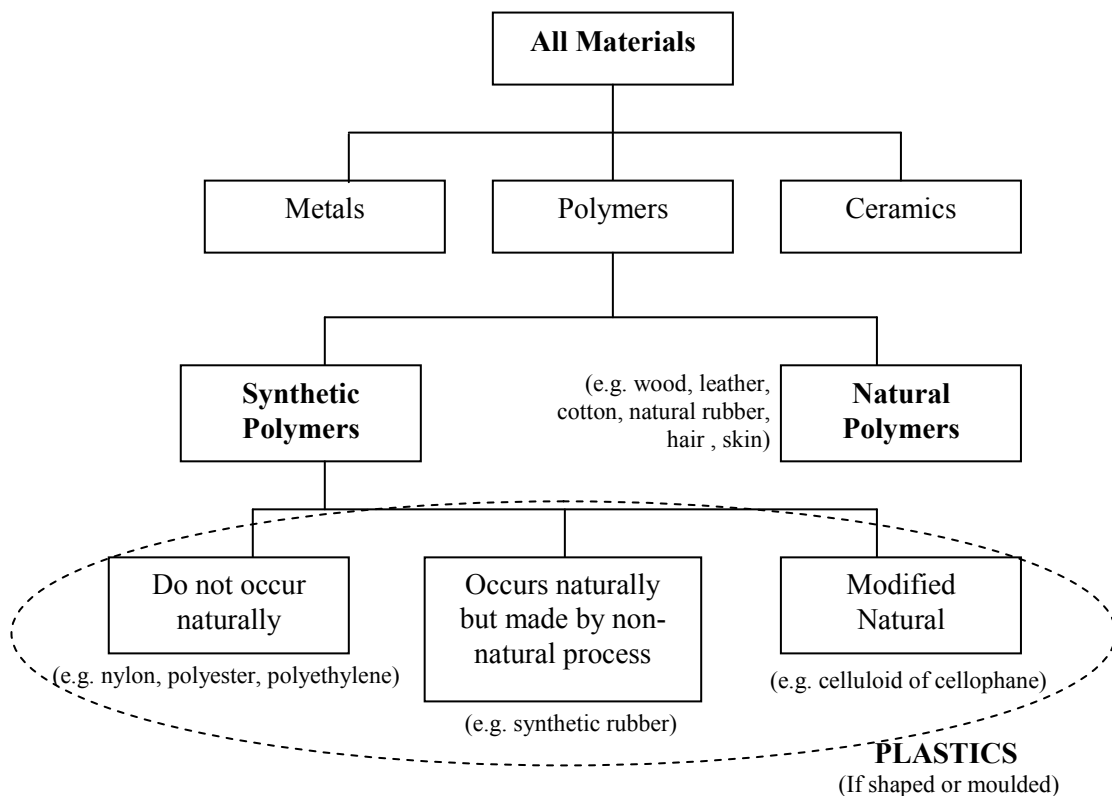
Figure 2.1: Definition of plastics (Strong 2000, p. 2).

2.3   Polymer Composites

The main constituent materials used to create fibre reinforced polymer composites are polymer matrix resins and reinforcing fibres. The addition of various fillers to matrix resins gives a range of desirable properties depending on the application.

Table 2.1 shows a wide variety of polymers and their applications when they are used in conjunction with a range of additives and created with different forming methods.

Table 2.1: Common polymers and applications

Polymer	Application
Thermoplastics	
Amorphous	
Polystyrene	Mass-Produced transparent articles, thermoformed packaging, Thermal Insulation (foamed)
Polymethyl methacrylate	Skylights, airplane windows, lenses, bulletproof windows, stop lights.
Polycarbonate	Helmets, hockey masks, bulletproof windows, blinker lights, headlights.
Un-plasticized poly vinyl chloride	Tubes, window frames, bottles, thermoformed packaging, gutters.
Plasticized poly vinyl chloride	Shoes, hoses, rotor-moulded hollow articles such as balls and other toys, calendered films for raincoats and tablecloths.
Semi-crystalline	
High density polyethylene	Milk and soap bottles, mass production of household goods of higher quality, tubes, paper coating.
Low density polyethylene	Mass production of household goods, grocery bags.
Polypropylene	Goods such as suitcases, tubes, engineering application (fibre glass reinforced), housings for electrical appliances.
Polytetrafluoroethylene	Coating of cooking pans, lubricant-free bearings.
Polyamide	Bearings, gears, bolts, skate wheels, pipes, fishing line, textiles, ropes.
Thermosets	
Epoxy	Adhesives, automotive leaf springs (with glass fibre), bicycle frames (with carbon fibre).
Melamine	Decorative heat resistant surfaces for kitchens and furniture, dishes.
Phenolics	Heat resistant handles for pans, irons and toasters, electric outlets.
Unsaturated polyester	Toaster sides, iron handles, satellite dishes, breaker switch housing (with glass fibre), automotive body panels (with glass fibre).

Source: 'Materials science of polymers for engineering' T.A. Oswald, G. Menges, Hanser published NY, 1996

2.3.1   Thermoplastics and Thermosets

All polymer resin can be placed into two major categories, thermoplastics and thermosets. Table 2.1, above, has been organised into these categories.

Thermoplastics are polymers that solidify as they cool, no longer allowing the long molecules to move freely. When heated these materials regain, "flow," or viscosity as the molecules become able to slide past one another with ease.   Furthermore, thermoplastics are again sub-divided into two classes: amorphous and semi-crystalline polymers.   Amorphous thermoplastics have a random molecular structure as the molecules remain in disorder as it cools. Semi-crystalline thermoplastics solidify with a certain order in their molecular structure and are usually leathery or rubbery materials at room temperature due to a sub-zero glass transition temperature.

Thermosetting polymers are chemically cured causing the long macromolecules to crosslink with each other. This results in a network of molecules that cannot slide past one another. The crosslinking in these networks causes the material to lose its ability to regain viscousness or "flow" on reheating. Thermosetting materials are stiff and brittle as a result of the high density of crosslinking. The matrix resin used in this project is a thermosetting type resin and they are explored in the following section.

2.4   Thermosetting Resins

One of the major advantages of thermosetting resins is that they can be liquids at room temperature when the moulding process commences. This allows fillers and other additives like colorants, reinforcements, and processing aids to be easily mixed by simply stirring through. The most commonly known and used thermosetting resins in composites today include phenolics, amino plastics, unsaturated polyesters, epoxies, vinyl ester, polymides, and polyurethanes. Each group has different properties which make them more appealing in certain applications than others. An understanding of the formation and structure of the resin is vital for material selection and application.

2.4.1   Phenolics

Phenolics are made by the reaction of phenol (an aromatic molecule) and formaldehyde (a common organic liquid). The reaction of phenol with formaldehyde simultaneously forms polymer linkages and crosslinks. The resulting material is very hard and stiff. The properties of phenolics suggest that this material is highly crosslinked and that the crosslinks are three-dimensional.

2.4.2   Amino Plastics

Amino plastics are formed by simultaneous polymer and crosslinking reactions, but use amines in place of phenol as the reactant with formaldehyde. Aminos have a very tightly bonded crosslink structure as each molecule can present multiple amine sites. The material is hard and brittle, like phenolics. Amino plastics have a very high surface energy and hardness which makes them ideal for applications in adhesives and as materials for bench tops.

2.4.3   Unsaturated Polyesters

Unsaturated polyesters are low molecular weight condensation polymers that contain carbon-carbon double bonds that can be used to form crosslinks at a time chosen by the moulder. The reactive polymers, usually liquids at room temperature, become cured after the addition of an initiator and, occasionally, heat. The material created is less rigid than phenolics and aminos but are still reasonably brittle and stiff. Unsaturated polyesters are the most common thermoset materials and are principally used in composites with fibreglass reinforcement. Vinyl esters are closely associated with unsaturated polyesters and cure in much the same way.

2.4.4   Epoxies

Epoxies are polymers with three member rings on the ends of the polymer chains. The rings are bonding sites for a wide variety of materials. Crosslinks are created when the bonding sites react with the polymer and form a bridge to another polymer. Epoxies are stiff and strong and are commonly used as adhesives. They are also used as the resin in advanced composite applications with carbon fibre, which requires a higher performance from the resin than can be obtained with polyesters.

2.4.5   Polymides

Polymides crosslink by condensation polymerization between molecules that contain the imide group. The imide group is a group somewhat like an aromatic group, like phenolics, but they are even stiffer and stronger. Polymides are stiff, strong materials with extremely high thermal stabilities.

2.4.6   Polyurethanes

Polyurethanes are created by the reaction between polyols and isocyanates, accomplished simply by mixing the two reactants, which form a urethane linkage. No condensation product is made. Urethanes can be bot thermoplastics and thermosets, although the thermosets are more important in commercial application. Generally flexible, these materials can posses a wide range of flexibilities and other properties. The polyurethanes can be easily adjusted for stiffness and strength versus flexibility and toughness. This is done by changing the aromatic content of the monomers. This freedom of choice in properties along with their generally excellent abrasion resistance and durability, has led to a rapid increase in the use of polyurethanes, perhaps the most important being as the principal material in athletics shoes.

2.5   Phenolics

Phenolic resin is the matrix used in the project and therefore will be further explained in this section.

In this project, the resin used is phenol formaldehyde resin solution J-2027L produced and distributed by Hexion Speciality Chemicals Pty Ltd. Its official name is Hexion Cellobond J2027L (Chemwatch, 2005a). The catalyst or hardener used to crosslink the resin is is Hexion Phencat 15 (Chemwatch, 2005b) and is also produced by Hexion Speciality Chemicals Pty Ltd. The recommended ratio by weight to mix the resin to catalyst is 20:1.

Phenolics were the first thermoset materials to be synthesized, under the name of Bakelite[TM] by Leo Bakeland in 1907. They are among the most widely used thermosets, undoubtedly because they are some of the lowest cost engineering materials on a cost per volume basis. Phenolics are formed from the condensation polymerization reaction between phenol, an aromatic molecule, and formaldehyde, a small organic compound often used as a solvent or as a preservative (Strong 2000). Figure 2.2 shows the condensation polymerisation reaction between phenol and formaldehyde to produce Phenolformaldehyde (PF).
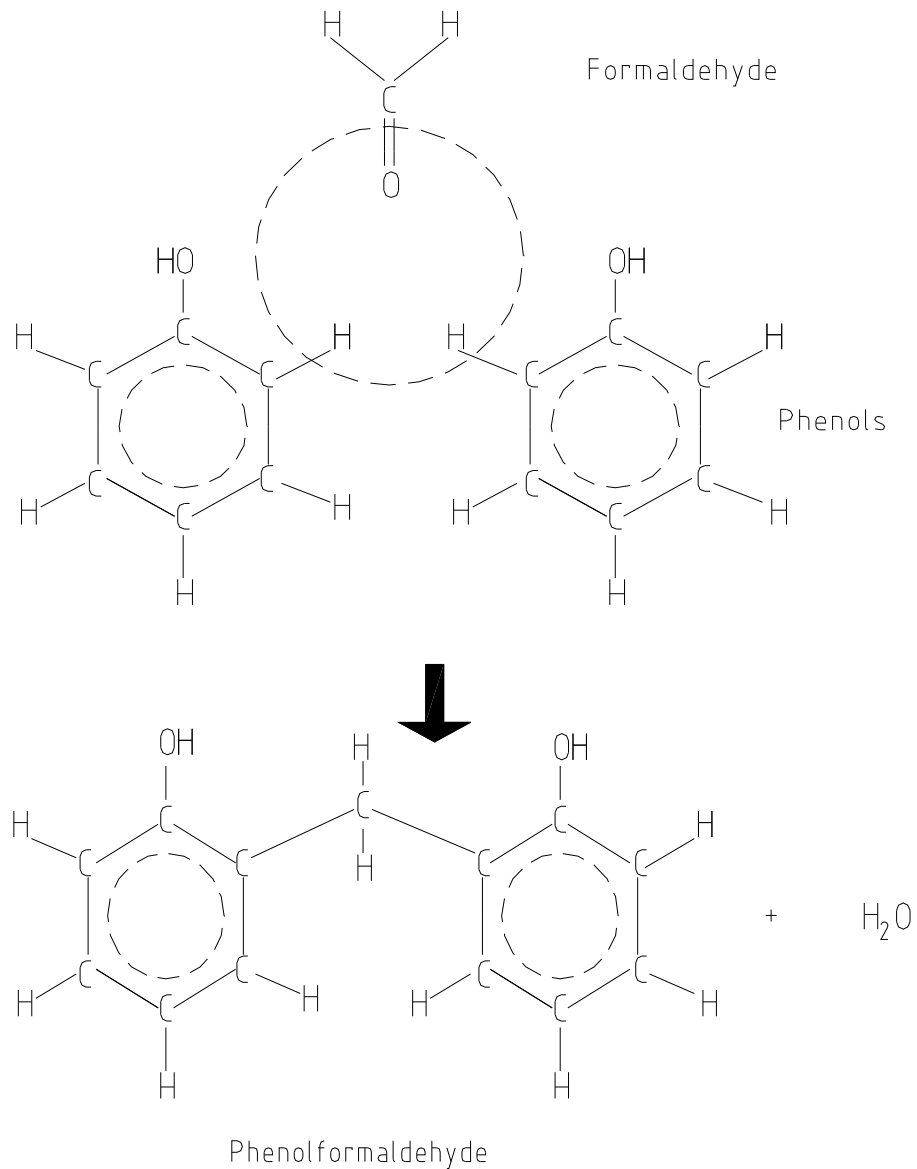
Figure 2.2: Condensation polymerization of Phenolformaldehyde resins

Cross linking requires that at least one of the reactants have more active reaction sites than the minimum needed for polymerization. Phenol has three active sites on the benzene ring, as indicated in Figure 2.3, which is one more than polymerization condensation requires and therefore cross linking can occur.
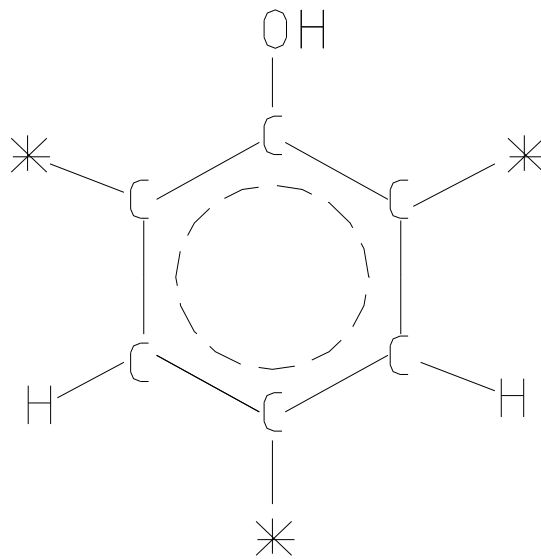
Figure 2.3: Phenol with active sites marked ✳

The condensation reaction for phenolics can be carried out under two different conditions, producing very different intermediate materials. The intermediates called resoles and novolacs are the materials usually sold to the moulder. Most moulded phenolic components are made from novolacs.

Resoles are created by conducting the condensation polymerization process in an alkali solution with excess formaldehyde, the reaction is carefully controlled so that a linear, non-crosslinked polymer liquid, a resole, is produced. The resole can then be used for moulding. Resoles are called one-stage resins because they can form cross links by simply heating without having to add any other materials (Strong, 2000).

Novolacs are formed by reacting phenol and formaldehyde in an acid solution but with insufficient formaldehyde to complete the reaction. This is the opposite conditions from those used to create resoles. The resulting novolac material is the first stage of the reaction and is a brittle thermoplastic resin that can be melted but will not crosslink to form a solid with just the addition of heat, as resoles do. Novolacs require a curing agent, the most common of which is hexamethylene tetramine, or simply hexa. When heat and pressure are applied to the novolac containing hexa, the hexa decomposes, producing ammonia which provides the methylene cross linkages to form a network

structure. Novolacs are called two stage resins because a second material must be added to complete the reaction. (Strong 2006; Clarke 1996)

2.6   Filler (Slg)

If moulded without fillers or reinforcements, phenolic components can be brittle and have high shrinkage in the mould. This is expected from the highly aromatic and multiple cross linked nature of cured phenolic resins. The resin is therefore usually blended with fillers and reinforcements to reduce shrinkage and increase the strength and toughness of the material. Electrical and thermal insulating properties and chemical resistance is improved by the addition of fillers and also the cost of the part is reduced. The most common filler is wood flour, which is purified sawdust. Other common fillers and reinforcements are cotton fibres, fibreglass, and chopped thermoplastic fibres such as nylon. The filler used in this project was Envirospheres and they are further explained in the following section.

2.6.1   Envirospheres (E-Spheres)

Enviroshperes (E-spheres) will be used as the slg in this project. E-spheres are a mineral additive that can improve a product by reducing its weight, improving performance and substantially lowering its cost. E-spheres are white microscopic hollow ceramic spheres that are ideal for a wide range of uses. The particle size of this general purpose E-spheres ranges from $20 - 300$ μm with an approximate average of 130 μm. The relative density of E-spheres is about 0.7. Envirospheres are a combination of Silica, SiO_2 (55-60%), Alumina, Al_2O_3 (36-44%), Iron Oxide, Fe_2O_3 (0.4-0.5%) and Titanium Dioxide, TiO_2 (1.4-1.6%). E-sphere is an inert material similar to talcum powder. The material may be prone to dusting in use. Grinding, milling or otherwise generating dust may create a respiratory hazard. In high dust areas the use of goggles and a National Institute of Occupational Health and Safety (NIOSH) approved dust respirator is recommended.

Envirospheres are used in a variety of manufacturing applications because of their unique properties and they are (E-spheres, n.d.):

- extreme heat resistance;

- high compressive strength;

- pure, clean and white.

Envirospheres can be used in most composite manufacturing methods including casting, spray-up, hand lay-up, cold/hot press molding, resin transfer molding and also in the creation of syntactic foam.

Chapter 3

Fracture Mechanics

3.1 Introduction to Fracture Mechanics

Fracture mechanics is the discipline concerned with the behaviour of materials containing cracks or other small flaws. A flaw is considered to be a potential crack producing feature such as small pores, inclusions, or micro-cracks. What we wish to know is the maximum stress that a material can withstand if it contains flaws of a certain size and geometry (Askeland, 2003).

Failure of engineering materials is almost always an undesirable event for several reasons; these include human lives that are put in jeopardy, economic losses, and the interference with the availability of products and services. Major material failures such as that show in Figure 3.1 and the brittle failure of normally ductile materials has lead to extensive research and developments in the field of fracture mechanics since World War Two. The increased understanding of material properties has lead to better understanding and application of materials since the mid 1900's.
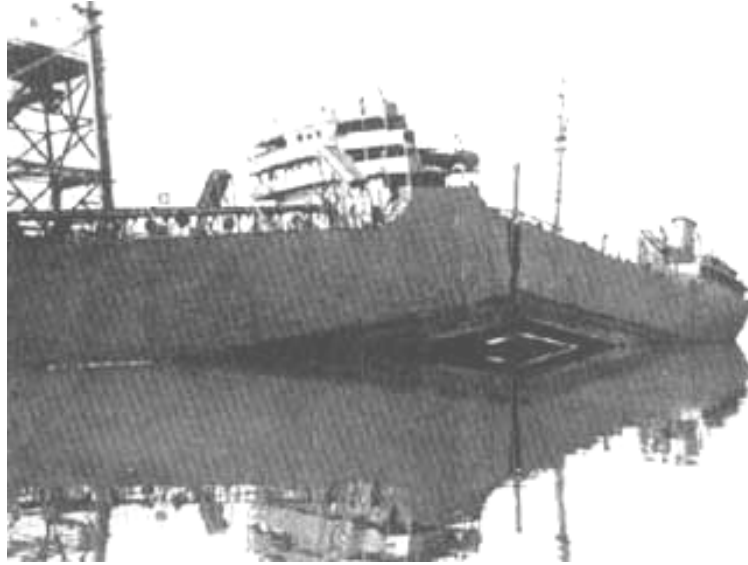
Figure 3.1: The S.S.Schenectady destroyed by brittle fracture while in harbor (1944)

(source: www.wikipedia.org)

3.2   Fracture Toughness

Fracture toughness is the ability of a material containing a flaw to withstand an applied load. A typical fracture toughness test can be conducted by applying a tensile stress to a specimen prepared with a flaw of know size and geometry, Figure 3.2(a). The stress applied to the specimen is intensified at the flaw, which acts as a stress raiser, Figure 3.2(b).
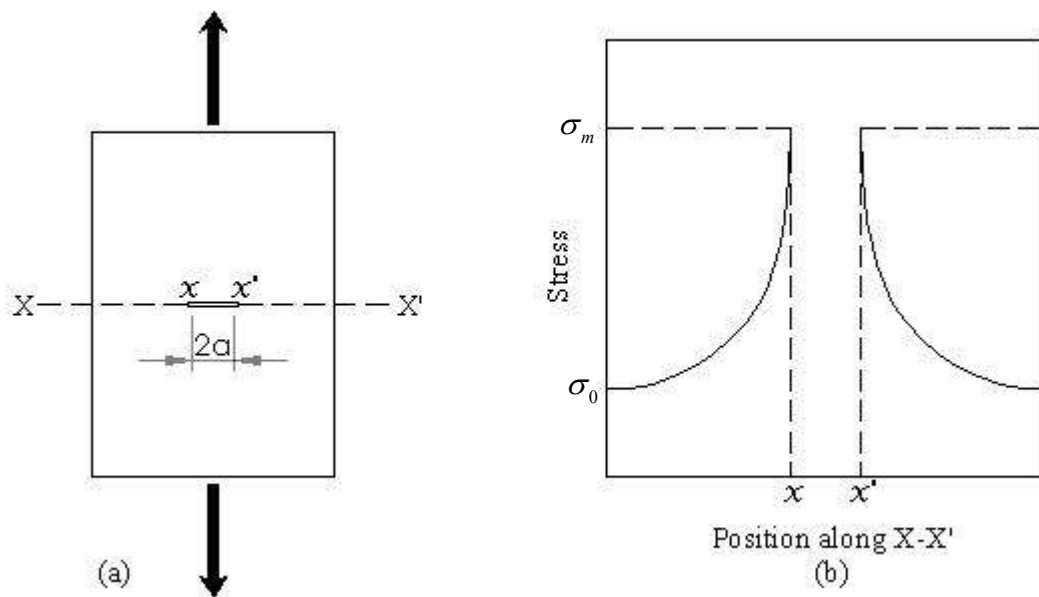
Figure 3.2: (a) The geometry of a typical fracture toughness test with an internal crack. (b) Schematic stress profile along the line X-X' in (a), demonstrating stress amplification at crack or flaw tips. (Callister 1994, p. 188)

For a simple stress loading case, the *stress intensity factor*, K, is given by (Askeland 2003, eqn. 6-18):

$$K = f\sigma\sqrt{\pi a} \qquad\qquad (3.1)$$

Where f is a geometry factor for the specimen and flaw, [given in Figure 3.3];

              σ is the tensile stress applied to the specimen, and;

              a is the flaw size.

From the analytical expression for K, equation 3.1, it can be noted that the stress intensity changes with the geometry of both the flaw and specimen. If the specimen is assumed to have an 'infinite' width, then $f \cong 1.0$.

σ (a) σ (b)
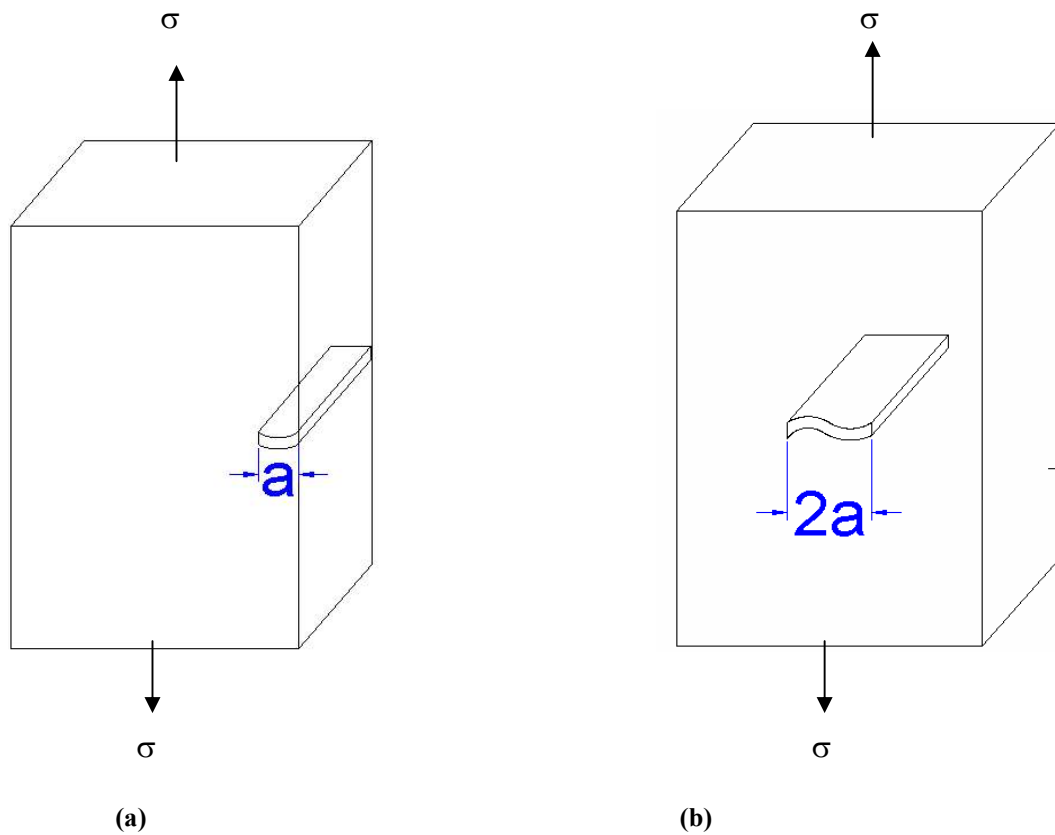
Figure 3.3: Schematic drawing of fracture toughness specimens with (a) edge and (b) internal flaws. (Askeland, 2003, p. 265)

By performing a tensile test on a specimen with a known flaw size, the value of K that causes the flaw to grow, and cause failure, can be determined. This critical value of the stress intensity factor, K, is defined as the *fracture toughness, K_c*, which is given by (Askeland 2003, eqn. 6-19):

$$K_c = f\sigma_c\sqrt{\pi a} = K \text{ required for crack to propagate} \qquad (3.2)$$

Where σ_c is the stress applied to the specimen when crack propagation occurs.

Fracture toughness is dependent on the thickness of the sample: As thickness increases, fracture toughness K_c decreases to a constant value where only a condition of plain strain exists, Figure 3.4. This constant is called the *plane strain fracture*

toughness, K_{IC}. Because K_{IC} does not depend upon the thickness of the sample it is therefore the most commonly reported fracture property of materials.
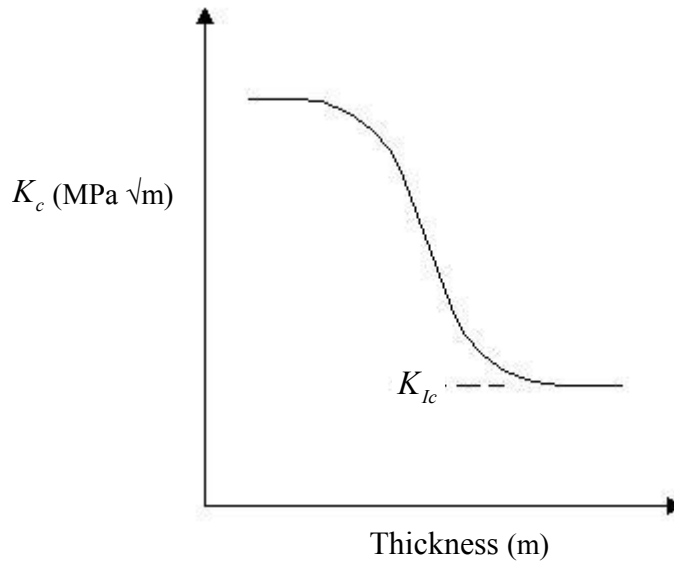
Figure 3.4: The fracture toughness, K_C, decreases with increasing thickness, eventually

levelling off at the plane strain fracture toughness, K_{IC}.

Table 3.1 is a comparison of the K_{IC} to yield strength of some commonly used engineering materials. Fracture toughness has the unusual units of $MPa\sqrt{m}$.

Table 3.1: The plane strain fracture toughness K_{IC} of common engineering materials.

Material	Yield Strength (MPa)	KIC (MPa√m)
	Metals	
Aluminium Alloy		36-50
Alloy Steel		50-90
Titanium Alloy		44-66
	Ceramics	
Aluminium Oxide	-	3.0-5.3
Soda-lime Glass	-	0.7-0.8
Concrete	-	0.2-1.4
	Polymers	
Polymethyl methacrylate	-	1.0
Polystyrene	-	0.8-1.1

Brittle materials have a low K_{IC} and are more susceptible to catastrophic failure. Ductile materials however have higher K_{IC} values.

The ability of a material to resist the growth of a crack depends on a large number of factors (Askeland 2003, p. 266-267);

- Larger flaws reduce the permitted stress. Therefore a reduced flaw size will mean an improved fracture toughness.

- The ability of a material to deform is critical. In ductile materials, the material near the tip of the flaw can deform, causing the tip of any crack to become blunt, reducing the stress intensity factor, and preventing growth of the crack. Increasing the strength of a given metal usually decreases the ductility and gives a lower fracture toughness. Brittle materials such as ceramics and many polymers have a much lower fracture toughness than metals.

- Thicker, more rigid pieces of a given material have a lower fracture toughness than thin materials.

- Increasing the rate of application of the load, such as in an impact test, typically reduces the fracture toughness of the material.

- Increasing the temperature normally increases the fracture toughness, just as in the impact test.

- A small grain size normally improves fracture toughness, whereas more point defects and dislocations reduce fracture toughness. Thus, a fine-grained ceramic material may provide improved resistance to crack growth.

- In certain ceramic materials we can also take advantage of stress-induced transformations that lead to compressive stresses that cause increased fracture toughness.

3.3   Importance of Fracture Mechanics

The fracture mechanics approach to material selection allows us to design and select materials without neglecting the inevitable presence of flaws.   There are three important variables to consider: the properties of the material (K_c or K_{IC}), the stress, σ, that the material must withstand, and the size of the flaw, a. If two of these variables are known we can determine and design for the third (Askeland, 2003).

3.3.1   Selection of Material

If we know the maximum size, a, of flaws in the material and the magnitude of the applied stress, σ, a material can be selected from tables and other sources that has a fracture toughness K_c or K_{IC} large enough to prevent the flaw from propagating. Equation (3.2) is used to calculate the fracture toughness requirement of the material (Askeland, 2003).

3.3.2   Design of a Component

If maximum flaw size, and the material and its fracture toughness values are known the maximum or critical stress that the component can withstand can be calculated by rearranging equation (3.2) to give:

$$\sigma_C \le \frac{K_{IC}}{f\sqrt{\pi a}} \qquad\qquad (3.3)$$

With equation (3.3) we can design the appropriate size of the component to assure that the maximum stress is not exceeded in the component (Askeland 2003).

3.3.3   Design of a Manufacturing or Testing Method

If a material is selected to be tested, the applied stress is known, and the size of the component is constant, the maximum size of the flaw that can be tolerated can be determined. Once again rearranging equation (3.2) for flaw size yields:

$$a_C = \frac{1}{\pi} \left(\frac{K_{IC}}{\sigma f} \right)^2 \qquad\qquad (3.4)$$

To ensure a part functions safely a non-destructive testing technique that detects any flaw greater than the critical size be performed. Additionally, the selection of an acceptable manufacturing process can assist in ensuring flaw sizes are below this critical size (Askeland, 2003).

3.4   Theories of Fracture

The first successful brittle fracture analysis was conducted on glass by Griffith (1920). Griffith concluded that an existing crack would propagate if the systems total energy was lowered, assuming a simple energy balance was present. The energy was balanced by a decrease in elastic strain energy within the stressed component as the crack propagated and the increase in energy required to create a new crack. Griffiths theory estimated the theoretical strength of brittle materials and offered a relationship between fracture strength and defect size (Elwads and Wanhill, 1984).

Fracture mechanics today has two major theories which tend to give similar results. One approach assumes that materials lose plasticity at lowered temperature. The other is an analytical approach derived from the stresses and plastic zones at the tip of the crack. The two different approaches are outline in the following sections.

3.5   Transitional Temperature Approach

The transitional temperature approach assumes that all materials will become brittle below a certain temperature. When cold, plastic yielding is restricted, so stresses can not be absorbed at crack tips leading to fracture at lower stresses.
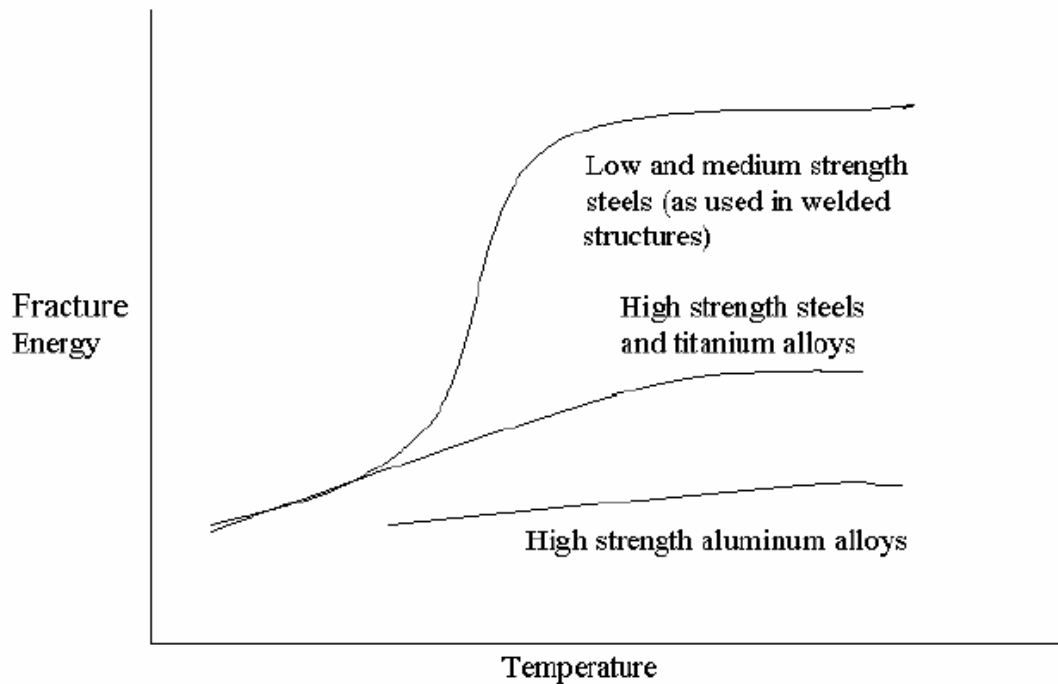
Figure 3.5: Materials exhibiting both ductile and brittle behaviour at different temperatures.

Figure 3.5 depicts this transitional temperature theory and it shows that at lower temperatures the materials need less fracture energy for failure, thus being brittler. The higher the fracture energy the more ductile the material is behaving.

3.6   Analytical Approach

The analytical approach is derived around the stresses that occur near the crack tip. The relationship between the change in potential and surface energy of the material and the stresses gives rise to a analytical method of calculating the stress present, assuming the stress distribution around the crack tip is constant.   Linear Elastic Fracture Mechanics (LEFM) was developed as a result of this approach. LEMF can,

however, only predict material behaviour if the crack tip remains mostly elastic. For brittle materials, it accurately establishes the criteria for catastrophic failure. Limitations arise when large regions of the material are subject to plastic deformation before a crack propagates. Elastic Plastic Fracture Mechanics (EPFM) is another approach can analyse mixed mode behaviour and large plastic zones. The equations involved are past the scope required in this discussion, only a understanding of the various methods is necessary.

Chapter 4

Fracture Toughness Tests

4.1   Standard Tests

There have been many tests developed for evaluating the fracture toughness, K_{IC}, of materials.   This section will explain the most commonly applied methods both standard and non-standard. Similar testing procedures have been implemented by the United States of America (USA) and the United Kingdom (UK) and these tests are regarded as standard. These tests are outlined in The American standard, ASTM: E399 and the British standard, BS: 5447. The standard tests are outlined in the following sub- sections.

4.1.1   C-Shape Section

The C-Shape Sections primary application is in checking the fracture toughness of hollow cylinders or pipes. The geometry of the C-Shape Section is shown in Figure 4.1. The specimen has a small notch at the centre of its curve where the crack propagates from. The specimen is fatigue loaded through pins by means of a two-point bending test.
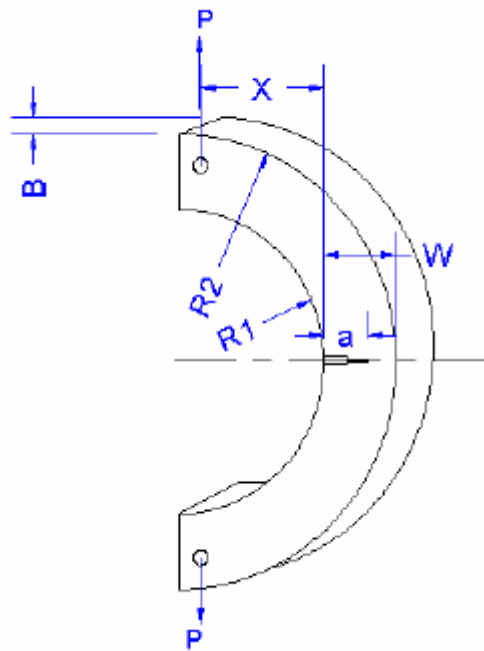
Figure 4.1: C-Shape Specimen fracture toughness test geometry.

4.1.2   Compact Tensile Specimen

A Compact Tensile Specimen fracture toughness test is a thin plate that has a fatigue load applied to two pins either side of the crack. The geometry of the test specimen is shown in Figure 4.2.
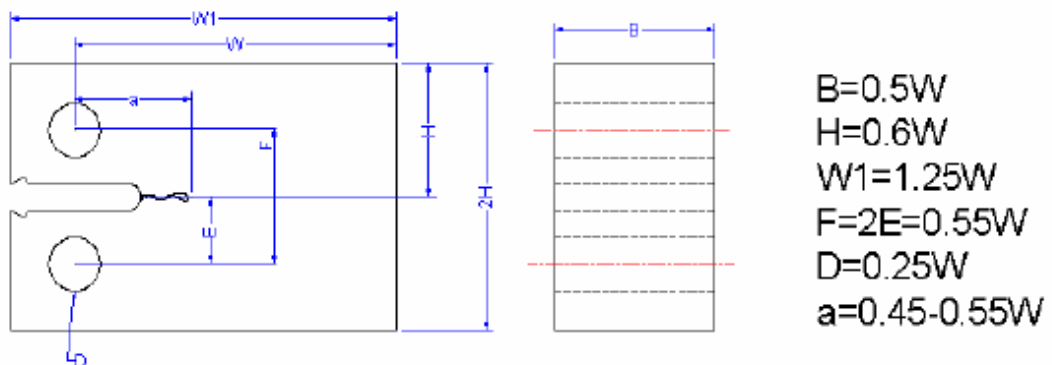
Figure 4.2: Compact Tensile Specimen fracture toughness test geometry.

4.1.3   Single Edge Notch Bend (SENB)

A Single edge notch bend or three point bend test has a simple rectangular geometry with a notch machined into the fracture toughness specimen. A fatigue crack is then grown by applying cyclic loading to the specimen. SENB specimens are usually immersed in a bath for low temperature tests. The geometry and load application points of a single edge notch bend test are shown in Figure 4.3.
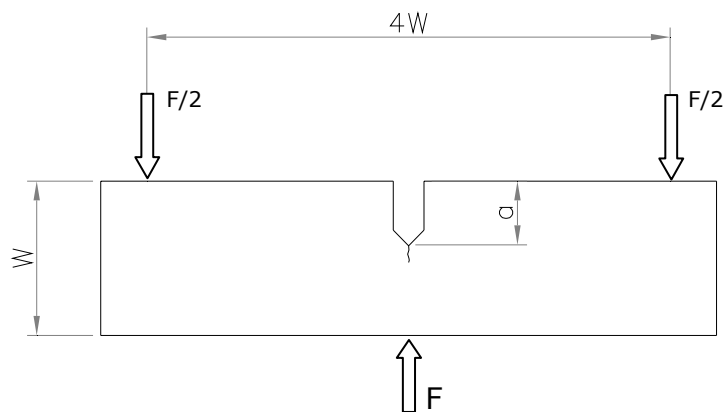
Figure 4.3: Single edge notch bend test geometry

4.2   Non-Standard Tests

The standard tests outlined above are usually high cost and have a complicated geometry making them hard to manufacture and test. Non-Standard tests are therefore commonly used to evaluate the fracture toughness of materials as they are a cheaper alternative and easier to test and create. Non-standard test results are related to the mechanical properties of the materials. These properties can then be converted into a more meaning fracture toughness value by mathematical models.

4.2.1   Charpy V-Notch Impact Test

The Charpy V-Notch Impact Test determines the resistance of a material to an impact. The Charpy test is conducted by swinging a large pendulum through a specimen and recording the starting and finishing height of the pendulum. The difference in heights of the pendulum is the impact energy absorbed by the specimen upon failure (Askeland

2003). The Charpy test specimen is a 10mm square by 55mm long bar containing a small notch to direct the crack. The Charpy test equipment and Charpy test specimen is pictured in Figure 4.4.
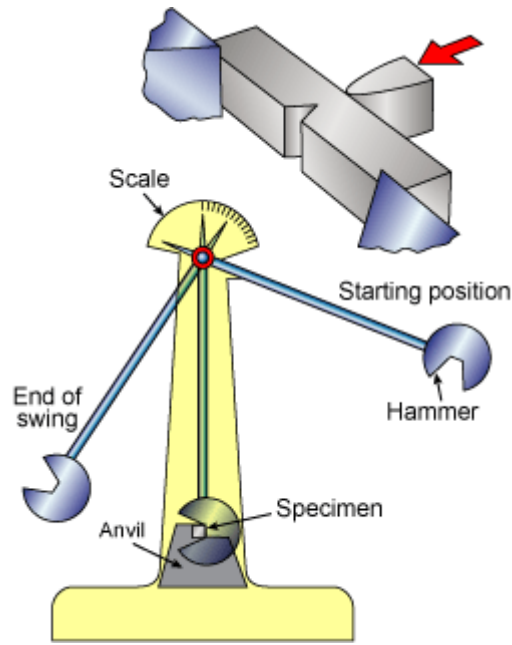
Figure 4.4: Charpy V-notch impact test.
(Source: www.twi.co.uk/j32k/servlet/getFile/jk71.html)

Equation (4.1) can be used to relate a charpy V-notch impact test result, *CVN*, to fracture toughness, K_{IC};

$$K_{IC}^{2} = 2 \times E \times CVN^{3/2} \tag{4.1}$$

Where E is the Modulus of Elasticity of the material in Pascals, Pa;

CVN is the Charpy V-Notch test result in Joules, J.

4.2.2   Short Rod/Short Bar Test

Barker (1977) created a simple method to measure fracture toughness that is applicable to a wide range of materials. The method uses small rod or bar specimen, as in Figure 4.5. The mouth or grip groove is where a load is applied to the specimen. The applied load causes fracture to initiate at a point, of known distance, called the chevron slot tip. A toughness measurement is made when the crack has developed and is in the central region of the specimen, to achieve a more reliable fracture toughness result.

Using the measured load, analysis methods have been derived to calculate the plane strain fracture toughness, as measured by the chevron-notched short rod method, K_{ICSR}.

Advantages of the short rod/short bar method include;

- Reduced sample size;

- Smaller specimen sizes can be created;

- Cheaper to create;

- Cheaper to test; and

- It is applicable to a wide variety of materials.

Unlike the other fracture toughness tests outlined in this chapter fatigue pre-cracking is not required due to the chevron slot. This is a major advantage over other fracture toughness tests as it simplifies the testing procedure.
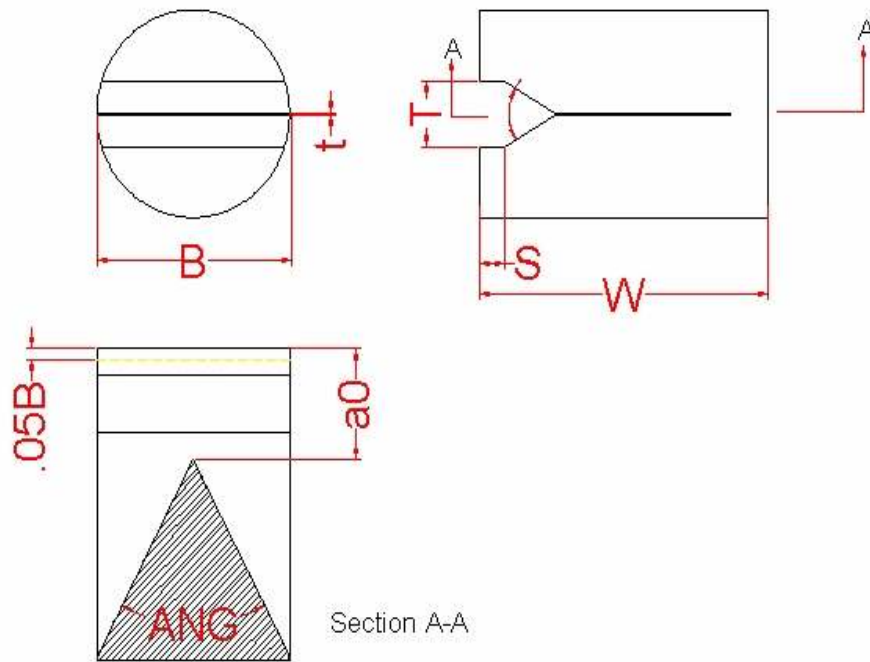
Figure 4.5: Short Rod Fracture Toughness Specimen

Chapter 5

Short Rod/Short Bar Test

5.1   Introduction

The need exists for a simple, less expensive method of measuring the fracture toughness of metallic materials in terms of their plain-strain critical stress-intensity factor (Barker 1981). The short rod/short bar method is a new test specimen with circular and rectangular cross-sections, respectively. Short rod/short bar specimens have been shown to be applicable to a wide variety of materials, like metals, polymers, ceramics, and rocks (Barker 1981). The short rod/short bar specimens are proficient in producing valid measurements using smaller specimens than other tests for plain-strain fracture toughness of metallic materials (E399-78a). These characteristics have created a considerable interest in the short bar geometry and it is being increasingly used today to evaluate the impact properties of a range of materials.

Specimens of the rectangular short bar configuration have been found to have test characteristics that are experimentally indistinguishable from those of the round short rod specimens. Therefore statements about short bar specimens are equally applicable to short rod specimens, and visa-versa (Barker 1981).

The short bar and rod geometry developed by Barker (1981, p. 457) can be seen in Figure 5.1.

SHORT BAR   (a)

SYMBOL	DEFINITION	VALUE	TOLERANCE
B	BREADTH	B	
W	LENGTH	1.5B	±.010B
H	HEIGHT	.870B	±.005B
a_0	INITIAL CRACK LENGTH	.513B	±.005B
θ	SLOT ANGLE	55.2°	± 1/2°
t	SLOT THICKNESS	SEE FIG 5.5	-
S	GRIP GROOVE DEPTH	.130B	±.010B
T	GRIP GROOVE WIDTH	.313B	±.005B

SHORT ROD   (b)

SYMBOL	DEFINITION	VALUE	TOLERANCE
B	DIAMETER	B	
W	LENGTH	1.5B	±.010B
a_0	INITIAL CRACK LENGTH	.513B	±.005B
θ	SLOT ANGLE	55.2°	± 1/2°
t	SLOT THICKNESS	SEE FIG 5.5	-
S	GRIP GROOVE DEPTH	.130B	±.010B
T	GRIP GROOVE WIDTH	.313B	±.005B

Figure 5.1: Short bar (a) and short rod (b) specimens with straight chevron slots. The LOAD LINE is the line along which the opening load is applied in the mouth of the specimen. (Barker 1981, p. 457)

5.2   Short Rod/Short Bar Geometry

5.2.1   Development of Short Bar Geometry

The dimensional relationships were selected on the basis of a large number of tests of specimens with different length-to-diameter ratios and various chevron slot geometries. From these tests the short bar specimen geometry configurations were selected as a reasonable compromise in an attempt for an optimum geometry (Barker 1981). The optimum geometries are pictured in Figures 5.1 and 5.2. The criteria on which this geometry was created is as follows (Barker 1981, p. 459);

- The tendency for the crack to "pop in" at initiation should be reduced; the crack initiation should be as smooth as possible.

- The crack should be well guided by the chevron slot.

- The width of the crack front should be an appreciable proportion of the specimen diameter at the time of the fracture toughness measurement.

- The crack should be near the centre of the specimen at the time of the fracture toughness measurement.

- The load should be at or near its peak value at the time of the toughness measurement.

- The specimen geometry should be as simple as possible for ease of specimen fabrication.

- The specimen should be economical in its use of sample material.

The short rod/short bar geometry for curved chevron slots is shown in Figure 5.2.

SHORT BAR   (a)

SYMBOL	DEFINITION	VALUE	TOLERANCE
B	BREADTH	B	
W	LENGTH	1.5B	±.010B
H	HEIGHT	.870B	±.005B
a_0	INITIAL CRACK LENGTH	SEE FIG 5.4	±.005B
θ	SLOT CHORD ANGLE	SEE FIG 5.4	±1/2°
t	SLOT THICKNESS	SEE FIG 5.5	-
S	GRIP GROOVE DEPTH	.130B	±.010B
T	GRIP GROOVE WIDTH	.313B	±.005B
R	RADIUS OF SLOT CUT	SEE FIG 5.4	±2.5B

SHORT ROD   (b)

SYMBOL	DEFINITION	VALUE	TOLERANCE
B	DIAMETER	B	
W	LENGTH	1.5B	±.010B
a_0	INITIAL CRACK LENGTH	SEE FIG 5.4	±.005B
θ	SLOT ANGLE	SEE FIG 5.4	±1/2°
t	SLOT THICKNESS	SEE FIG 5.5	-
S	GRIP GROOVE DEPTH	.130B	±.010B
T	GRIP GROOVE WIDTH	.313B	±.005B
R	RADIUS OF SLOT CUT	SEE FIG 5.4	±2.5B

Figure 5.2: Short bar (a) and short rod (b) specimens with curved chevron slots. The LOAD LINE is the line along which the opening load is applied in the mouth of the specimen. (Barker 1981, p. 460)

5.2.2   Specimen Geometry Options

Four basic geometries are revealed in Figure 5.1 and 5.2, all of which give accurate results of fracture toughness. The specimen size parameter, B, is the specimen diameter (short rod) or the specimen breadth (short bar) shown in the respective tables of Figures 5.1 and 5.2. These Figures show two different chevron slot geometries, straight or curved, as a result of the different methods of machining or creating the chevron slot. Figure 5.1 (a) and (b) show the short bar and short rod geometries, respectively, for straight chevron slots. Straight chevron slots are created by feeding a saw or cutter through the specimen or by placing a thin piece of material cut to size into the mould before pouring. 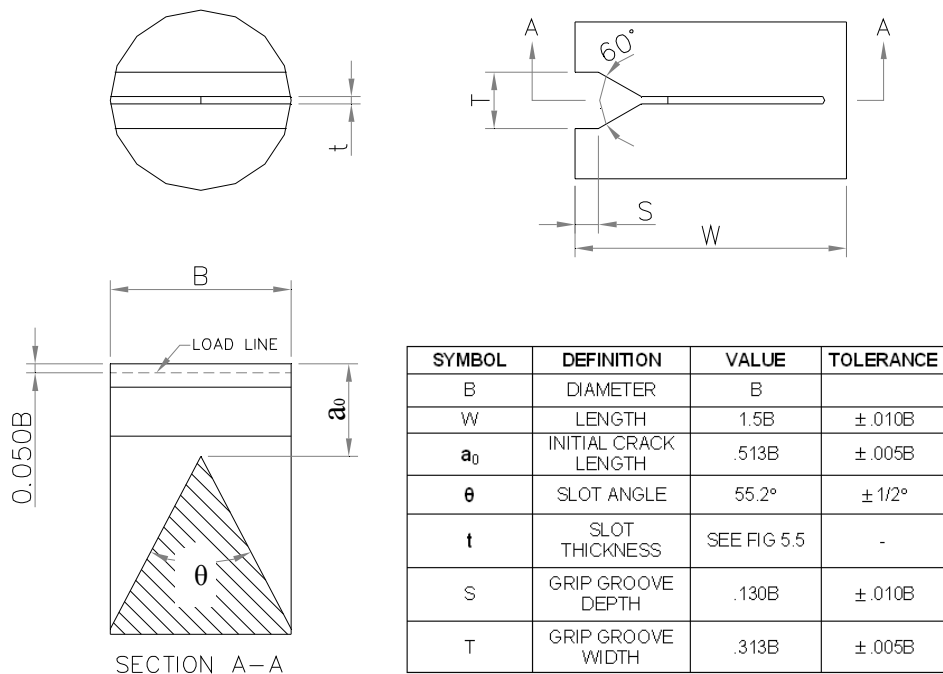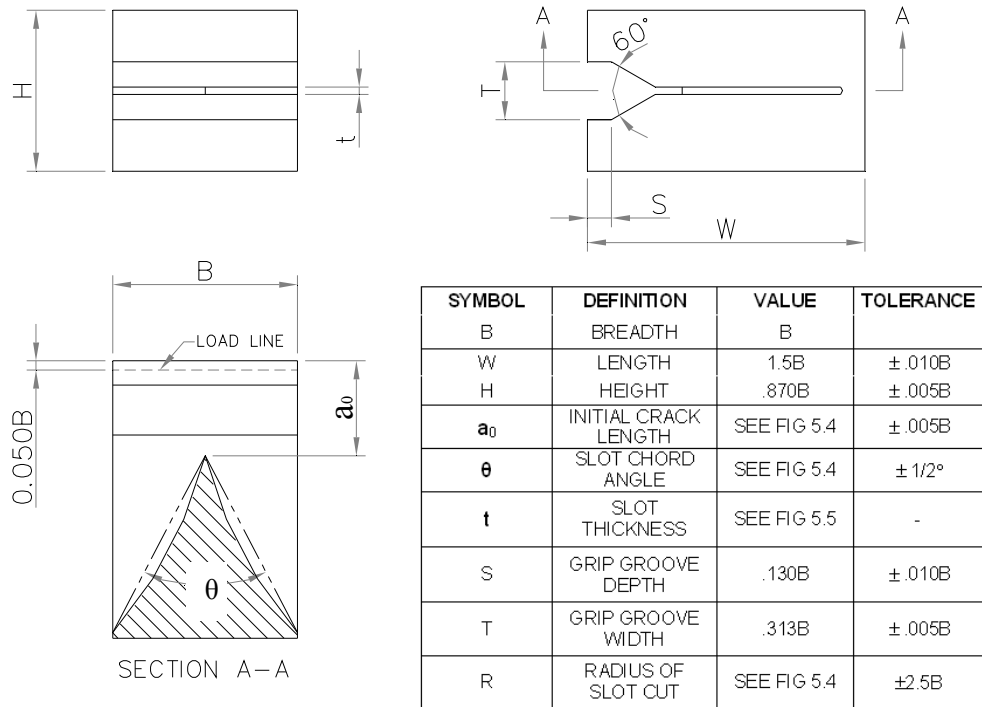 Figure 5.2 (a) and (b) show the short bar and short rod geometries, respectively, for curved chevron slots. Curved chevron slots are created from a plunge-type feed of a saw blade into the specimen. In Figures 5.1 and 5.2 it is noticeable that the section views (section A-A) of the rectangular short bars are identical with those of the circular short rods (Barker 1981).   By making the height of the short bar specimen 0.870B the short rod and bar geometries therefore have the same calibrations, this has been proven in experimental studies (Barker 1981).

Another desirable calibration is that between straight-slotted specimens, Figure 5.1, and curved-slotted specimens, Figure 5.2. This is done by superimposing the section views of the two different slot geometries, and then adjusting the slot configurations until the straight and curved slot bottoms are tangent to one another at the critical crack length, a_C, where the peak load occurs in an LEFM test, that is, where the fracture toughness measurement is made. Figure 5.3 shows the superimposed slot geometries tangent at a_C. This means that when the crack is near the position where the toughness measurement is taken, both slot geometries have essentially the same crack-front width, rate of change of crack-front width with crack length, and compliance derivative, which causes their calibrations to be effectively equivalent (Barker 1981).

Barker (1981) has discovered that when machining the chevron slots in a curved-slotted specimen, it is easier to measure the distance to the point of the chevron slot, a_0, and the slot chord angle, θ, than to measure the slots passing through the desired tangency point at the required angle. The values of a_0, and θ which produce the

desired tangency have been calculated as a function of saw blade diameter. This is plotted in Figure 5.4.
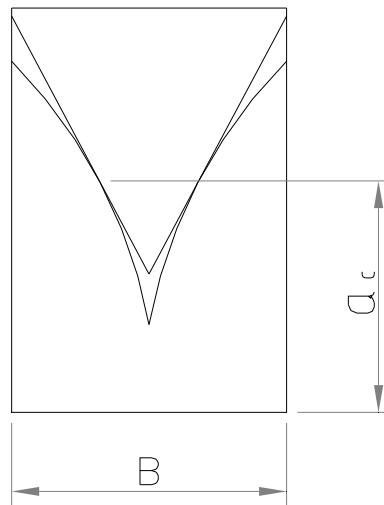
Figure 5.3: Superimposed curved and straight chevron slots tangent at a_C.
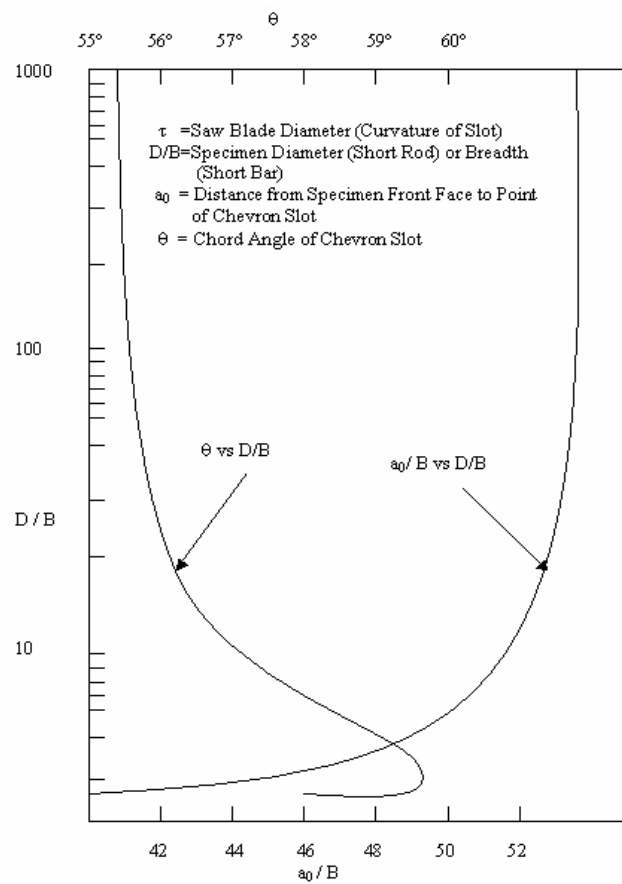
Figure 5.4: Chevron slot angle, θ, and initial crack length, a_0, for curved chevron slots.

Using a_0 and θ derived from Figure 5.4 for the saw blade diameter, an effectively constant specimen calibration can be obtained, regardless of specimen size, when the crack is in the vicinity of the critical crack length, a_C (Barker 1981, p. 461).

5.2.3   Specimen Tolerances and Correction
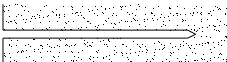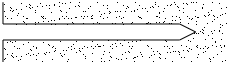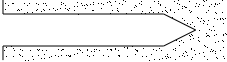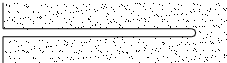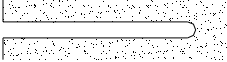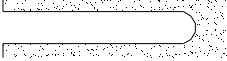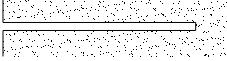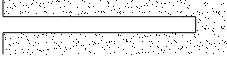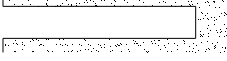
The variation in a specimens calibration is a related to the parameters, a_0, θ, and W, when B is assumed to be constant. This variation should be measured to determine the allowable dimensional tolerances on the parameters in manufacturing specimens (Barker 1981). Barker (1981) conducted a sensitivity study on these parameters and it was found that the dimensional tolerances listed in the tables in Figure 5.1 and 5.2 were selected to ensure the effect of within-tolerance variations of any one parameter is within about ±0.5 percent of the calculated fracture toughness (Barker 1981).

When the parameters, a_0, θ, and W, are out of tolerance the sensitivities of the test results to variations in parameters are well enough known to permit the application of a correction factor. Barker (1981, p. 463), Table 1, contains the equations used in the calculation of the configuration correction factor, C_C. This factor is multiplied by test results to correct inaccurate specimen geometries. By using the C_C factor, test results for specimens which are out of tolerance by up to three times the tolerances of the tables in Figures 5.1 and 5.2 can be corrected to within ±0.5 percent toughness uncertainty of nominal specimens (Barker 1981).

5.2.4   Chevron Slot Thickness and Sharpness

The thickness and sharpness of the bottom of the chevron slot can have a major effect on the fracture toughness result. Properly designed slots can greatly enhance the degree of plain-strain along the crack front. Better slot geometries lead to a smaller plain-stress or plastic zone in comparison to the size of the specimen and therefore an enhanced plain-strain region (Barker 1981). Controlling the plain-strain constraint

with the slot geometries means that a range of materials can be tested accurately from very tough, brittle low yield materials, to high yield ductile materials. Figure 5.5 is the result of a study into the chevron slot geometries and depicts the best slot configurations.

SLOT CONFIGURATION	SLOT THICKNESS (mm)	EFFECT ON SLOT CALIBRATION	PLAIN −STRAIN CONSTRAINT*
	0.38	0	Excellent
	0.8	−1%	Excellent
	1.6	−3%	Excellent
	0.38	0	Excellent
	0.8	−1%	Good
	1.6	−3%	Poor
	0.38	0	Good
	0.8	−1%	Poor
	1.6	−3%	Poor

* Excellent = less than +2% effect on the measurement
  Good = less than +5% effect on the measurement
  Poor = more than +5% effect on the measurement

Figure 5.5: Effect of chevron slot geometry. (Barker 1981, p. 466)

5.3   Short Bar Fracture Toughness Test

Specimen geometry and preparation are important to obtain accurate fracture toughness results, but the testing procedure must also be controlled in order to obtain accurate testing data (Barker 1981).

In fracture toughness testing of short bar specimens a load is applied to the mouth of the specimen to initiate crack growth at the point of the chevron slot. In an ideal test the load to initiate crack growth is smaller than the load that is needed to further advance the crack. The test therefore requires an increasing load to be applied to the specimen until the crack length reaches its critical length, a_C. Figure 5.6 shows the load variation with crack length of an ideal test.
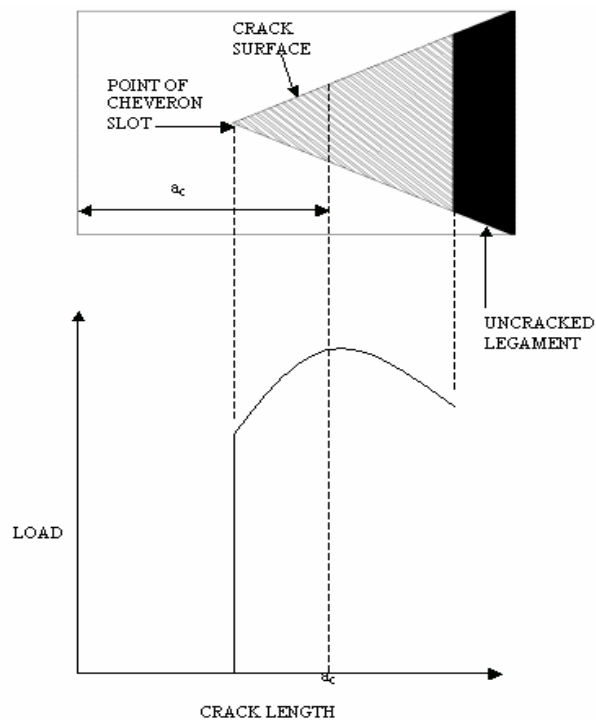
Figure 5.6: Variation of load versus crack length.

Using linear elastic fracture mechanics principles (LEMF) the equation for fracture toughness in a short bar test specimen can be derived. The material plane strain critical stress intensity factor, F_{ICSB}, is given by the equation (Munz 1981):

$$F_{ICSB} = \frac{\left(F_{max} Y_m^*\right)}{B\sqrt{W}}$$

(5.1)

Where F_{max} is the peak load

Y_m^* is the compliance calibration according to ASTM E-399-78

The compliance calibration, Y_m^*, for the short bar test method from ASTM E-399-78 is given by:

$$Y_m^* = \{-0.36 + 5.48\omega + 0.08\omega^2 + (30.56 - 27.49\omega + 7.46\omega)\alpha_0$$
$$+ (65.90 + 18.44\omega - 9.7\omega)\alpha_0^2\}\left\{\frac{\alpha_1 - \alpha_0}{1 - \alpha_0}\right\}^{\frac{1}{2}} \qquad (5.2)$$

Where:

$$\omega = \frac{W}{H} \qquad (5.3)$$

$$\alpha_0 = \frac{a_0}{W} \qquad (5.4)$$

$$\alpha_1 = \frac{a_1}{W} \qquad (5.5)$$

In the equations, above, W, H, a_0 and a_1 are the measured specimen dimensions in millimetres, shown in Figure 5.7.
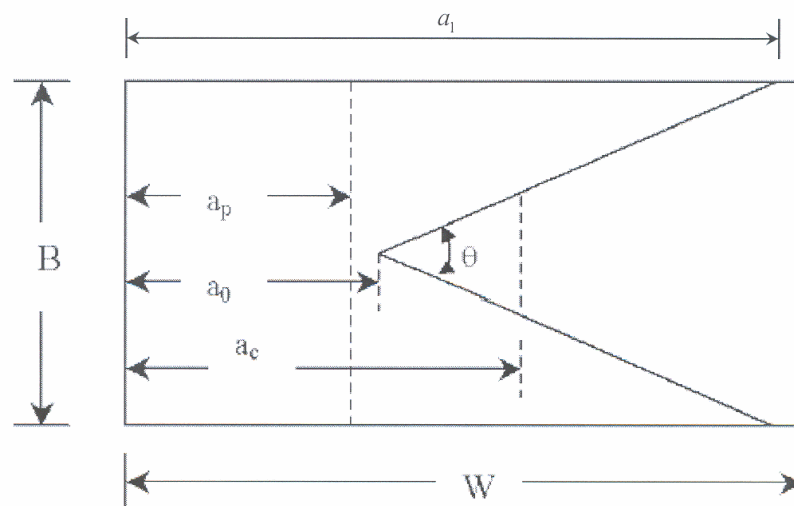
Figure 5.7: Cross-sectional dimensions of short bar specimen showing a_1.

After testing the specimens the measurements in Figure 5.7 need to be recorded for use with equations (5.3), (5.4) and (5.5). In this project these measurements can be seen tabulated in Appendix F, Table F.1

Chapter 6

Experimental Methodology

6.1   Specimen Design

Having selected the short bar test as the method of fracture toughness measurement the size of the specimen had to be determined as this would have a major effect on the mould material and construction properties.   From the standard ISRM short bar geometry, Figure 5.1(a), a size of B = 50mm was selected. The resulting dimensions of the specimen are shown in Appendix B.1, Figure B.2. This size gives a practical specimen for testing because is easy to handle and also it reduces the cost of the testing as mould and composite materials are reduced. This step of the selection of geometry size was done in conjunction with the design and construction of the mould step that is described in section 6.2 because size, cost and material selection are all interconnected.

6.2   Mould Design and Construction

A mould for a sample of short bar test specimens was required to be designed and built as the previous or common method of constructing the specimens had many limitations in design and construction of the test piece. The limitations found that the new mould had to improve on included;

- Re-use – old method used cardboard and therefore had a finite mixture life, usually one use.

- Accuracy – the dimensional accuracy of the cardboard mould was poor and was rarely within the designed dimensional limits, there was also a difference between different percentages as moulds were made separately and non-reusable.

- Manufacture – should be easy to manufacture and accurate, the old mould was constructed with cardboard, scissors and glue using a difficult and inaccurate procedure.

As well as improving on the old design limitations, listed above, there were other requirements that the new mould needed to fulfil, theses were;

- Flexibility – be able to be used with a wide variety of composites (Epoxies, Vinyl Esters, and Phenolics) and also different post-curing methods (Microwaves and Ovens).

- Ease of use – the mould should be easy to assemble and disassemble without destroying both test piece and mould components.

- Strength – be strong enough to withstand the sometimes violent chemical reaction that occurs with certain composite mixtures and when mixtures are made poorly or inaccurately.

The above mould and specimen requirements meant that the mould needed to be made of a material that is strong, heat and microwave resistant, machineable, and able to obtain and maintain dimensional accuracy throughout its lifetime. The material selected was 6mm poly vinyl chloride (PVC) sheets which is a hard thermoplastic polymer material.

The design of the mould has a major bearing on the flexibility, ease of manufacture and ease of use. The mould was designed to ensure all the criteria were met and is pictured in Figure 6.1 and 6.2, below. Rubber bands will be used during casting to hold the mould tightly together. An AutoCAD draft of the mould that was used for construction can be viewed in Appendix C.

Side component placed in grooves in base component

Division components placed in machined grooves of corresponding side components

Base component with machined grooves
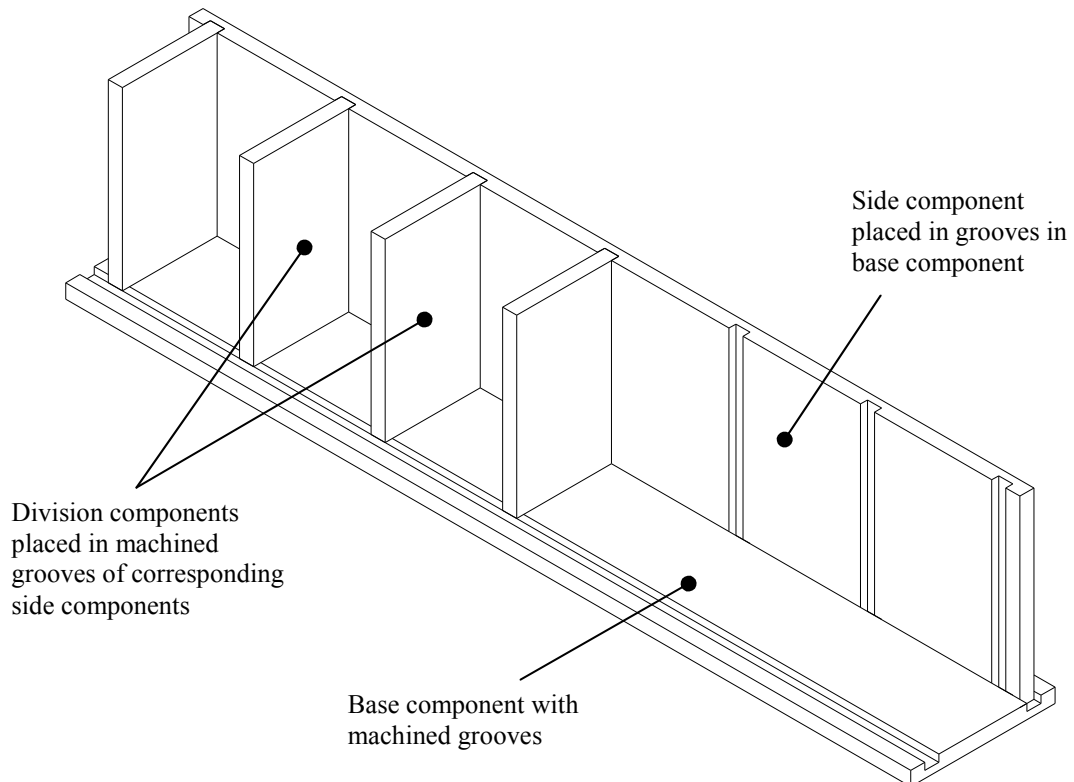
Figure 6.1: AutoCAD 2006 Isometric view of half assembled mould.

The design of the mould permits the grip groove and chevron slots to be created by various different methods, either during moulding or post moulding, depending on the users judgment. Methods in which the grip groove and chevron slot can be created include insertion of moulding components, like cardboard and plastic, or machining and cutting after curing. Because phenolics are generally brittle and hard to machine the method selected to create the grip grooves and chevron slots in this project was to incorporate them into the mould using the notch component. The assembled mould and the moulding notch component are shown in Figure 6.2.
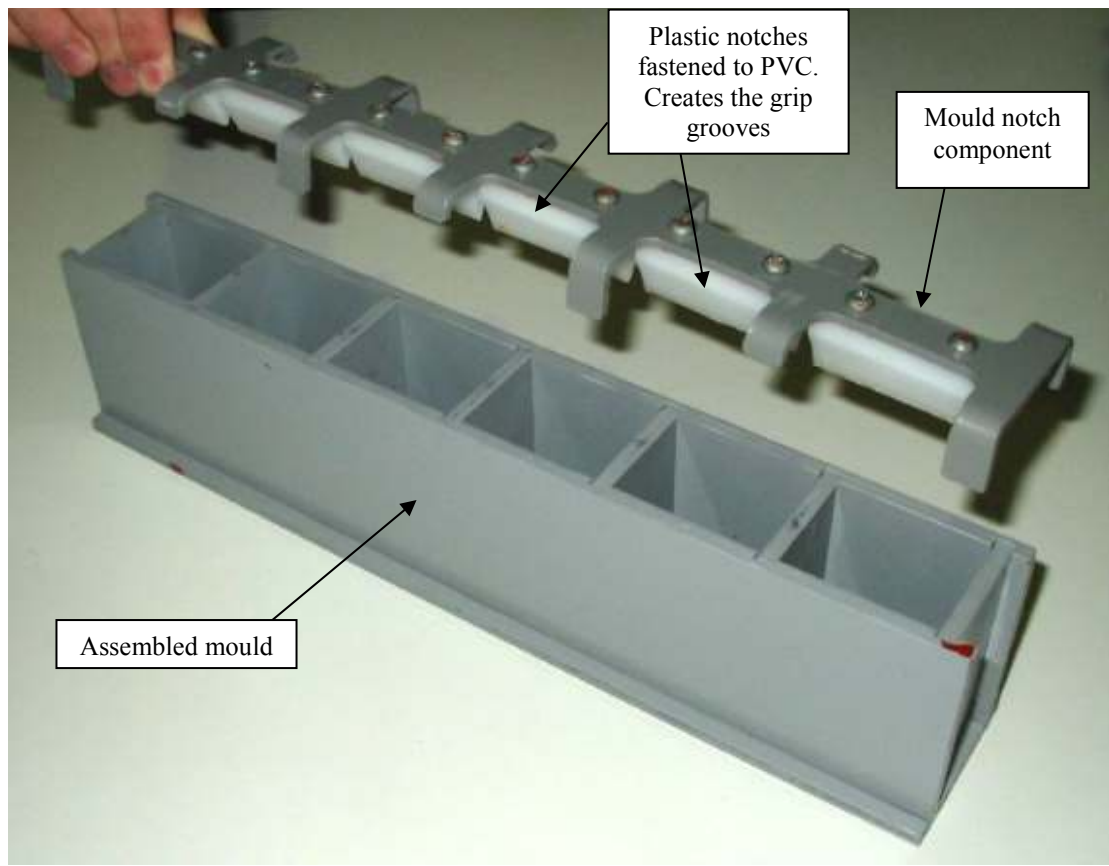
Figure 6.2: Assembled mould and notch component.

From Figure 6.2, the six notch mould components created from plastic and fastened in a line along a piece of 3mm thick PVC with 6mm spacings, can be seen. In this case the notches were fastened to the PVC with small metal screws. Depending on the curing method, microwaves or ovens, other fastening methods can be used such as plastic screws, to prevent arching, or even glue. The PVC in the notch component has been machined and shaped to allow for pouring of the composite and to clamp the mould together. The notch component guarantees that accurate grip grooves will be created repeatedly and with ease, thus each sample set will be almost exactly the same.

6.3   Mould Preparation

The steps carried out in the preparation of the mould are as follows;

Firstly, chevron slots were constructed from over-head projector transparency (OHT) plastic as it had desirable properties in that it was thin , approximately 0.15mm (Refer section 5.2.4), whilst still being strong.   The slot components were drafted in AutoCAD 2006 to the required size and then printed out onto OHT plastic sheets. Figure 6.3 depicts the A4 layout containing an optimum of fifteen chevron slots per page.   Creation of the chevron slots from OHT plastic sheets ensured greater dimensional accuracy and was a much faster technique than machining slots or hand drafting slot geometries onto cardboard.
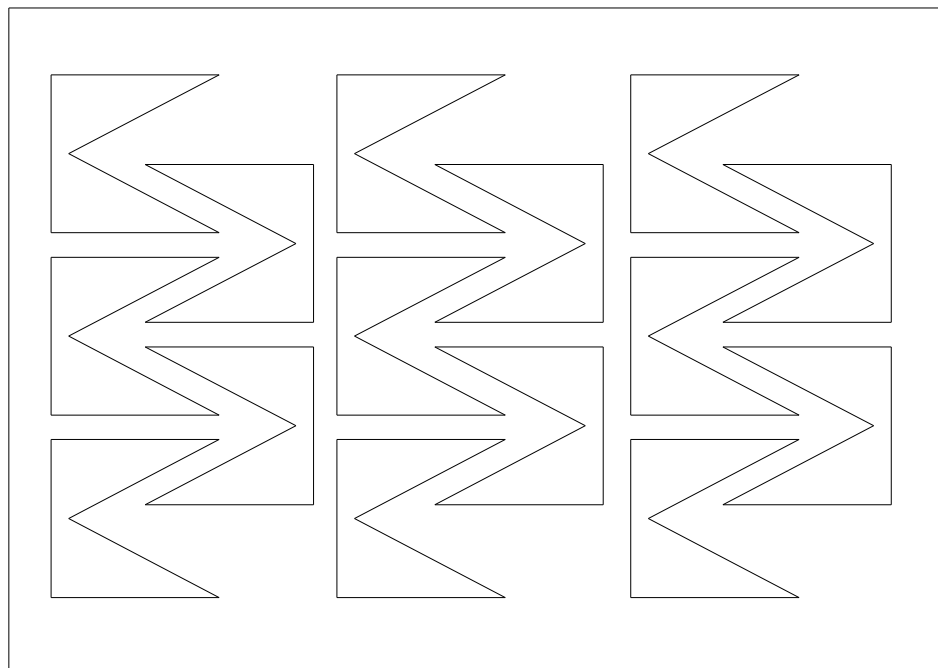
Figure 6.3: AutoCAD draft of chevron slot A4 layout that was printed onto over-head transparency paper.

The stiff plastic slots were then cut out carefully and sticky taped to the point of the mould notch component as shown in Figure 6.4.
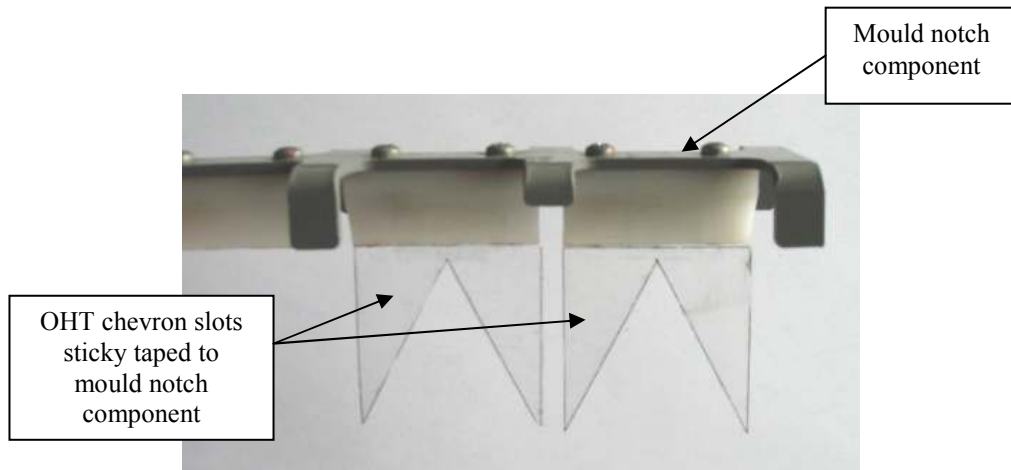
Figure 6.4: OHT chevron slots attached to mould notch component.

Secondly, the mould was built up from the designed components and the notch component was placed into the assembled mould. Rubber bands were placed at each division to make certain the mould would stay together during pouring and curing operations. The finished ready to pour mould can be seen in Figure 6.5, below.
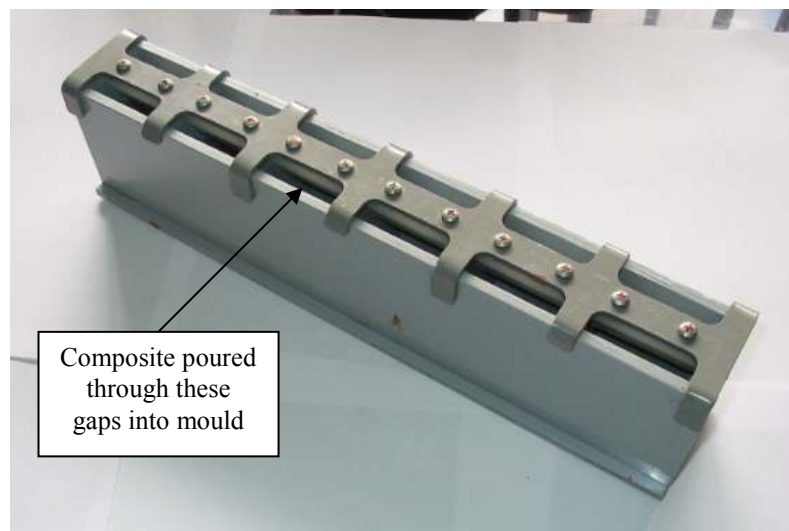
Figure 6.5: Assembled mould ready for pouring.

6.4   Composite Preparation

To determine the percentage test range of the specimens a few test mixes were conducted to determine the maximum amount of filler that can be practically added to the resin and mould. At 40% by weight it was found that the mixture was extremely hard to mix by hand and it was extremely viscous and therefore hard to pour into the mould before it began curing. From here it was decided that mixtures will be done in steps of 5% by weight up to approximately 35%. The aim of this project is partially cost based so the higher percentages of filler are desirable as the filler is the cheaper material. Therefore, the percentages to be tested were, 15%, 20%, 25%, 30% and 35% by weight. Previous USQ dissertations and other studies have found that the best mixture percentage of filler, for other composites, is approximately 33% or a third by volume.   20% by weight is, for phenolic resin and micro-spheres, 32.4% (approximately 33%) by volume. The 20% by weight mixture is therefore an expected important mixture for comparison.

The amount or volume of resin to be mixed needed to be determined and this was done by approximating the volume of the mould using the basic equation:

$$V = B \times W \times H \times n \qquad (6.1)$$

Where B, W, and H are specimen dimensions in (cm) from Figure B.2, and;

n is the number of specimens that the mould can produce.

The approximate volume of the mould from equation (6.1) is:

$$V \approx B \times W \times H \times n$$
$$\approx 5.0 \times 7.5 \times 4.75 \times 6$$
$$\approx 1068.75 cm^{3}$$

Since 1 g of water is 1 cm^{3}, by making 1000 g of resin mixture it would be almost ensured that for all percentage by weight mixtures there would be enough composite to fill the mould without running out because the resin is denser than water and it is also the major constituent. The mixtures below 40%, by weight of slg, will always be more

dense than water so therefore 1000 g is an over estimation and it is desirable to have some mixture left over than to run out halfway through and have an inconsistent sample of specimens.

The resin (Hexion Cellobond J2027L) is required to be mixed at a ratio of 20:1 of resin to catalyst (Hexion Phencat 15), respectively. A table of mixture constituents was derived for each mixture percentage based on this ratio and the 20% by weight mixture table is shown below, Table 6.1. The other mixture tables used can be found in Appendix D.

Table 6.1: Weight of materials required to make 1000 g of PF/SLG (20%).

	Materials	Resin (R)	Catalyst (C)	R + C	Slg	Composite
Parameters						
Percentage by weight		20	1	---	---	---
Percentage by weight		---	---	8	2	---
Weight of materials in 1000 g of PF/SLG (20%)		762 (g)	38 (g)	800 (g)	200 (g)	1000 (g)

Before any moulding or material handling could occur safety precautions needed to be made. Appropriate footwear, clothing, respirator and goggles were required to be worn throughout the process (refer section 1.2 for risk assessment). After safety was addressed the composite material was prepared and specimens moulded through the following process for each percentage;

    1.   Measure the specified amount of slg in grams (g) using the appropriate mixture table (Appendix D), scales and an ice-cream container.

    2.   Measure the specified amount resin in grams (g) using the appropriate mixture table (Appendix D), scales and an ice-cream container.

3.   Slowly pour the filler into the resin whilst mixing with a plastic spoon, ensuring a fully mixed paste.

4.   Add the indicated amount of catalyst using the appropriate mixture table (Appendix D) and a syringe. Then stir with spoon thoroughly in the exhaust cabinet to avoid toxic fumes.

5.   Spray the mould with cooking oil to avoid the specimen sticking and to make removal easier.

6.   Pour the mixture into the mould and let cure under the exhaust fan in the exhaust cabinet for approximately one day (overnight).

7.   Carefully remove the specimens from the mould and label the specimens by percentage and designate a specimen number (1-6) each.

The apparatus used in the above process is depicted in Figure 6.7.
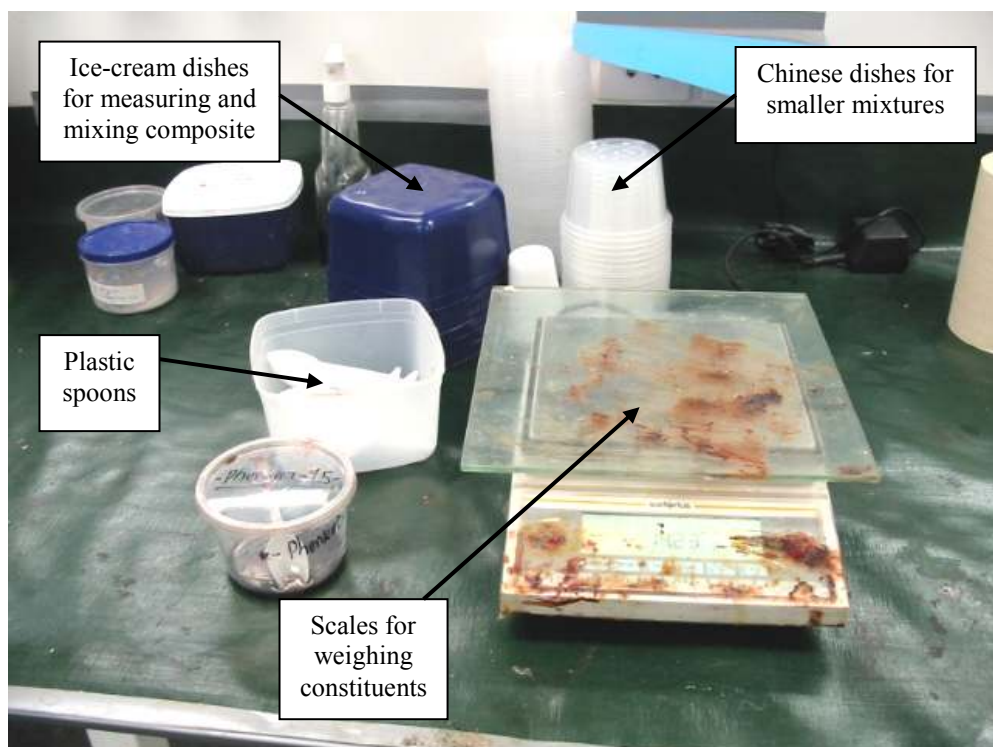
Figure 6.7: Apparatus used in the composite preparation process.

6.5   Viscosity Testing

Viscosity of the selected test percentages were measured at the Fibre Composite Design and Development Centre of Excellence using the Brookfield RDVD-II+ viscosity testing machine, Figure 6.8. Throughout the tests the viscosity was recorded at a constant temperature as the viscosity would be constantly changing due to the reaction taking place, this information was recorded in Table 6.2. Data was also recorded for a longer period of time for the 35% by weight mixture to determine the change in viscosity as a result of the chemical reaction taking place, Table 6.3.

Table 6.2: Data recorded from Brookfield RDVD-II+ viscosity testing machine

Percentage by weight of slg	Viscosity (cP)	Spindle No.	Temperature (°C)	R.P.M.
0	3240	6 (32.2%)	18.4	100
15	3760	6 (37.5%)	26.1	100
20	4550	7 (11.3%)	26.2	100
25	5680	7 (14%)	26.1	100
30	7900	7 (20.1%)	26.5	100
35	13360	7 (33.2%)	27.4	100

Table 6.3: Viscosity change of 35% mixture during reaction.

Temperature (°C)	Viscosity (cP)	Spindle No.	R.P.M.
27.4	13360	7 (33.2%)	100
28	12870	7 (30.6%)	100
29	11600	7 (28%)	100
29.6	10700	7 (25.7%)	100
30	10240	7 (24%)	100
31.7	9040	7 (22%)	100
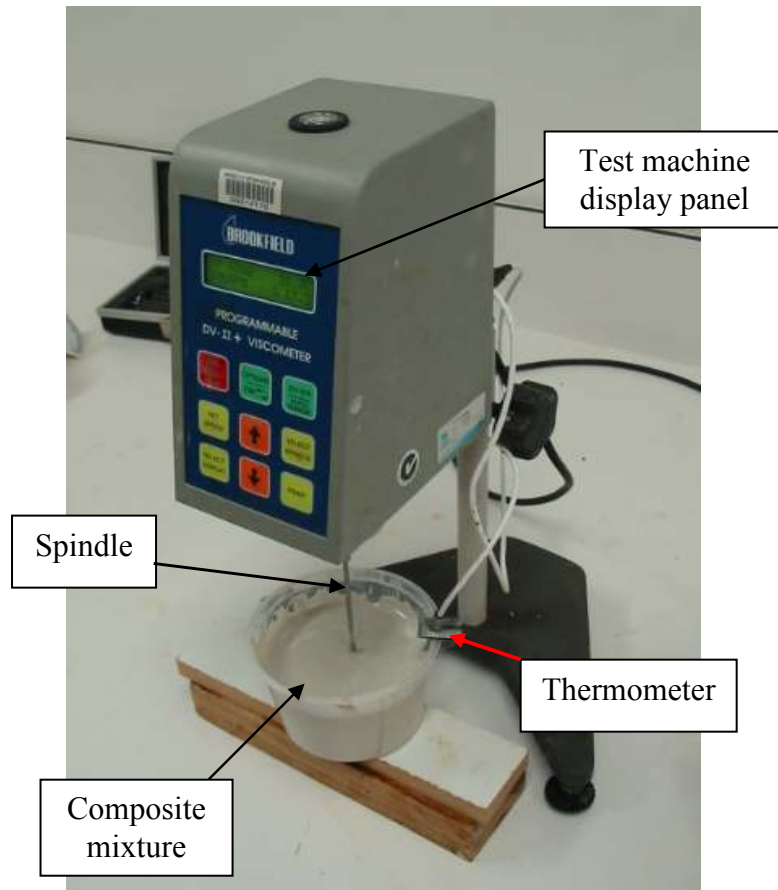
Figure 6.8: Brookfield RDVD – II+ Viscosity machine

Figure 6.9: Brookfield RDVD – II+ Viscosity testing spindles

Figure 6.9 shows the different spindles used in the testing machine. Large spindles are used for non-viscous liquids, while smaller spindles are used for very viscous liquids. When the percentage noted alongside the spindle number in both Tables 6.1 and 6.2 reaches around 40%, the spindle was required to be changed to a smaller one to ensure accuracy of viscosity measurements. Spindle numbers range from 1-7.

6.6   Oven Curing

After the specimens had cured in the mould overnight they were removed from the mould and placed in the ovens, shown in Figure 6.10, to help fully cross-link the polymer chains before testing. The ovens are model CE MLM and manufactured by, Ceramic Engineering Furnace Manufacturers, Sydney.

Figure 6.10: Oven furnaces used for post curing of specimens

The oven curing involved three (3) stages at different temperatures, these were;

> 4 hours at 50ºC
>
> 4 hours at 80ºC
>
> 2 hours at 100ºC

After the specimens were subject to the ten (10) hour post-curing cycle the specimens were observed to be darker in colour, grittier or more sandy and seemed to feel lighter, and look more brittle.

After completing the oven curing for all the different percentages the specimens were cleaned and finished ready for testing. Finishing involved the removal of excess resin

from the top surface where the composite would puddle as a result of the resin expanding slightly in the early stages of curing. This expansion was noted to cause porosity. The excess resin was simply filed back using a normal file. The specimens were then ready to be tested and this is outlined in chapter 7.

6.7   Problems During Methodology

Throughout the methodology various obstacles were encountered that could have had a potentially adverse effect on the result. Problems encountered are explained in the following sections.

6.7.1   Chevron Slots

It was observed that after the chevron slots were placed in the cast some did not fit perfectly and therefore had to be trimmed by scissors, whilst others were slightly too small and didn't quite go to the edge of the mould and specimen. Therefore when cast a small number of slots were not fully through to the edge of the specimens but buried by a small amount of composite. Figure 6.11 exaggerates the slot not touching the mould and therefore being buried under a small layer of composite.
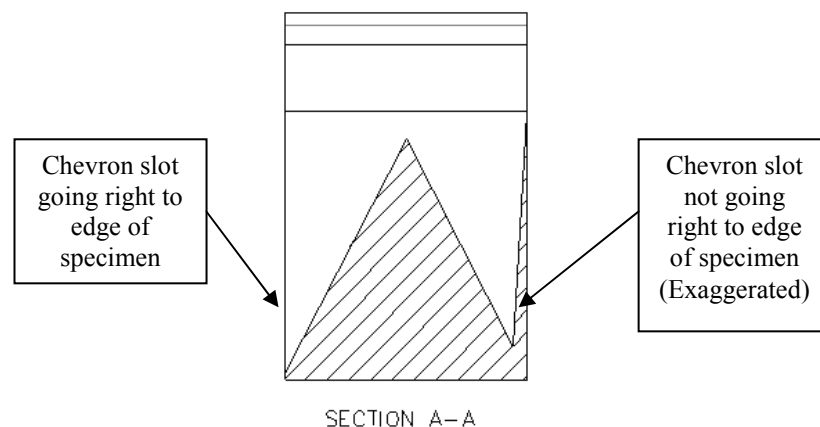
Figure 6.11: Section A-A, from Figure 5.1(a) of short bar geometry, showing a chevron slot not going right to edge of specimen.

After placing the specimens in the ovens for the ten (10) hour cycle, cracks appeared along the length of the specimen above where the slot should be protruding. These cracks completed the chevron slot right to the edge of the specimen and therefore would have a minimal effect on the fracture toughness measurements. Chevron slots that did not touch the edge of the specimen were therefore not a problem as first perceived. If this is believed to be a problem the slots could be machined at the expense of thicker slots and a lower plain-strain constraint, refer section 5.2.4 for slot geometries.

6.7.2   Composite mixture volatile reaction

It was noted that some percentage mixtures created a more violent curing, chemical reaction, than others which lead to a slightly higher porosity in some samples. The violent reactions are believed to be the result of in-exact measuring of composite constituents which is further exaggerated by the small size of the mixtures. The extremely violent reactions were re-mixed, as porosity was extremely high, to ensure that porosity as a result of violent cure had no effect on the results. A few test specimens were cracked to test if the porosity on the surface was any indication of the porosity in the centre of the sample. After cracking it was observed that the porosity on the surface of the specimen was not related to the porosity in the centre of the specimens with most cracked surfaces being extremely constant in porosity. Thus the effect on the final results would once again be minimal.

6.7.3   Oven Heat Variation

It was observed that whilst curing in the ovens the oven temperatures fluctuated dramatically about the set temperature. This fluctuation was because the ovens used are not overly accurate at lower temperatures. The ovens are recorded to perform best above temperatures of 400°C. The temperate effect this had on the specimens was as follows;

50°C cycle was at 65°C;

80°C cycle was at 95°C; and

100°C cycle was at 120°C.

There were two ovens used in the post-curing process, Figure 6.10, each with the capacity of approximately eight (8) specimens, depending on placement. Approximately sixteen (16) specimens could therefore be placed into ovens at a time. There was a total of thirty (30) specimens so another oven cycle, containing the remaining fourteen (14) specimens, needed to be conducted. After realising the first cycle temperatures were elevated it was decided that the second cycle be conducted in exactly the same manner to ensure curing was constant across all samples. This error in oven temperatures was therefore constant for all specimens so the results are comparable to one another thus the results are still valid in finding the best percentage by weight of micro-spheres as fillers in phenolic resins. The effect this may have had on the specimens is unknown but maybe they are more brittle than they would have become otherwise if the temperatures were exact. This may result in slightly lowered fracture toughness values.

Chapter 7

Testing and Apparatus

7.1   Testing System Requirements

There are many testing methods available for testing of short bar and rod specimens, the testing criteria that the selected testing method must fulfil is outlined in the following sub-sections.   These criteria ensure an improved and more accurate test result.

7.1.1   Test Machine Stiffness

Some materials exhibit an interesting behaviour called the, "pop in" effect.   This occurs when the load to initiate the crack at the point of the chevron slot is greater than the load during the test.   When "pop in" occurs a stiff testing machine is essential to ensure the mouth of the specimen continues opening at an almost constant rate as the load decreases due to crack propagation.   If the testing machine is not stiff enough the mouth opening of the specimen will increase in response to a load drop by means of additional elastic energy.   This is an undesirable effect and will invalidate the test results as the crack may propagate through the entire specimen catastrophically (Barker 1981).

Figure 7.1 displays "Pop in" and what occurs with two different testing machine characteristics.
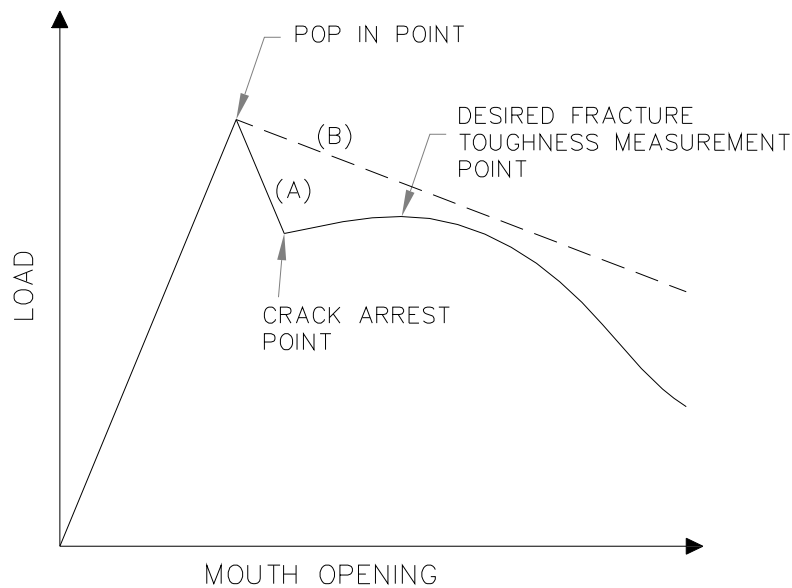
Figure 7.1: Effect of test machine stiffness.

In Figure 7.1 a sufficiently stiff testing machine (A) allows crack arrest, after pop in occurs, and therefore leads to an accurate fracture toughness measurement. A soft or un-stiff machine (B) maintains more load and this causes the crack to run through the entire specimen catastrophically leading to inaccurate fracture toughness results.

7.1.2   Load-Line Deviation

For accurate and repeatable tests, the specimens must be placed in the testing machine so the opening load is applied along the intended load-line which is shown in Figure 5.1(a). Variation in the load line position can cause invalid results due to ambiguities in the specimen calibration, as it is a function of load location, and therefore it is desirable that the position of the load does not change during the test (Barker 1981). Flexing of the specimen can significantly change the position of load application however with brittle materials this is not an extreme problem as elongation is minimal before crack propagation.

7.1.3   Friction

Friction between the load transducer and the specimen and also friction resulting from flexure of the specimen during the test can effect on the accuracy of the results. Any system for accurate testing must minimise any adverse friction effects (Barker 1981).

7.1.4   Plastic Deformation

Plastic deformation where the loading mechanism comes in contact with the test specimen must be minimised.   Plastic deformation can have unwanted effects if present at the load lines. These effects include increased friction, as specimen flexure occurs, and a change in the position of the load lines. The deformation itself can also produce inaccurate test results. The mechanism for applying the load to the specimen load lines must therefore be carefully designed to minimise plastic deformation thus producing a more accurate result (Barker 1981).

7.2   Short Rod and Bar Testing Methods

There are a few test methods available for testing the fracture toughness of short rod and short bar test specimens. All of which meet the above testing system requirements adequately. These tests are outlined in the following section.

7.2.1   Fracjack Testing Mechanism

The Fracjack loading mechanism is a successful short rod test configuration that meets the entire short rod testing system requirements listed above. The fracjack short rod testing system can be seen in Figure 7.2.
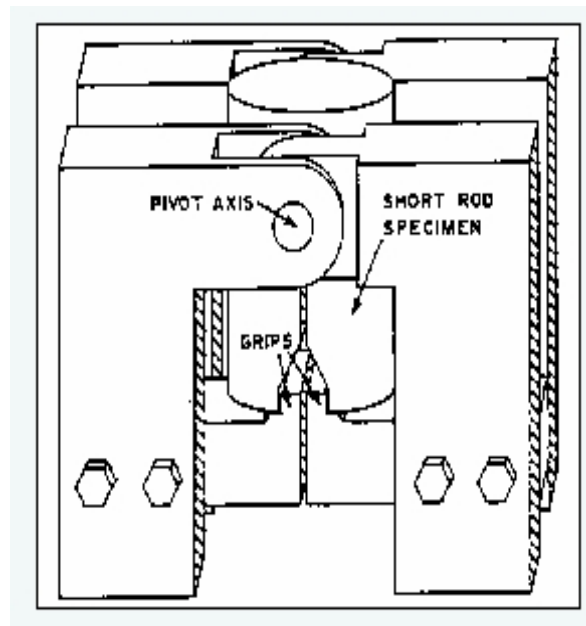
Figure 7.2: Fracjack Short Rod Fracture Toughness Test System.

The fracjack is a specimen loading mechanism that converts a load applied by the tensile test machine to an opening load at the load line of the specimen. Plastic and metal materials usually have high fracture toughness and therefore need a large load (50kN) which can be obtained accurately using this testing method. Other properties of the Fracjack testing mechanism include;

- Specimen installation and alignment is extremely accurate and easy.

- A wide variety of materials can be successfully tested.

- It has the added attribute of being able to control the specimens' temperature throughout the duration of the test.

7.2.2   Flatjack Testing Mechanism

The flatjack test method applies an opening load to the chevron-notched specimen mouth using an inflatable ultra-thin bladder shown in Figure 7.3. The bladder is inserted into the mouth of the specimen and pressure is applied to the fluid in the bladder causing fracture to initiate at the chevron tip. Stable crack growth can be controlled by increasing the applied pressure on the fluid.
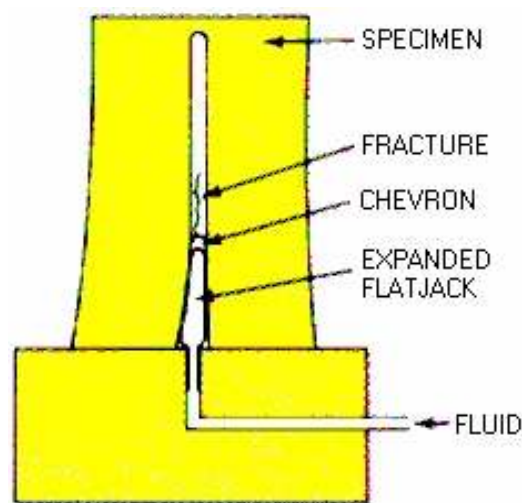
Figure 7.3: Flatjack testing mechanism.

An advantage of the flatjack method is that the load line does not need to be specifically defined. A major disadvantage of this testing method is that it is limited to materials with low fracture toughness and high elastic module, and brittle materials, such as ceramics and glasses.

7.2.3   Modified MTS 810 Material Testing System

The MTS 810 Material Testing System, located at the Faculty of Engineering and Surveying, at the University of Southern Queensland (USQ), has been used to conduct fracture toughness tests on short bar specimens for a range of different materials. A tensile force is applied to the load line of the specimen using grippers and a high

tensile bolt mechanism that has been specifically designed by Phelan (1990) for this purpose.

The MTS 810 Material Testing System is comprised of a Load Unit connected to a series of digital controllers and remote stations.   The major components of the MTS 810 Load Unit are shown in Figure 7.4, below, and Figure 7.5 shows the total operating system setup controls the testing and records data.

Crosshead
►Designed for a high natural frequency.
►High stiffness for precise displacement measurement and increased dynamic performance.

Grips and fixtures (optional)
►The largest variety of hydraulic and mechanical grips and loading fixtures are available from MTS.

Grip controls (optional)
►Provide fingertip control of hydraulic grips and clamping pressure.

Columns
►Solid steel for high stiffness and chrome plated for long life and easy cleaning.
►Precision machining maintains load unit alignment over their entire length.

Alignment fixture (optional)
►Precise load train alignment in minutes.

Force transducers
►Strain gage design is accurate for both static and dynamic testing.
►Many force ratings are available to meet your specific needs.

Load unit control module
►Puts control of the hydraulic lifts and locks for repositioning the crosshead at a convenient location.
►Emergency stop shuts off hydraulics.

Isolator pads

Figure 7.4: The MTS 810 Load Unit (MTS 810 FlexTest™ Material Testing Systems).
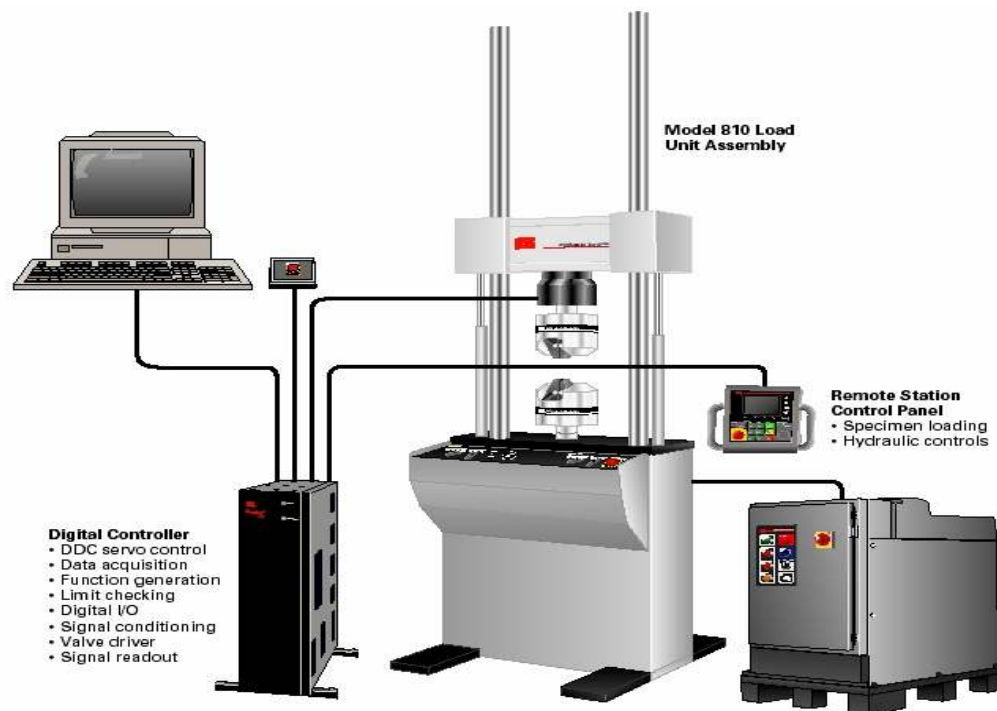
Figure 7.5: The operating system layout of the MTS 810 Material Testing

Systems (MTS 810 Material Testing Systems, 2003).

The MTS 810 Material Testing System has many advantages including;

- Flexible – Different tests can be conducted by changing and adjusting
  components. Tensile tests, fatigue tests and soil test are some of the tests that
  can be conducted.

- Accurate – The low weight crosshead and integrated force transducer design
  ensures that superior axial and lateral stiffness is achieved.

- User-friendly – The integration of the load unit with software, a digital
  controller, and a remote station control panel makes conducting tests simple
  and efficient. Comprehensive graphs and tables can be created for individual
  specimens and also for an array of samples. Means and standard deviations are
  also calculated in the result.

7.3   MTS 810 Short Bar Testing

The MTS 810 Material Testing System was selected to conduct the short bar fracture toughness tests in this project because of its availability, flexibility and accuracy. The modified MTS 810 Material Testing System meets all the testing machine requirements as outlined in section 7.1. A test being conducted using the MTS 810 system and the modified grippers can be seen in Figure 7.6, below. A tensile force is applied to the mouth of the specimen using the grippers until failure occurs.
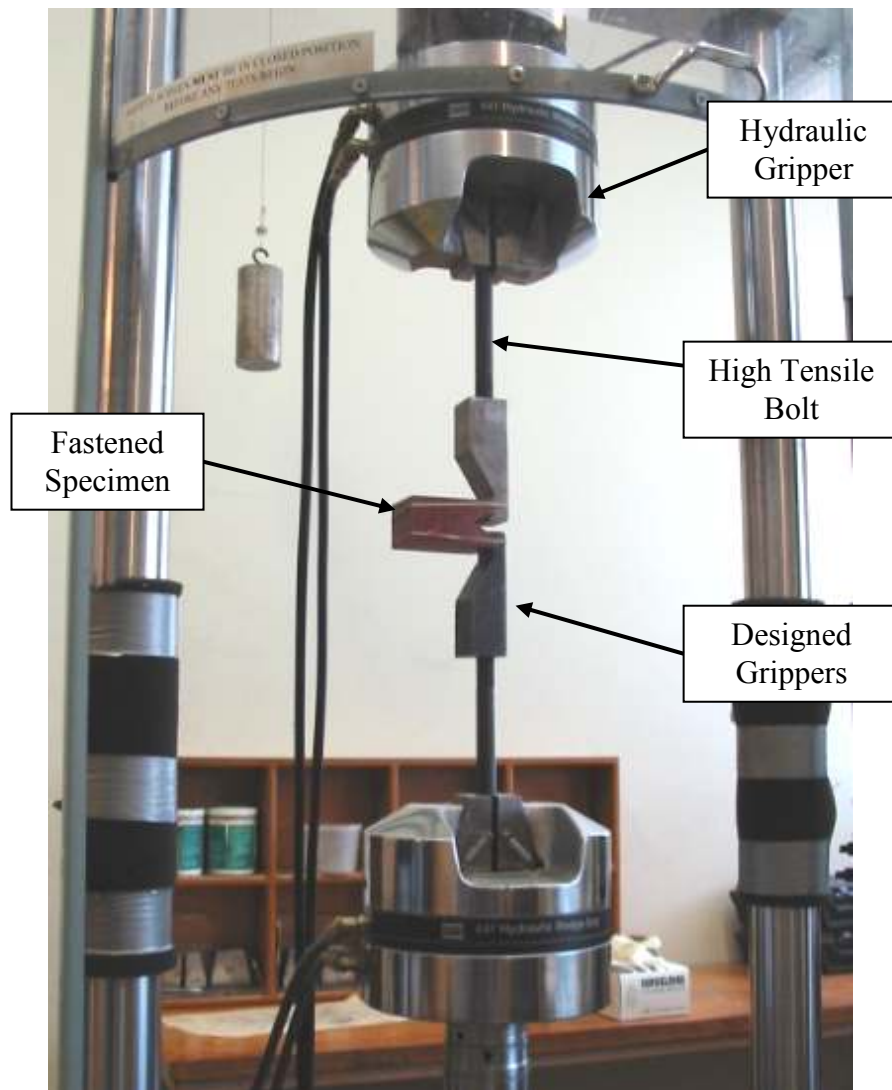
Figure 7.6: Test being conducted on a short bar specimen using the MTS 810 Material Testing System.

7.3.1   Gripper Selection

Phelan (1990) designed a set of grippers for short bar testing to be used with the Instron Universal Testing Machine. The grippers fulfil all requirements in section 7.1 and have been tested to withstand a load of up to 50 KN. Because of the similarities between the Instron Universal Testing Machine and the MTS 810 Material Testing System only a small modification was required for the grippers to be used. As can be seen in Figure 7.6, the grippers are attached to the end of a high tensile bolt which is held by the MTS 810 Load Units hydraulic grippers. A closer detail of the grippers can be seen in Figure 7.7.

Figure 7.7: Grippers used in MTS 810 Material Testing System

Specimens were mounted to the grippers selected using two rubber bands to pull the specimen against the grippers and ensure the load line does not deviate during the test.

7.3.2   Testing Results

After the MTS 810 Material Testing System had finished testing the specimen the results could be easily accessed and printed. A graph and corresponding list of results is shown in Figure 7.8 and the graphs and results for all specimens can be found in Appendix E.

Sample ID: robert20-1.mss
Specimen Number: 1
Tagged: False

Load (N)

Extension (mm)

Specimen Results:

Name	Value	Units
Thickness	50.000	mm
Width	30.000	mm
Area	1500	mm^2
Peak Load	356 N	
Peak Stress	0.24	MPa
Break Load	356 N	
Break Stress	0.24	MPa
Elongation At Break	0.482	mm
Stress At Offset Yield	0.181	MPa
Load At Offset Yield	271.679	N
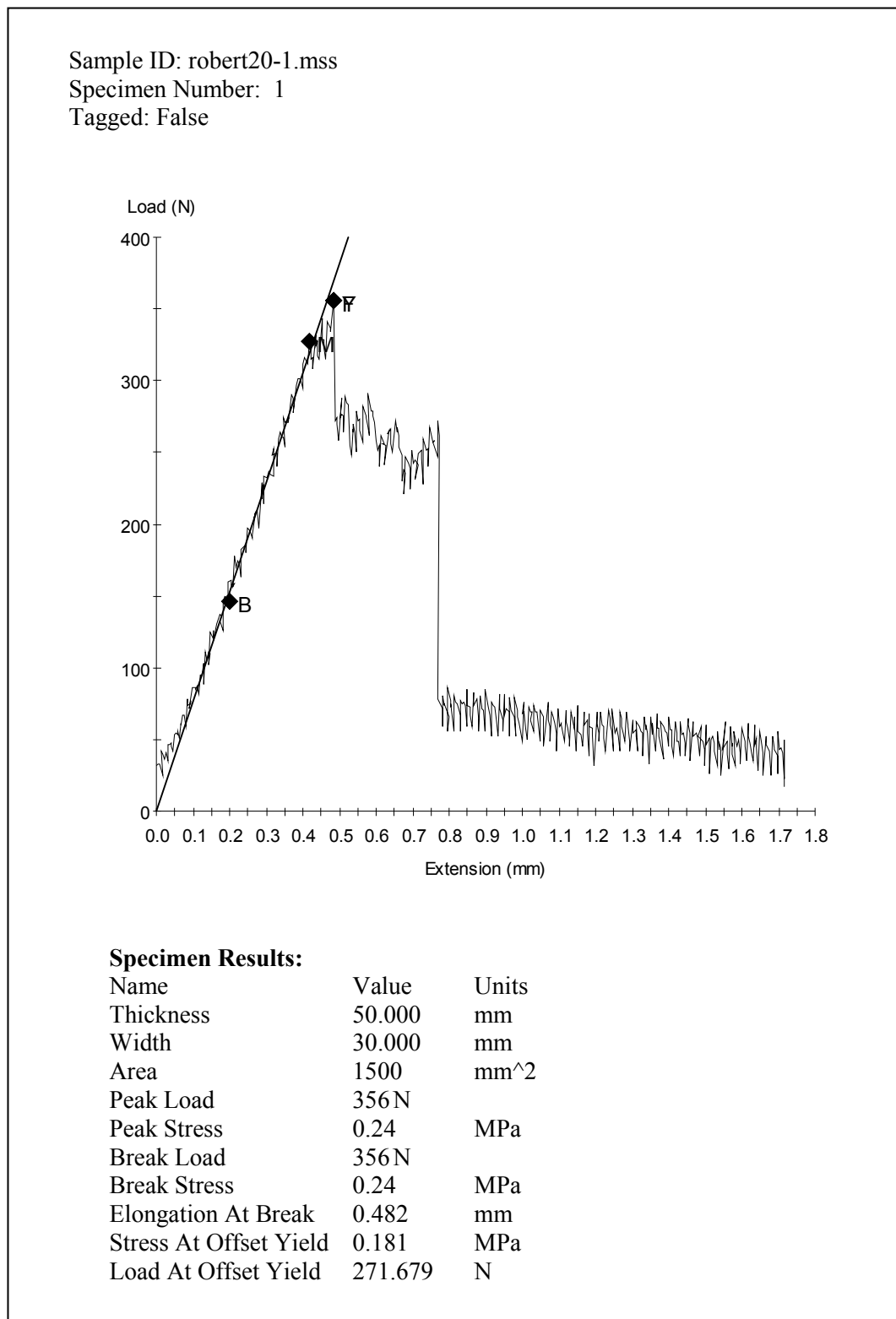
Figure 7.8: Results printout from the MTS 810 Material Testing System for a 20% by weight of filler specimen.

From Figure 7.8 the Peak Load is recorded and is used in the process outlined in section 5.3 to calculate the fracture toughness of each specimen. Appendix F, Table

F.1 contains the calculated fracture toughness results, the means and also the standard deviations associated with each different percentage by weight of filler sample set, are also calculated.

After the specimens have been tested you can clearly see the effect that the chevron slots had on crack propagation. Figure 7.9 displays a series of broken test specimens and their brittle fracture surface.

Figure 7.9: Tested specimens in half.

The measurements, as per Figure 5.7, of the tested specimens were then recorded using electronic vernier callipers, as in Figure 7.10. The measurements are contained in Table F.1 of Appendix F.
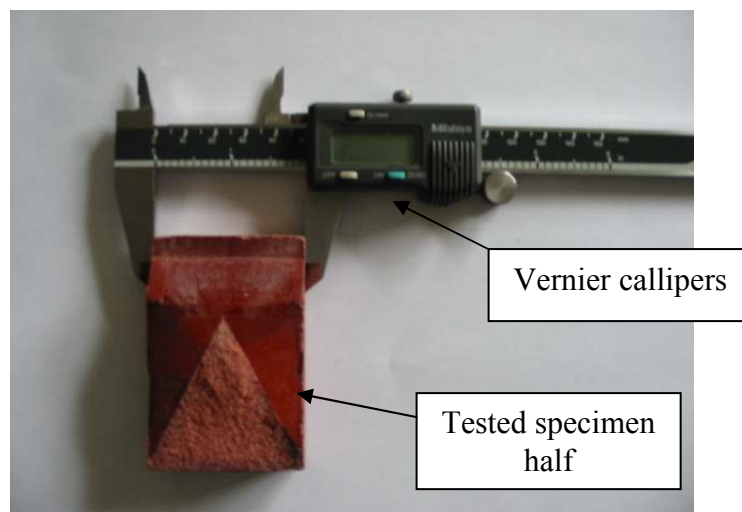
Figure 7.10: Measurements of tested specimen being recorded.

Chapter 8

Results and Discussion

8.1 Fracture Toughness

Using equations 5.1 to 5.5, from Chapter 5, the fracture toughness was calculated by the following procedure;

Specimen 1 of the 20% by weight mixture has been selected for this example.

Table 8.1 shows the actual geometry measurements of the created, 20% by weight of filler, specimen.

Table 8.1: Measured geometry of 20% by weight of filler specimens.

Specimen Number	$W^{\#}$	H	$a_0^{\#}$	$a_1^{\#}$
1	*73.2*	*43.8*	*22.7*	*70.9*
2	72.9	43.81	23.45	70.9
3	72.8	43.6	23.39	70.9
4	72.84	43.8	23.3	69.06
5	73.32	43.7	23.32	70.9
6	73.2	43.9	22.9	70.9

\# Derived from Table F.1 in Appendix F.
\# See Figure 5.7 for measurement explanations.

Using the measured values from Table 8.1 for specimen number 1 along with equations 5.3, 5.4, 5.5, respectively:

$$\omega = \frac{W}{H} = \frac{73.2}{43.8} = 1.671$$

$$\alpha_0 = \frac{a_0}{W} = \frac{22.7}{73.2} = 0.310$$

$$\alpha_1 = \frac{a_1}{W} = \frac{70.9}{73.2} = 0.969$$

The compliance calibration, Y_m^*, for the short bar test method for this specimen using equation 5.2 is as follows:

$$Y_m^* = \{ -0.36 + 5.48\omega + 0.08\omega^2 + (30.56 - 27.49\omega + 7.46\omega)\alpha_0$$
$$+ (65.90 + 18.44\omega - 9.7\omega)\alpha_0^2 \} \left\{ \frac{\alpha_1 - \alpha_0}{1 - \alpha_0} \right\}^{\frac{1}{2}} = 15.7002$$

Also, $B = 50$ (by design), and $F_{max} = 356N$ (from MTS 810 Results in Appendix E)

Fracture toughness from, equation 5.1, is calculated as:

$$F_{ICSB} = \frac{(356 \times 15.7002)}{50\sqrt{73.2}} = 13.07 \text{ MPa}\sqrt{\text{m}}$$

All values of fracture toughness have been calculated following the above process and are averaged and tabulated in table 8.2.

Table 8.2: Fracture toughness of PF/E-SPHERES.

Percentage by weight of slg (%)	15	20	25	30	35
Fracture toughness (MPa$\sqrt{m}$)	10.5* (0.80)#	12.5 (0.16)	9.62 (0.24)	8.82 (0.36)	8.12 (0.67)

* Average of all six specimens fracture toughness from Table G.1, Appendix G.
# standard deviation

Table 8.2 depicts the average fracture toughness PF/E-SPHERES with varying percentage by weight of slg, with the standard deviation given in bracket. As the standard deviation is small, it can be argued that the values of fracture toughness obtained are reliable.

Figure 8.1 is a plot of Table 8.2, the fracture toughness PF/E-SPHERES with varying percentage by weight of slg. It can be observed that the fracture toughness is highest when the percentage by weight of the filler, E-Spheres, is 20 %.
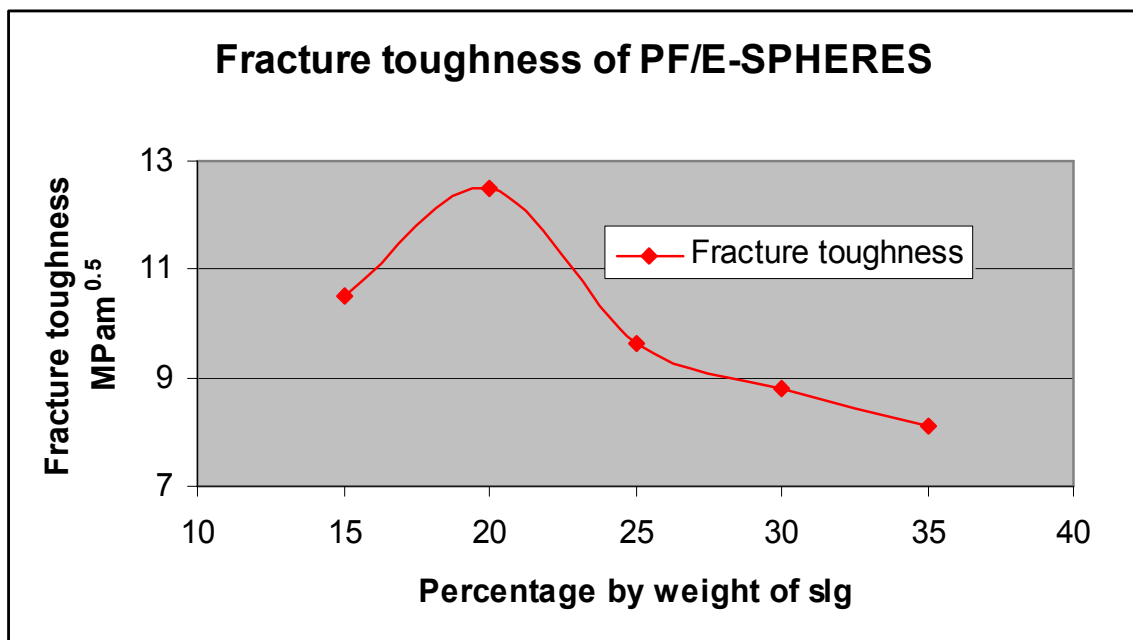
Figure 8.1: Fracture toughness of PF-E-SPHERES with varying percentage by weight

of slg.

The values of fracture toughness obtained are also very high and encouraging. Redjel (1995) recorded the fracture toughness of pure phenolic resin was 1.51 MPa$\sqrt{m}$; the fracture toughness of 20 percent by weight of slg reinforced phenolic resin, PF/E-SHPERES (20%), was averaged to be 12.5 MPa$\sqrt{m}$, which is 8.28 times the fracture toughness of pure phenolic resin, an increase of 728%.

8.2 Viscosity

A plot of the viscosity measured against the percentage by weight of filler was plotted and can be found in Figure 8.2 and the raw recorded data can be found in Table 6.1.
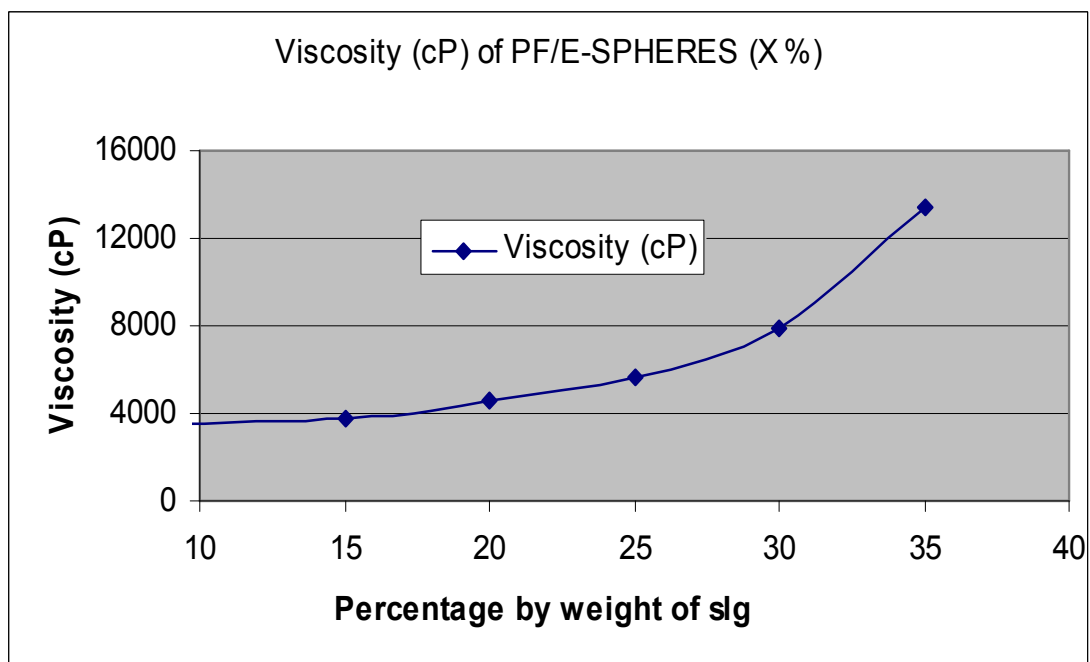
Figure 8.2: Viscosity of various composite mixtures at approximately 26°C.

It can be found that the viscosity increases with increasing percentage by weight of filler. At 35 % by weight of filler, the viscosity was recorded to be 13,360 cP, at which the composite was still fluid enough to be cast into moulds. However, at 40% by weight of filler, the composite was discovered to be too viscous for moulding; by extrapolation, its viscosity would be approximately 19,400 cP, which is very near to

the viscosity value (19,210 cP) that Davey et al. (2005) obtained when his composite mixture was also was also 40 % by weight of filler. It can be argued that the maximum percentage by weight of E-Spheres that can be present in the composite, while the composite is still fluid enough for casting would be around 37.5 %, at which its viscosity would be 16,600 cP. Since for maximum fracture toughness, the allowable percentage of filler in the composite was 20 %, at which the viscosity was 3,140 cP; there would be no fluidity problem for this percentage by weight of E-Spheres in the composite.

Chapter 9

Conclusion

The project has proved that by adding 20 % by weight of E-Spheres as filler to phenolic resin, the fracture toughness of the composite is 8.28 times of that of the pure resin. It has also proved that 20 % by weight of E-Spheres is the most suitable amount of filler to add to achieve maximum fracture toughness. Also at this percentage there is no fluidity problem for casting the composite into moulds.

References

Askeland, D R, The science and engineering of materials, Fourth Edition, Stanley Thornes, 1999, pp.163-164.

ASTM, Standard test method for impact resistance of plastic and electrical insulating materials, 1990, ASTM D256-288.

Astrom, B T, Manufacturing of polymer composites, Chapman and Hall, 1997, pp.74-83, 432-4.

Baddeley, D T and Ballard J, 1991, *Evaluate the Short Rod/Bar Fracture Mechanics Test*, BEng Thesis of Jennine Ballard, School of Mechanical and Manufacturing Engineering, Queensland University of Technology,

Barker, L M, Fracture mechanics applied to brittle materials, ASTM, STP 678, American Society for Testing and Materials, 1979, pp.73-82.

Baker, L M, Development of the short rod method of fracture toughness measurement, Proceedings, Conference on Wear and Fracture Prevention, 21-22 May 1980, ASM, Metals Park, Ohio, pp. 163-180.

Baker, L M, Short rod and short bar fracture toughness specimen geometries and test methods for metallic materials, Proceedings, Fracture Mechanics: Thirteenth Conference, ASMT STP 743, 1981, pp. 456-475.

Bolton, W, 1996, *Materials and Their Uses*, Butterworth and Heinemann, pp. 128-130.

Budinski, K G, Engineering materials, properties and selection, 4th edition, Prentice-Hall, 1992, pp. 32, 87, 231-3.

Callister, W D, Materials science and engineering: an introduction, 7th Ed., John Wiley and Sons, Inc., 2006, pp. 201-203.

Chemwatch, Material safety data sheet for Hexion Cellobond J2027L, 2005a, pp. 1-14.

Chemwatch, Material safety data sheet for Hexion Phencat 15, 2005b, pp. 1-14.

Clarke, J L (Editor), Structural design of polymer composites, E & FN Spon, U.K., 1996, pp.59-62, 343-5, 357.

E-spheres, www.envirospheres.com.au, Envirospheres Pty Ltd., P O Box 497, NSW 2070, Australia, undated.

Gottfried, W. E, Polymeric Materials – structure, properties, applications, Hanser, 2001.

Halloway, L., Handbook of polymer composites for engineers, Woodhead publishing, 1994.

Ku, H S, Baddeley, D, Snook, C and Chew, C. S., Fracture Toughness of Vinyl Ester Composites Cured by Microwave Irradiation: Preliminary Results, Journal of Reinforced Plastics and Composites, Vol. 24, No. 11/2005, pp. 1181-1201.

Matthews, F L and Rawlings, R.D, 1994, *Composite Materials: Engineering and Science*, 1st edn, Chapman and Hall, United Kingdom.

Morgan, M J, Engineering materials - Study Book 1, University of Southern Queensland, 2006, p. 9.13.

Munz, D, Determination of Fracture Toughness of High Strength Aluminum Alloys with Cheron Notched Short Rod and Short Bar Specimens, Engineering Fracture Mechanics, Vol. 15, No. 1-2, 1981, pp. 231-236.

Osswald, T A and Menges, G, 1995, *Materials Science of Polymers for Engineers,* Hanser Publishers, New York.
Peters, S T, 1998, *Handbook of Composites*, Chapman and Hall, United Kingdom.

Pritchard, G, 1999, *Reinforced Pastics Drability*, Woodhead publishing Ltd., United Kingdom.

Redjel, B, Mechanical Properties and Fracture Toughness of Phenolic Resin, Plastics, Rubber and Composites Processing and Applications, 1995, Vol. 24, pp. 221-228.

Shackelford, J F, Introduction to materials science for engineers, 3rd edition, Macmillan, 1992, pp.435-437.

Smith, W F and Hashemir, J, Foundations of material science and engineering, 4th edition, McGraw-Hill, 2006, pp. 523-525.

Strong, A B, Plastics: materials and processing, 3rd edition, Pearson/Prentice-Hall, 2006, pp. 182-183, 304-309, 323-333, 620-621.

Swallowe, G M, Mechanical properties and testing of polymers, Vol. 3, Kluwer, 1999.

Appendix A

Project Specification

University of Southern Queensland
Faculty of Engineering and Surveying

ENG 4111/4112 Research Project
PROJECT SPECIFICATION

Project title: **Investigation of the best percentage by weight**
                                        of microspheres as fillers, in phenolic resins.

Student: Robert Davey - 0050010155

Supervisor: Dr. Harry Ku

Project Synopsis:

The project involves the production of a range of phenolic resin specimens with
different percentage by weight of fillers. Tests will be conducted on the specimens to
evaluate the fracture toughness. Findings will be analysed in detail in order to
establish behavioural trends and formulas that can be used for theoretical prediction of
filled polymer behaviour.

Timeline:

1. Familiarization of equipment and literature reviews.

    Begin   : 6th March 2006
    Completion   : 20th March 2006
    Approx. Hours   : 30 hours

2. Design and manufacture of a cast/mould for short bar tests.

    Begin   : 20th March 2006
    Completion   : 3rd April 2006
    Approx. Hours   : 20 hours

3. Casting Components.

    Begin   : 4th April 2006
    Completion   : 7th April 2006
    Approx. Hours   : 15 hours

4. Preform fracture toughness test and examination of specimens.

    Begin   : 10th April 2006
    Completion   : 8th May 2006
    Approx. Hours   : 40 hours

5. Analysis of results.

    Begin   : 8th May 2006
    Completion   : 26th June 2006
    Approx. Hours   : 50 hours

6. Draw up conclusions.

    Begin   : 26th June 2006
    Completion   : 31st July 2006
    Approx. Hours   : 40 hours

7. Discussion for the thesis outline with supervisors.

    Begin   : 14th August 2006
    Completion   : 24th August 2006
    Approx. Hours   : 10 hours

8. Thesis initial drafting – each chapter in draft form and shown to supervisors so
    that the thesis can be read by 9th October 2006.
    Begin   : 24th August 2006
    Completion   : 9th October 2006
    Approx. Hours   : 70 hours

9. Final draft of thesis, to incorporate modifications suggested by supervisor.

    Begin   : 9th October 2006
    Completion   : 20th October 2006
    Approx. Hours   : 10 hours

10. Complete the thesis in requested format.

    Begin   : 20th October 2006
    Completion   : 2nd November 2006
    Approx. Hours   : 20 hours

As time permits:

11. Software package analysis.

AGREED:

_____ (Student)   _____ (Supervisor)

(Date) ___ / ___ / ___

Appendix B

Specimen Dimensions

After the short bar geometry was selected a size for the specimens needed to be selected. The following pages shows a picture of the short bar geometry, Figure B.1, and also the resulting dimensions of the specimens when a size of B = 50mm was selected, Figure B.2.

SHORT BAR GEOMETRY

Figure B.1: The selected geometry of specimens. (Barker 1981, p. 457)
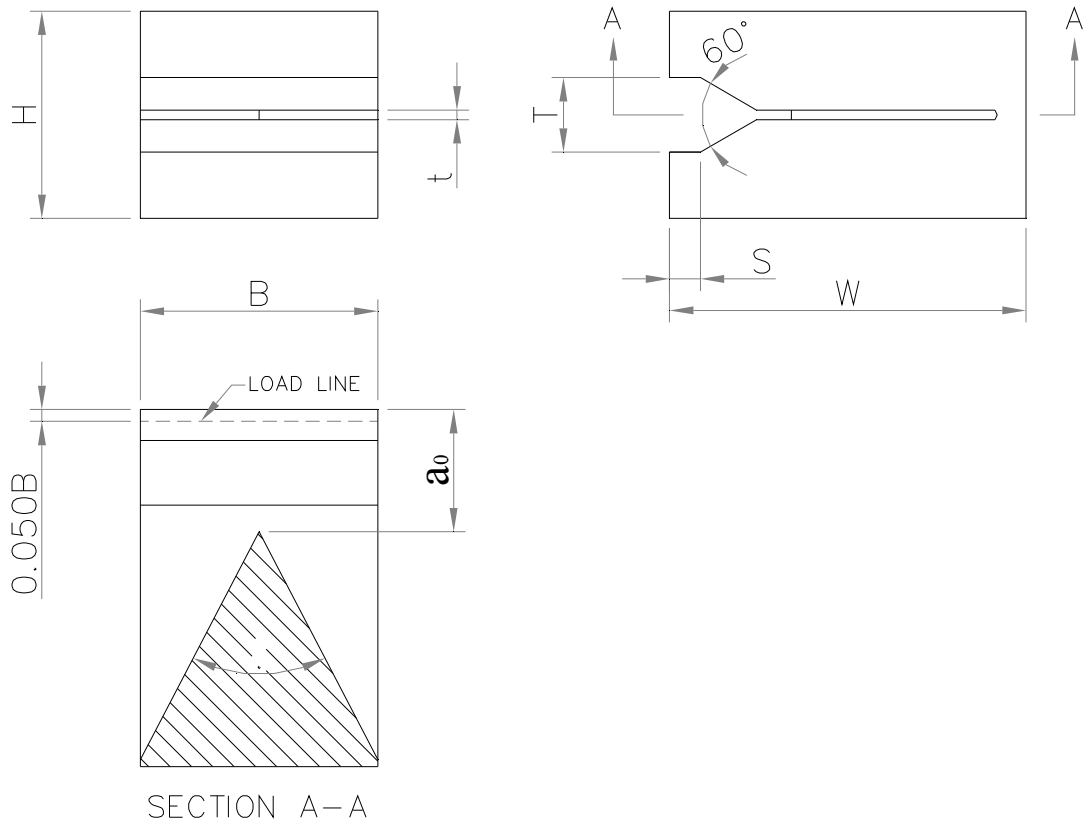
SYMBOL	DEFINITION	VALUE	TOLERANCE
B	BREADTH	B = 50mm	
W	LENGTH	1.5B	$\pm$ .010B
H	HEIGHT	.870B	$\pm$ .005B
a_0	INITIAL CRACK LENGTH	.513B	$\pm$ .005B
θ	SLOT ANGLE	55.2°	$\pm$ 1/2°
t	SLOT THICKNESS	SEE TABLE III (of Barker, 1981)	
S	GRIP GROOVE DEPTH	.130B	$\pm$ .010B
T	GRIP GROOVE WIDTH	.313B	$\pm$ .005B
R	RADIUS OF SLOT CUT	SEE FIG 4 (of Barker, 1981)	$\pm$2.5B

SECTION A–A
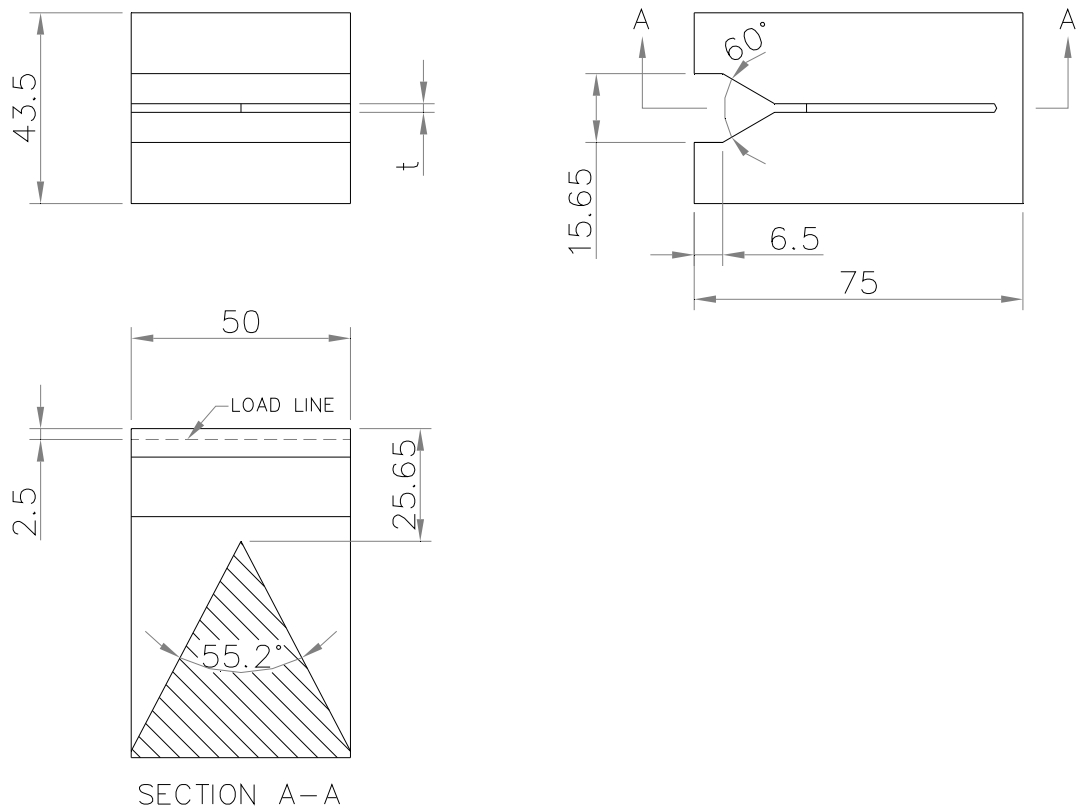
SYMBOL	DEFINITION	VALUE (mm)	TOLERANCE
B	BREADTH	B = 50	
W	LENGTH	75	± .010B
H	HEIGHT	43.5	± .005B
a_0	INITIAL CRACK LENGTH	25.65	± .005B
θ	SLOT ANGLE	55.2°	± 1/2°
t	SLOT THICKNESS	0.15	
S	GRIP GROOVE DEPTH	6.5	± .010B
T	GRIP GROOVE WIDTH	15.65	± .005B

Figure B.2: The dimensions of the specimens using geometry in Figure B.1.

Appendix C

Mould Design

The following page is an A3 draft of the specimen mould that was used for construction purposes.

3 | 4 | 5 | 6 | 7 | 8 | 9 | 10

354

TOP VIEW

6mmx3mm DEEP
MACHINED GROOVES

3
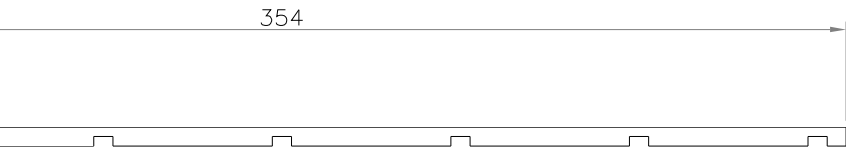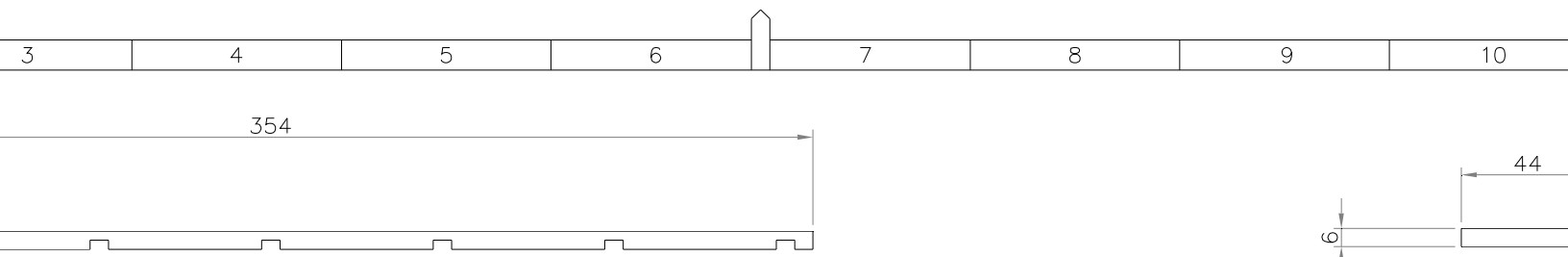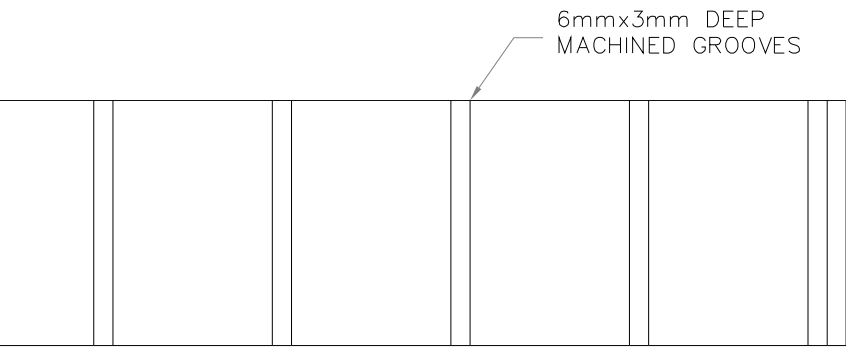
FRONT VIEW

END VIEW

SIDES
TWO (2) REQUIRED

44

6

TOP VIEW

49.5

75
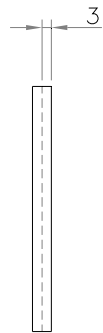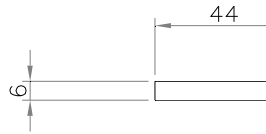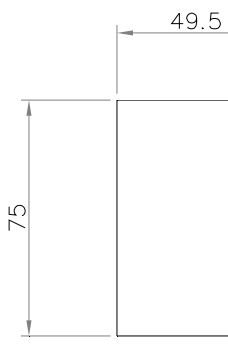
FRONT VIEW

DIVISIONS
SEVEN (7) REQ

6mmx3mm DEEP
MACHINED GROOVES

TOP VIEW

360
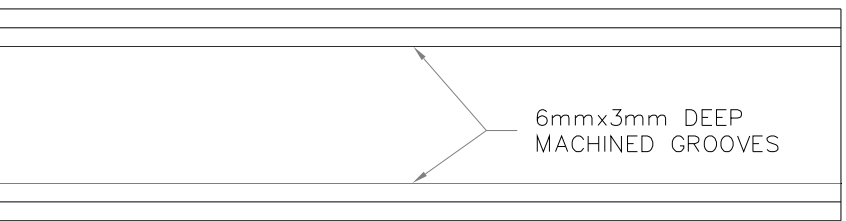
FRONT VIEW

BASE
ONE (1) REQUIRED

9 | (49.5) | 9

3

END VIEW

30°

(13.553)

60°

15.65±0.25
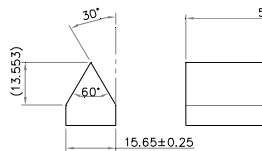
NOTCH
SIX (6) RE
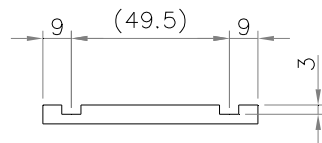
SHORT

SCALE: 1:1 U.N.O.

NOTE: ALL COMPONENTS
MADE FROM 6mm PVC
SHEETS U.N.O

ROBERT DAVEY

3 | 4 | 5 | 6 | 7 | 8 | 9 | 10
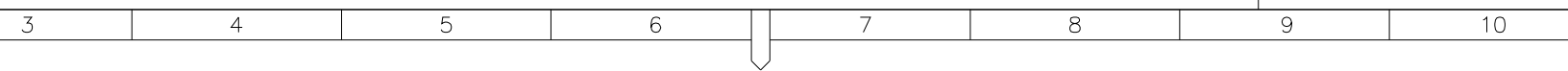
Appendix D

Composite Mixture Tables

A ratio of 20:1 of resin (Hexion Cellobond J2027L) to catalyst (Hexion Phencat 15), respectively, is required for each different percentage by weight mixture. A table of mixture constituents was derived for each mixture percentage based on this ratio and the tables are on the following pages.

Table D.1: Weight of materials required to make 1000 g of PF/SLG (15%)

	Materials	Resin (R)	Catalyst (C)	R + C	Slg	Composite
Parameters						
Percentage by weight		20	1	---	---	---
Percentage by weight		---	---	8.5	1.5	---
Weight of materials in 1000 g of PF/SLG (15%)		810 (g)	40 (g)	850 (g)	150 (g)	1000 (g)

Table D.2: Weight of materials required to make 1000 g of PF/SLG (20%)

	Materials	Resin (R)	Catalyst (C)	R + C	Slg	Composite
Parameters						
Percentage by weight		20	1	---	---	---
Percentage by weight		---	---	8	2	---
Weight of materials in 1000 g of PF/SLG (20%)		762 (g)	38 (g)	800 (g)	200 (g)	1000 (g)

Table D.3: Weight of materials required to make 1000 g of PF/SLG (25%)

	Materials	Resin (R)	Catalyst (C)	R + C	Slg	Composite
Parameters						
Percentage by weight		20	1	---	---	---
Percentage by weight		---	---	7.5	2.5	---
Weight of materials in 1000 g of PF/SLG (25%)		714 (g)	36 (g)	750 (g)	250 (g)	1000 (g)

Table D.4: Weight of materials required to make 1000 g of PF/SLG (30%)

	Materials	Resin (R)	Catalyst (C)	R + C	Slg	Composite
Parameters						
Percentage by weight		20	1	---	---	---
Percentage by weight		---	---	7	3	---
Weight of materials in 1000 g of PF/SLG (30%)		667 (g)	33 (g)	700 (g)	300 (g)	1000 (g)

Table D.5: Weight of materials required to make 1000 g of PF/SLG (35%)

	Materials	Resin (R)	Catalyst (C)	R + C	Slg	Composite
Parameters						
Percentage by weight		20	1	---	---	---
Percentage by weight		---	---	6.5	3.5	---
Weight of materials in 1000 g of PF/SLG (35%)		619 (g)	31 (g)	650 (g)	350 (g)	1000 (g)

Appendix E

MTS 810 Testing System Data

As the MTS 810 Material Testing System conducted the tests on the short bar specimens the data was logged. This data is reproduced here as graphs and tables in the format that the MTS 810 outputs it for each specimen and sample.

MTS 810 Testing System Data

15% by Weight of Filler

Sample ID: robert15-1.mss
Specimen Number: 1
Tagged: False
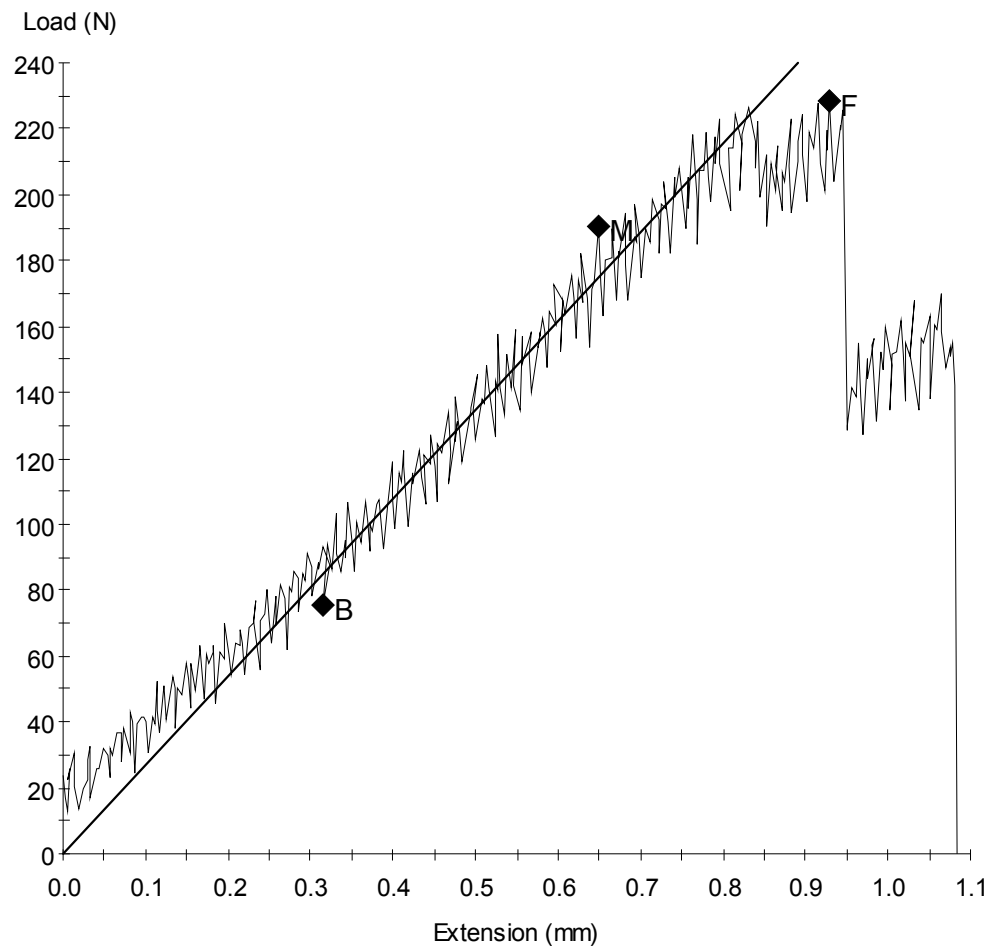
Specimen Results:
Name Value Units
Thickness   50.000 mm
Width 30.000 mm
Area   1500   mm^2
Peak Load   228   N
Peak Stress   0.15   MPa
Break Load   228   N
Break Stress   0.15   MPa
Elongation At Break   0.930   mm
Stress At Offset Yield 0.133   MPa
Load At Offset Yield 199.016   N

Sample ID: robert15-2.mss
Specimen Number: 2
Tagged: False

Specimen Results:
Name   Value   Units
Thickness   50.000 mm
Width   30.000 mm
Area   1500   mm^2
Peak Load   283   N
Peak Stress   0.19   MPa
Break Load   264   N
Break Stress   0.18   MPa
Elongation At Break   0.712   mm
Stress At Offset Yield 0.167   MPa
Load At Offset Yield 250.099   N

Sample ID: robert15-3.mss
Specimen Number: 3
Tagged: False

Specimen Results:
Name   Value   Units
Thickness   50.000 mm
Width 30.000 mm
Area   1500   mm^2
Peak Load   298   N
Peak Stress   0.20   MPa
Break Load   290   N
Break Stress   0.19   MPa
Elongation At Break   0.859   mm
Stress At Offset Yield 0.156   MPa
Load At Offset Yield 234.589   N

Sample ID: robert15-4.mss
Specimen Number: 4
Tagged: False

Specimen Results:
Name Value Units
Thickness   50.000 mm
Width 30.000 mm
Area   1500   mm^2
Peak Load   332   N
Peak Stress   0.22   MPa
Break Load   300   N
Break Stress   0.20   MPa
Elongation At Break   1.496   mm
Stress At Offset Yield 0.193   MPa
Load At Offset Yield 289.212   N

Sample ID: robert15-5.mss
Specimen Number: 5
Tagged: False
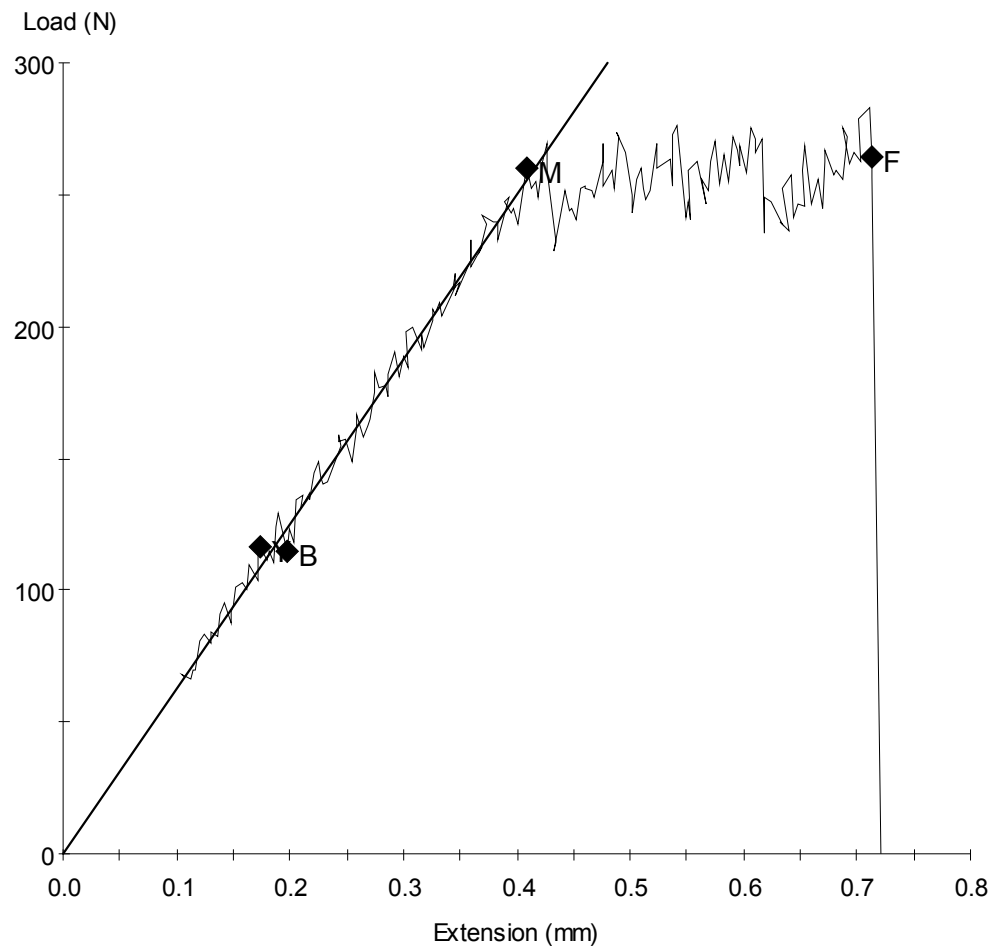

Specimen Results:
Name Value Units
Thickness   50.000 mm
Width 30.000 mm
Area   1500   mm^2
Peak Load   345   N
Peak Stress   0.23   MPa
Break Load   345   N
Break Stress   0.23   MPa
Elongation At Break   0.407   mm
Stress At Offset Yield 0.187   MPa
Load At Offset Yield 280.614   N

Sample ID: robert15-6.mss
Specimen Number: 6
Tagged: False
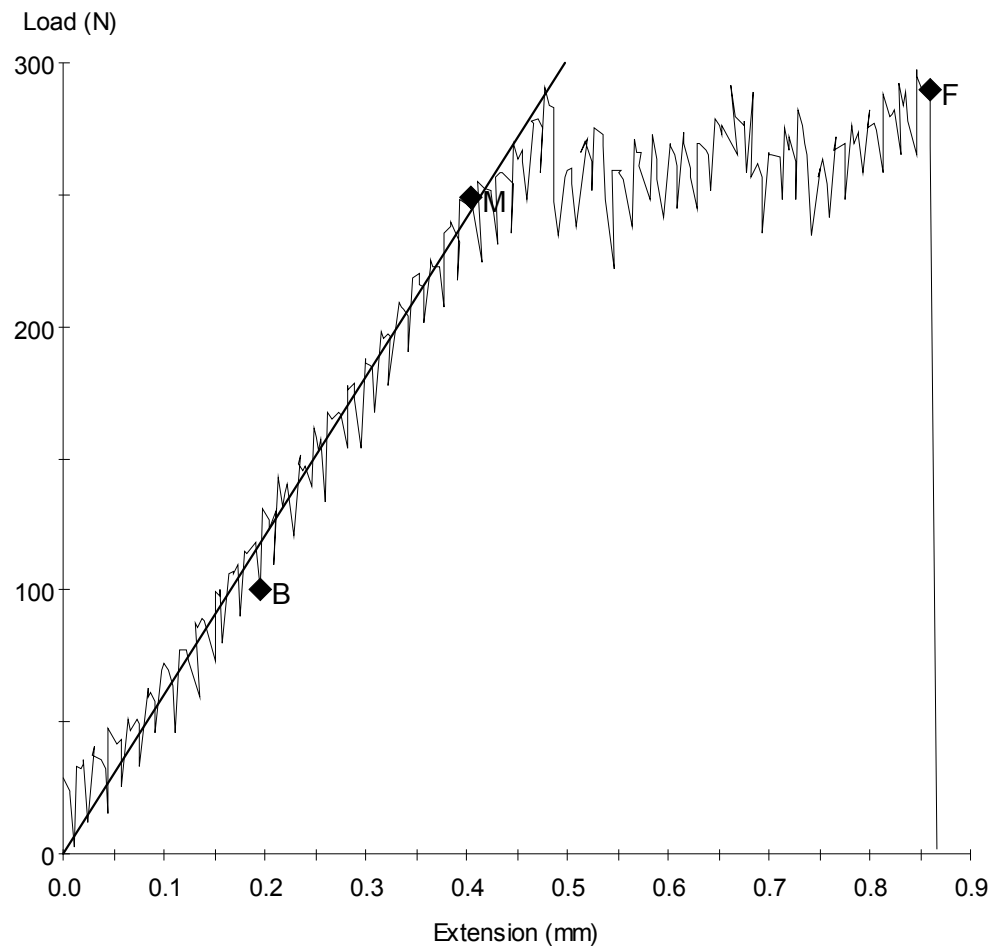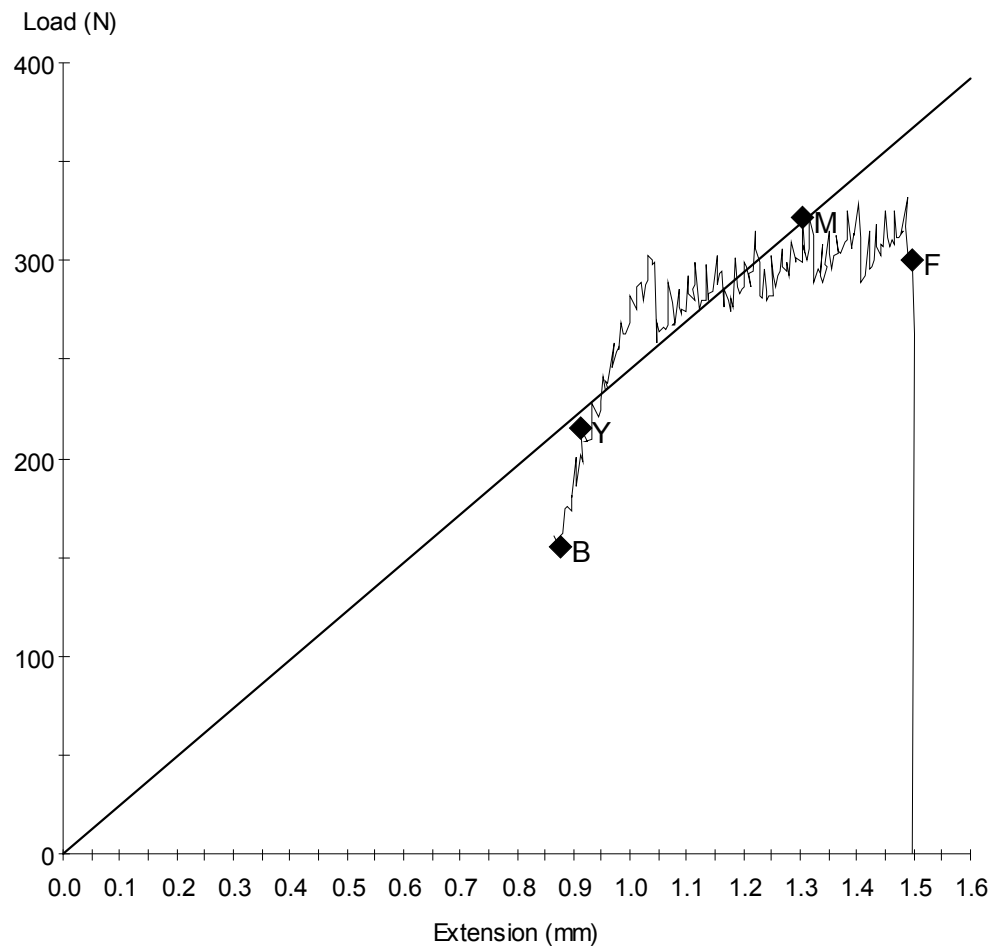

Specimen Results:
Name Value Units
Thickness   50.000 mm
Width 30.000 mm
Area   1500   mm^2
Peak Load   182   N
Peak Stress   0.12   MPa
Break Load   182   N
Break Stress   0.12   MPa
Elongation At Break   0.836   mm
Stress At Offset Yield -0.044 MPa
Load At Offset Yield -66.133   N

Test Date   : 05-Sep-06
Method   : MMT fracture toughness Test .msm

Specimen Results:

Specimen #	Thickness mm	Width mm	Area mm^2	Peak Load N	Peak Stress MPa	Break Load N	Break Stress MPa
1	50.000	30.000	1500	228	0.15	228	0.15
2	50.000	30.000	1500	283	0.19	264	0.18
3	50.000	30.000	1500	298	0.20	290	0.19
4	50.000	30.000	1500	332	0.22	300	0.20
5	50.000	30.000	1500	345	0.23	345	0.23
6	50.000	30.000	1500	182	0.12	182	0.12
Mean	**50.000**	**30.000**	**1500**	**278**	**0.18**	**268**	**0.18**
Std Dev	**0.000**	**0.000**	**0**	**63**	**0.04**	**57**	**0.04**

Specimen #	Elongation At Break mm	Stress At Offset Yield MPa	Load At Offset Yield N				
1	0.930	0.133	199.016				
2	0.712	0.167	250.099				
3	0.859	0.156	234.589				
4	1.496	0.193	289.212				
5	0.407	0.187	280.614				
6	0.836	-0.044	-66.133				
Mean	**0.873**	**0.132**	**197.900**				
Std Dev	**0.357**	**0.089**	**133.391**				

MTS 810 Testing System Data

20% by Weight of Filler
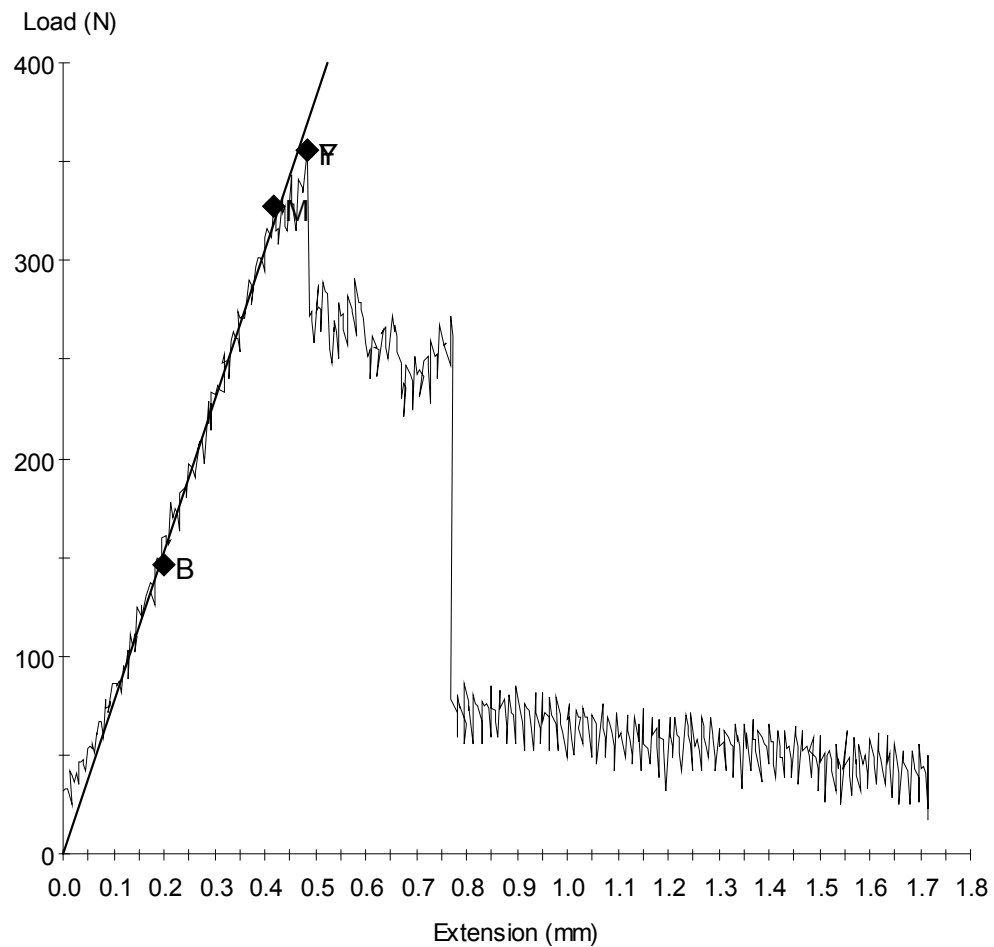
Sample ID: robert20-1.mss
Specimen Number: 1
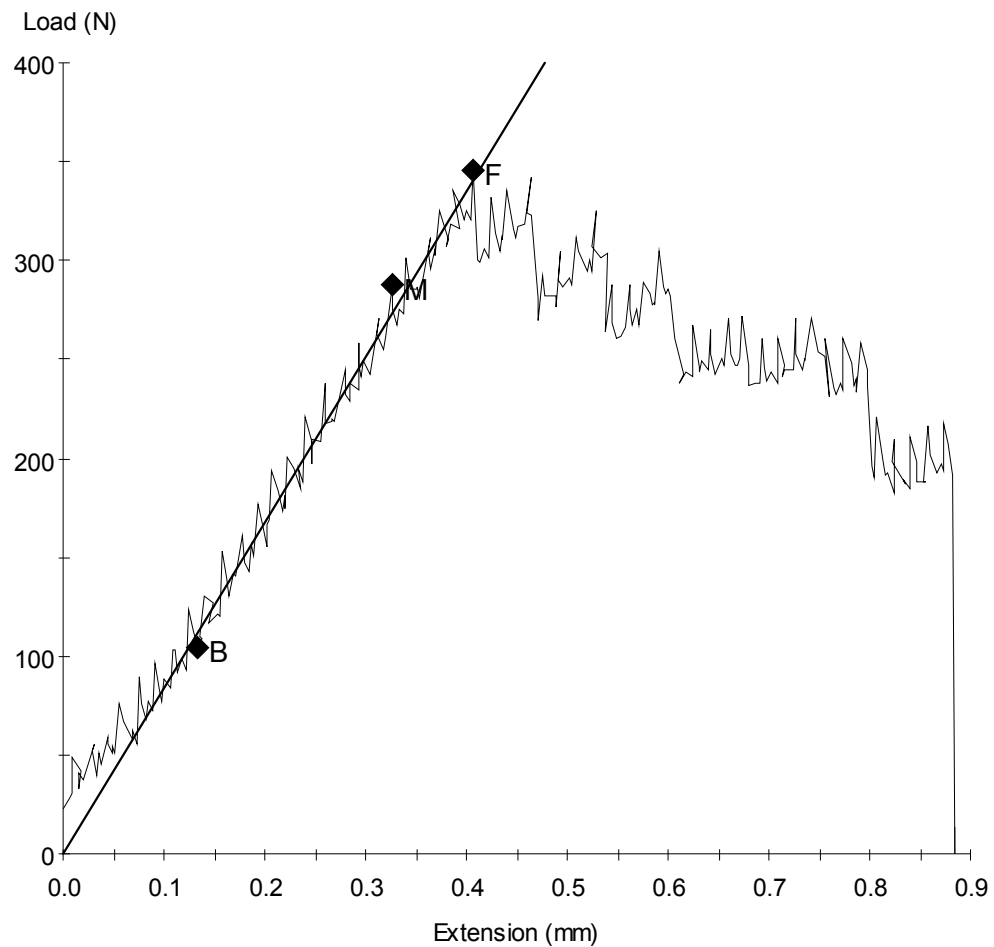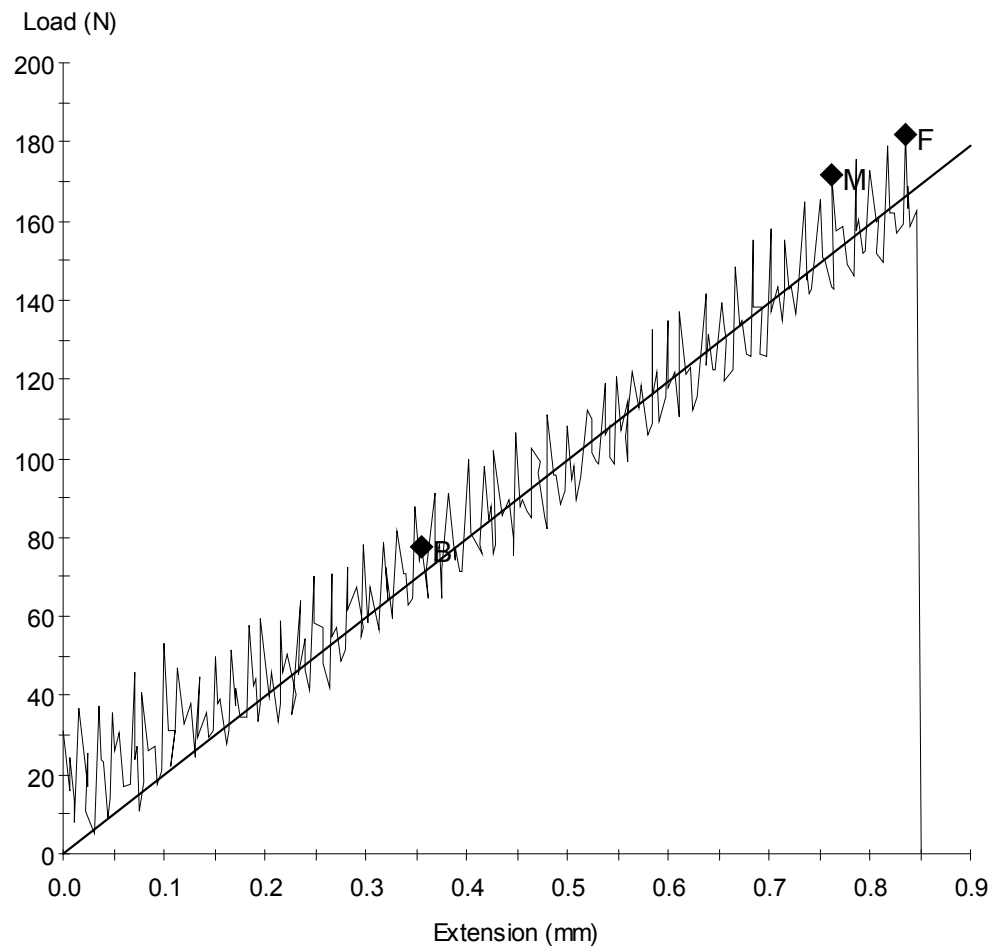Tagged: False

Specimen Results:
Name Value Units
Thickness 50.000 mm
Width 30.000 mm
Area 1500 mm^2
Peak Load 356 N
Peak Stress 0.24 MPa
Break Load 356 N
Break Stress 0.24 MPa
Elongation At Break 0.482 mm
Stress At Offset Yield 0.181 MPa
Load At Offset Yield 271.679 N

Sample ID: robert20-2.mss
Specimen Number: 2
Tagged: False

Specimen Results:
Name   Value   Units
Thickness   50.000 mm
Width 30.000 mm
Area   1500   mm^2
Peak Load   315   N
Peak Stress   0.21   MPa
Break Load   302   N
Break Stress   0.20   MPa
Elongation At Break   0.676   mm
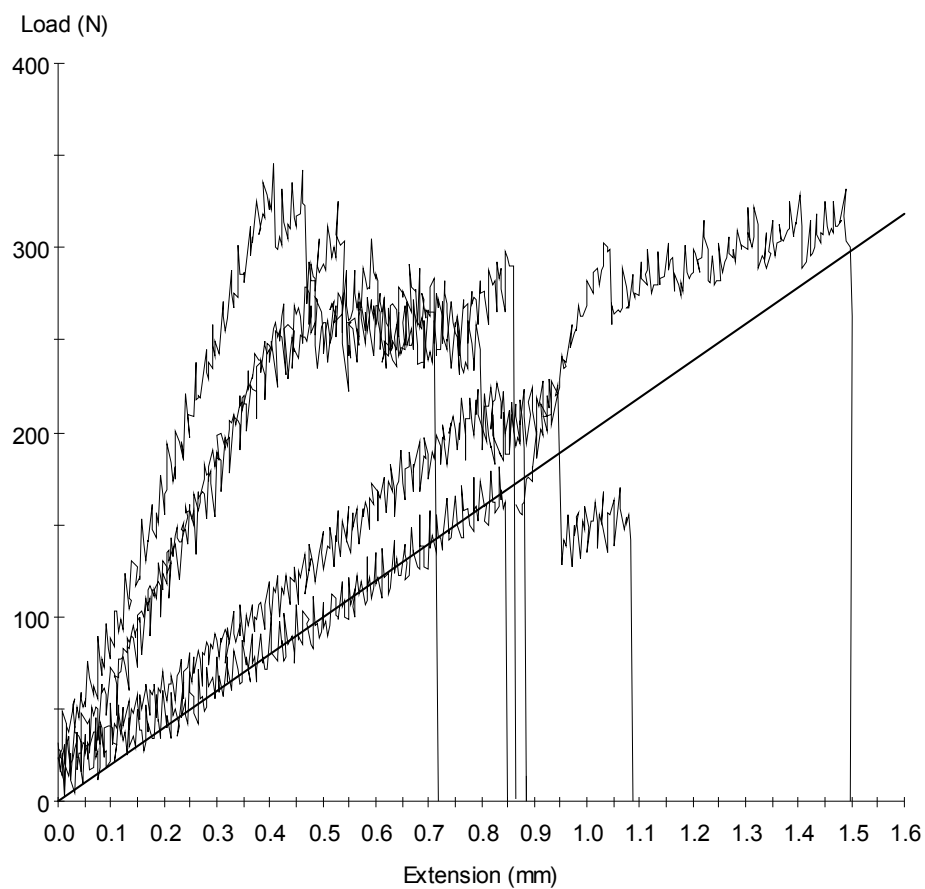Stress At Offset Yield 0.184   MPa
Load At Offset Yield 276.737   N

Sample ID: robert20-3.mss
Specimen Number: 3
Tagged: False

Specimen Results:
Name Value Units
Thickness   50.000 mm
Width 30.000 mm
Area   1500   mm^2
Peak Load   314   N
Peak Stress   0.21   MPa
Break Load   294   N
Break Stress   0.20   MPa
Elongation At Break 0.760   mm
Stress At Offset Yield 0.141   MPa
Load At Offset Yield 211.324   N

Sample ID: robert20-4.mss
Specimen Number: 4
Tagged: False

Specimen Results:
Name   Value   Units
Thickness   50.000 mm
Width 30.000 mm
Area   1500   mm^2
Peak Load   341   N
Peak Stress   0.23   MPa
Break Load   336   N
Break Stress   0.22   MPa
Elongation At Break   0.409   mm
Stress At Offset Yield 0.183   MPa
Load At Offset Yield 274.376   N

Sample ID: robert20-5.mss
Specimen Number: 5
Tagged: False
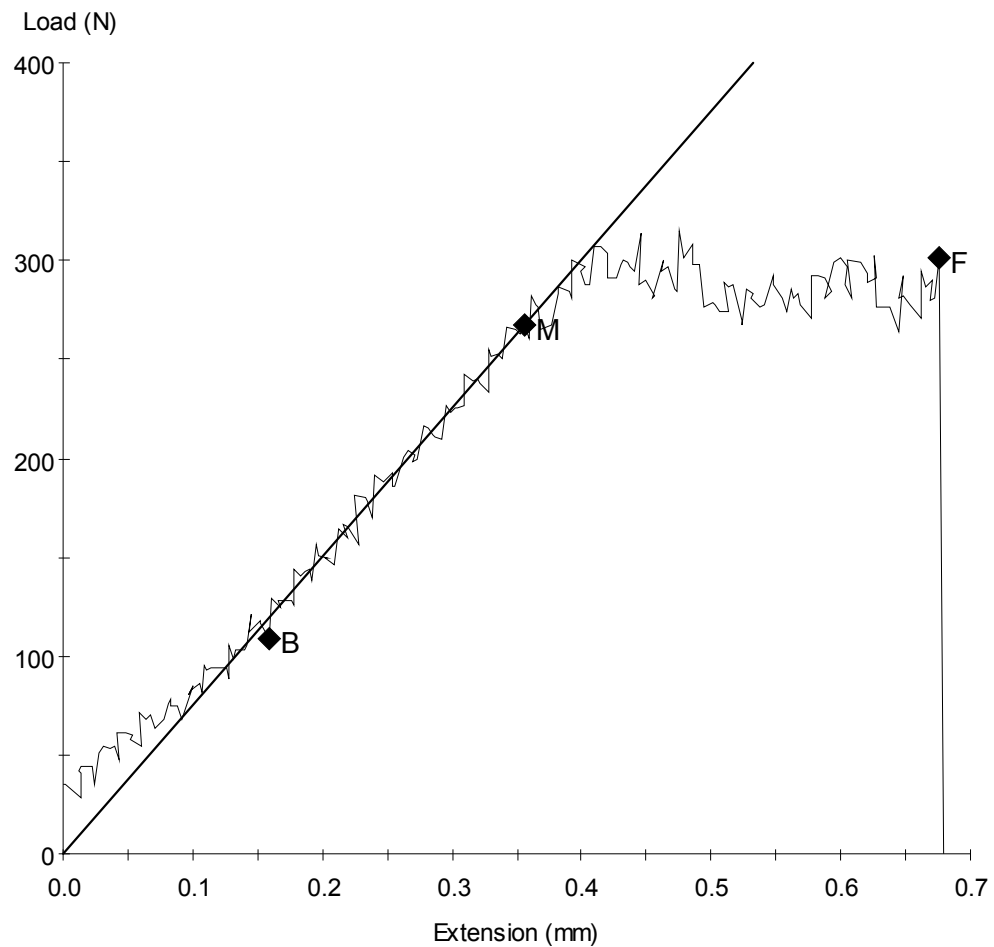

Specimen Results:
Name Value Units
Thickness   50.000 mm
Width 30.000 mm
Area   1500   mm^2
Peak Load   336   N
Peak Stress   0.22   MPa
Break Load   320   N
Break Stress   0.21   MPa
Elongation At Break   0.860   mm
Stress At Offset Yield 0.190   MPa
Load At Offset Yield 284.323   N

Sample ID: robert20-6.mss
Specimen Number: 6
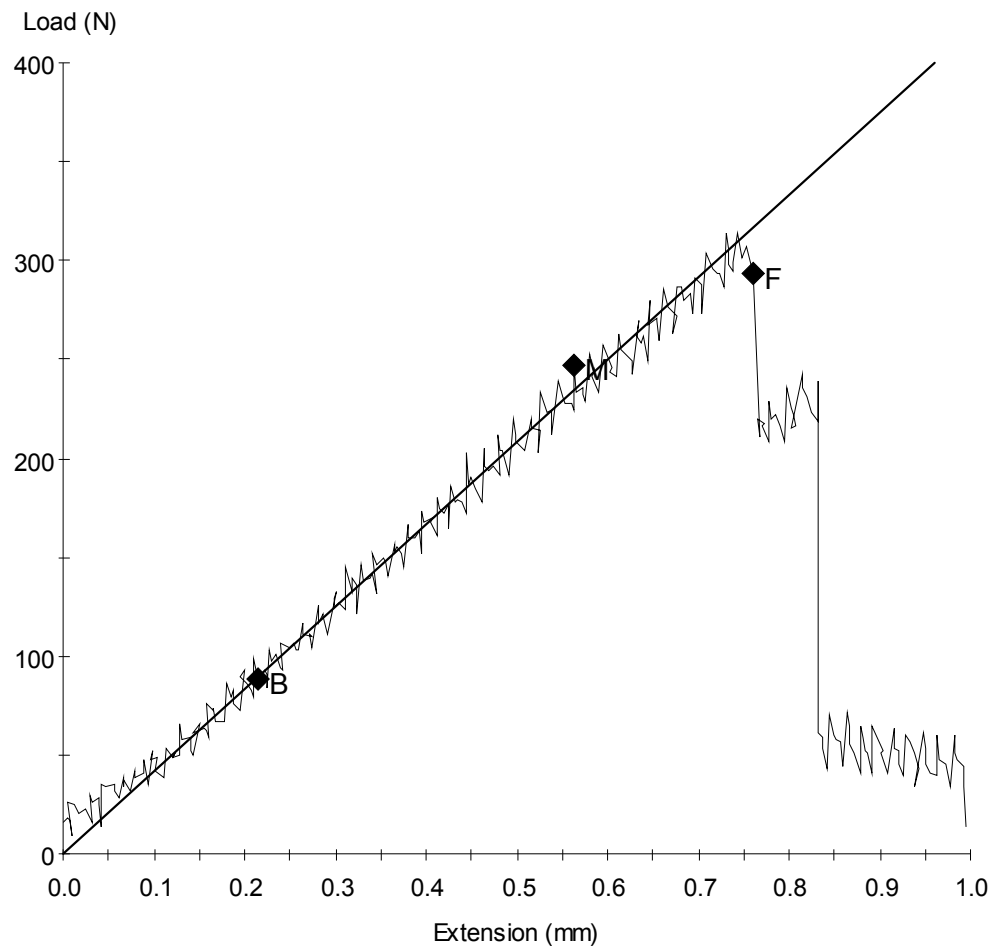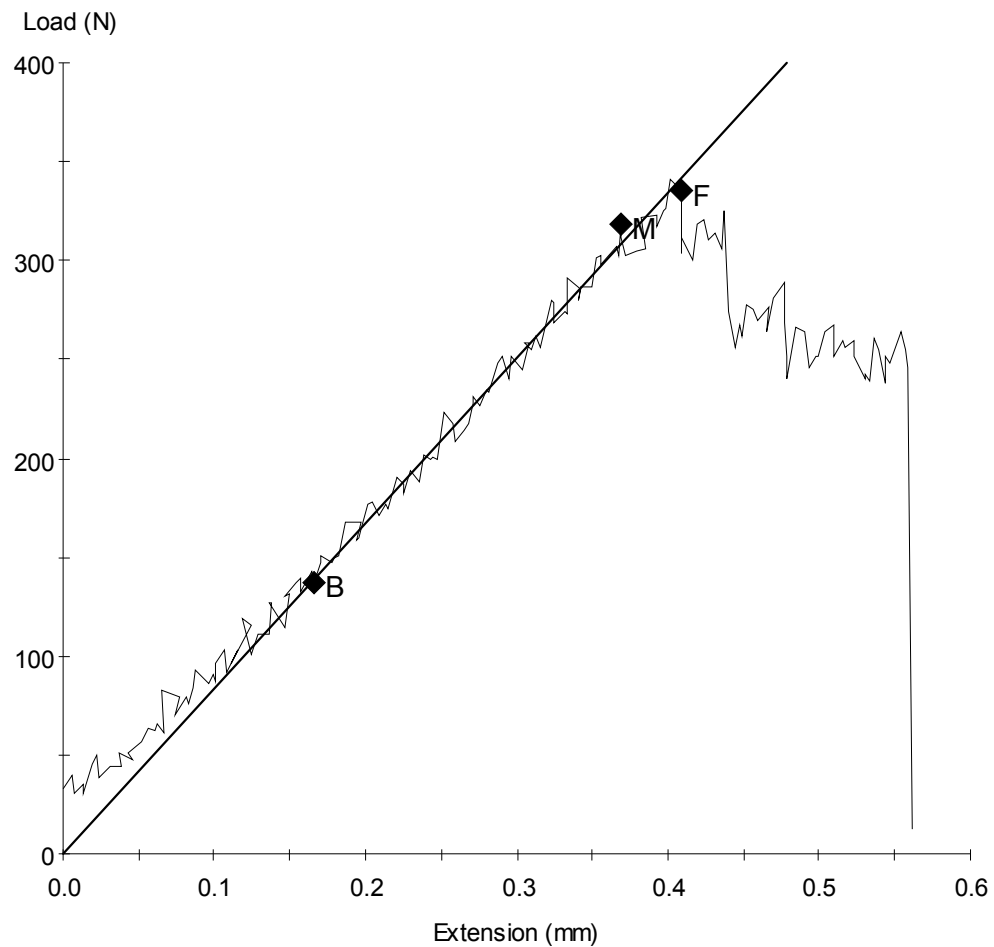Tagged: False

Specimen Results:
Name Value Units
Thickness   50.000 mm
Width 30.000 mm
Area   1500   mm^2
Peak Load   340   N
Peak Stress   0.23   MPa
Break Load   333   N
Break Stress   0.22   MPa
Elongation At Break 0.493   mm
Stress At Offset Yield 0.186   MPa
Load At Offset Yield 278.928   N

Test Date   : 05-Sep-06
Method   : MMT fracture toughness Test .msm

Specimen Results:

Specimen #	Thickness mm	Width mm	Area mm^2	Peak Load N	Peak Stress MPa	Break Load N	Break Stress MPa
1	50.000	30.000	1500	356	0.24	356	0.24
2	50.000	30.000	1500	315	0.21	302	0.20
3	50.000	30.000	1500	314	0.21	294	0.20
4	50.000	30.000	1500	341	0.23	336	0.22
5	50.000	30.000	1500	336	0.22	320	0.21
6	50.000	30.000	1500	340	0.23	333	0.22
Mean	**50.000**	**30.000**	**1500**	**333**	**0.22**	**323**	**0.22**
Std Dev	**0.000**	**0.000**	**0**	**16**	**0.01**	**23**	**0.02**

Specimen #	Elongation At Break mm	Stress At Offset Yield MPa	Load At Offset Yield N				
1	0.482	0.181	271.679				
2	0.676	0.184	276.737				
3	0.760	0.141	211.324				
4	0.409	0.183	274.376				
5	0.860	0.190	284.323				
6	0.493	0.186	278.928				
Mean	**0.613**	**0.177**	**266.228**				
Std Dev	**0.179**	**0.018**	**27.239**				

MTS 810 Testing System Data

25% by Weight of Filler

Sample ID: robert25-1.mss
Specimen Number: 1
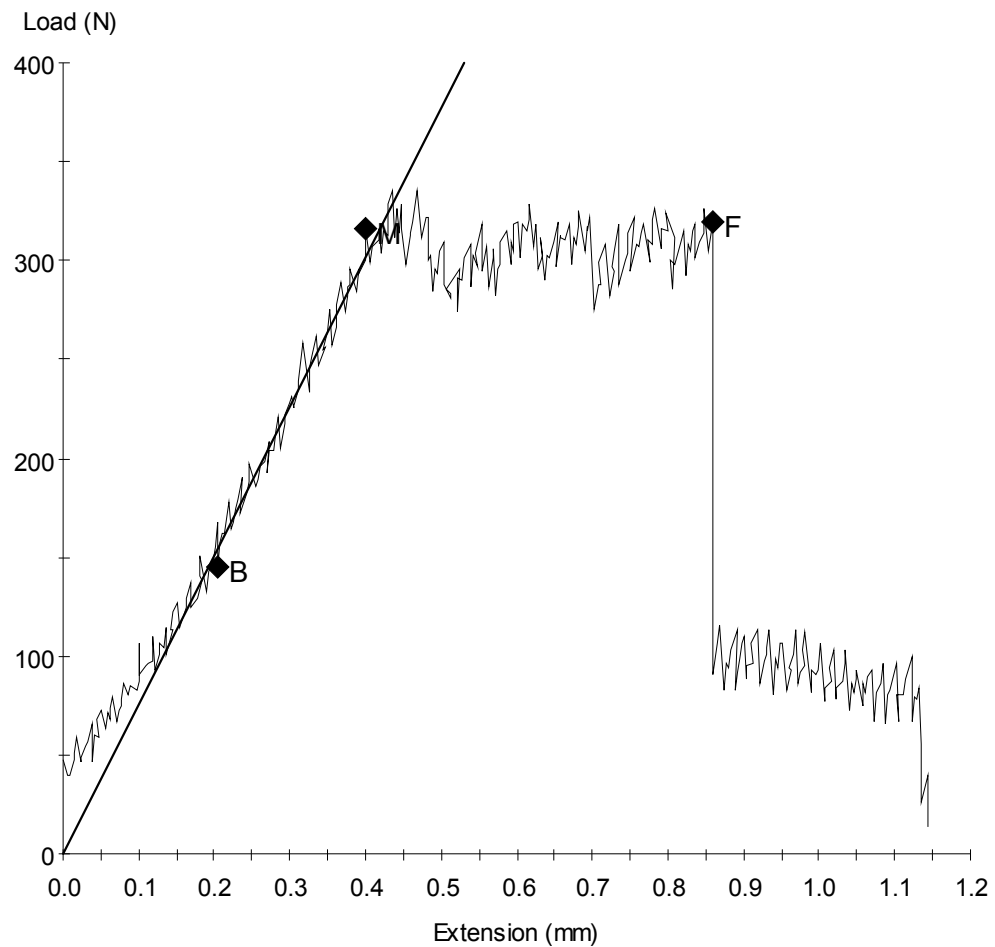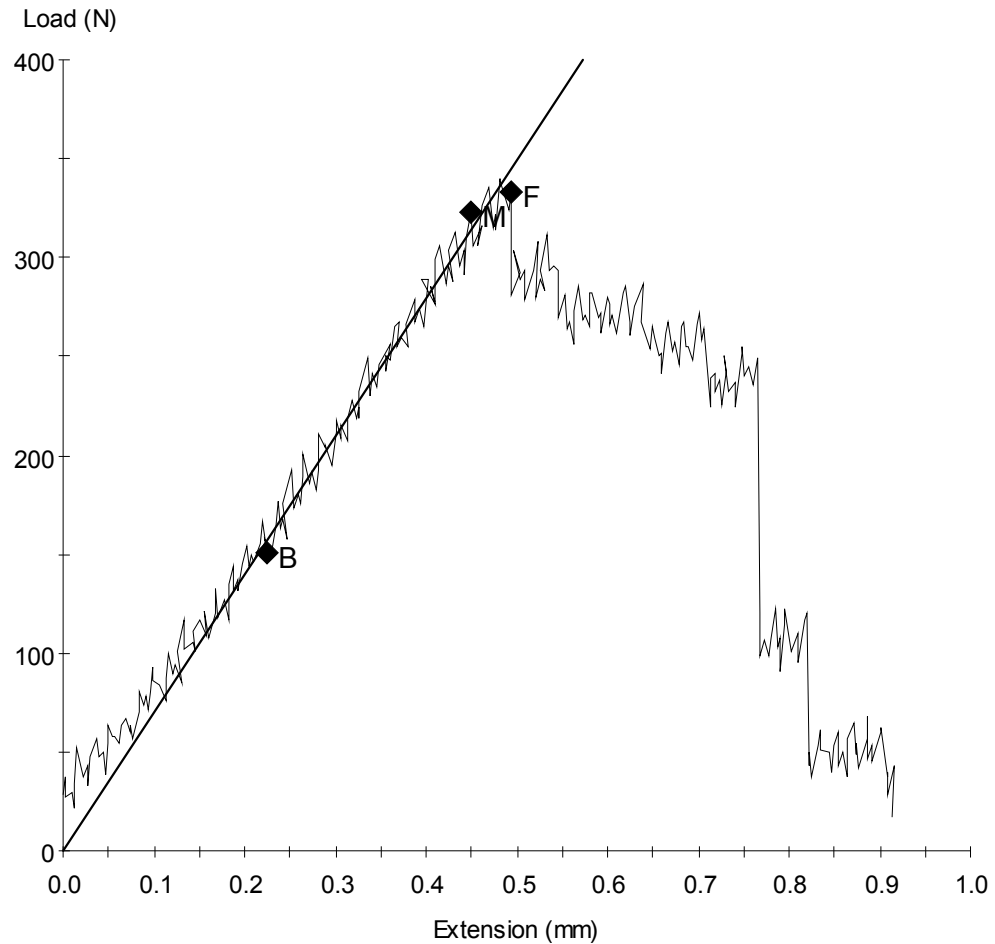Tagged: False
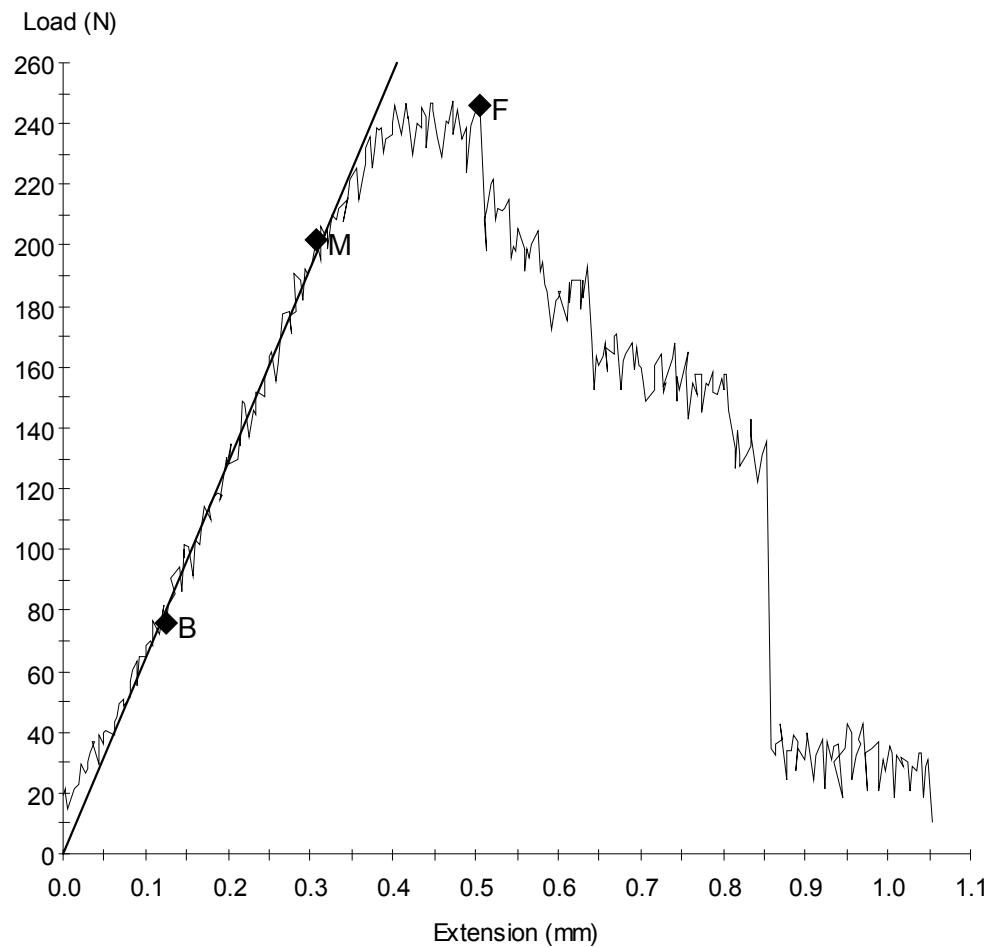
Specimen Results:
Name   Value   Units
Thickness   50.000 mm
Width 30.000 mm
Area   1500   mm^2
Peak Load   248   N
Peak Stress   0.16   MPa
Break Load   246   N
Break Stress   0.16   MPa
Elongation At Break   0.506   mm
Stress At Offset Yield 0.153   MPa
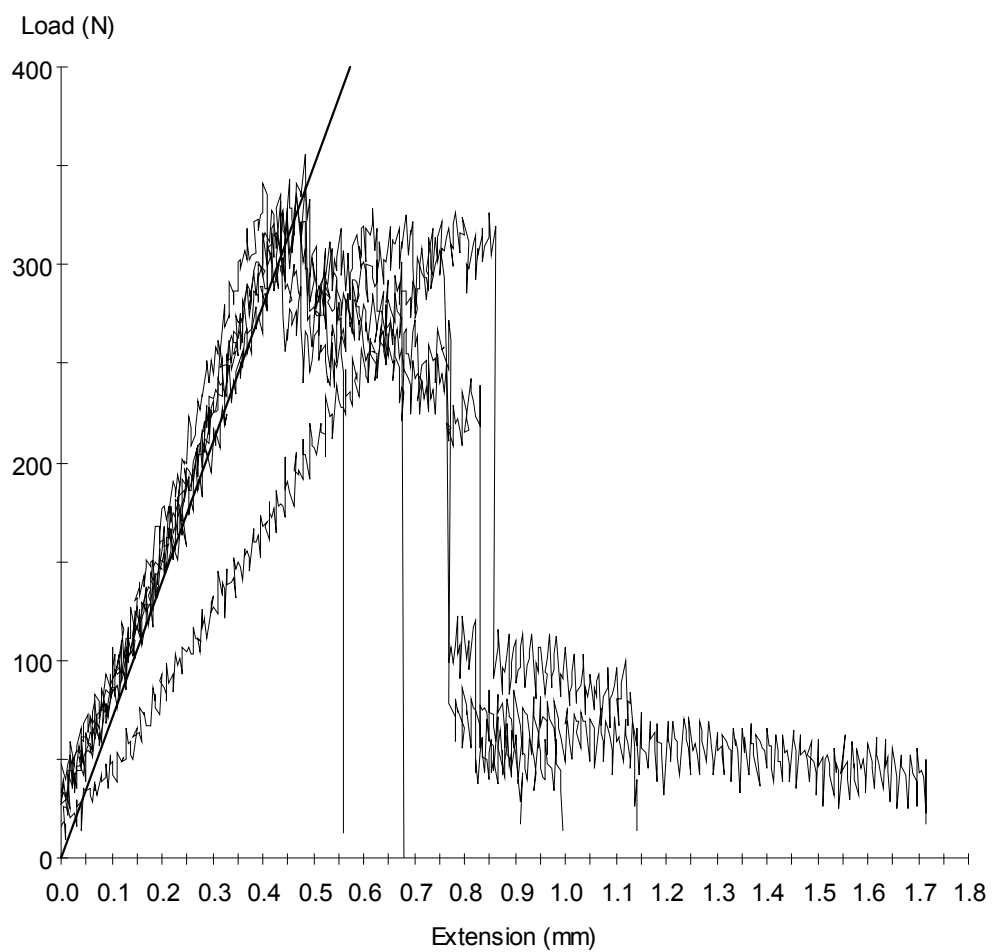Load At Offset Yield 229.363   N

Sample ID: robert25-2.mss
Specimen Number: 2
Tagged: False

Load (N)

Extension (mm)

Specimen Results:
Name   Value   Units
Thickness   50.000 mm
Width 30.000 mm
Area   1500   mm^2
Peak Load   248   N
Peak Stress   0.16   MPa
Break Load   217   N
Break Stress   0.14   MPa
Elongation At Break 0.738   mm
Stress At Offset Yield 0.138   MPa
Load At Offset Yield 207.615   N

Sample ID: robert25-3.mss
Specimen Number: 3
Tagged: False

Specimen Results:
Name   Value   Units
Thickness 50.000 mm
Width 30.000 mm
Area   1500   mm^2
Peak Load 274 N
Peak Stress 0.18 MPa
Break Load 255 N
Break Stress 0.17 MPa
Elongation At Break 0.560 mm
Stress At Offset Yield 0.172 MPa
Load At Offset Yield 258.360 N

Sample ID: robert25-4.mss
Specimen Number: 4
Tagged: False

Specimen Results:
Name Value Units
Thickness   50.000 mm
Width 30.000 mm
Area   1500   mm^2
Peak Load   268   N
Peak Stress   0.18   MPa
Break Load   268   N
Break Stress   0.18   MPa
Elongation At Break 0.407   mm
Stress At Offset Yield 0.157   MPa
Load At Offset Yield 235.938   N

Sample ID: robert25-5.mss
Specimen Number: 5
Tagged: False

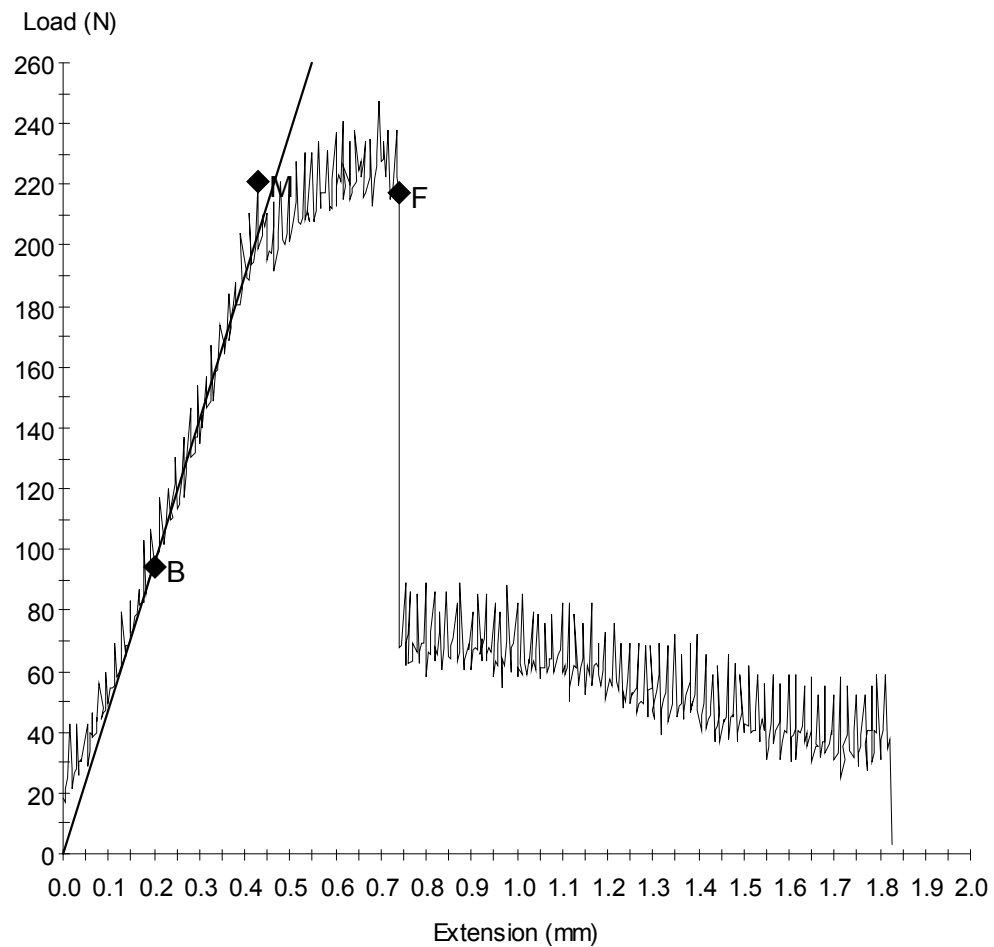**Specimen Results:**
Name Value Units
Thickness   50.000 mm
Width 30.000 mm
Area   1500   mm^2
Peak Load   274   N
Peak Stress   0.18   MPa
Break Load   256   N
Break Stress   0.17   MPa
Elongation At Break 0.589   mm
Stress At Offset Yield 0.169   MPa
Load At Offset Yield 253.134   N

Sample ID: robert25-6.mss
Specimen Number: 6
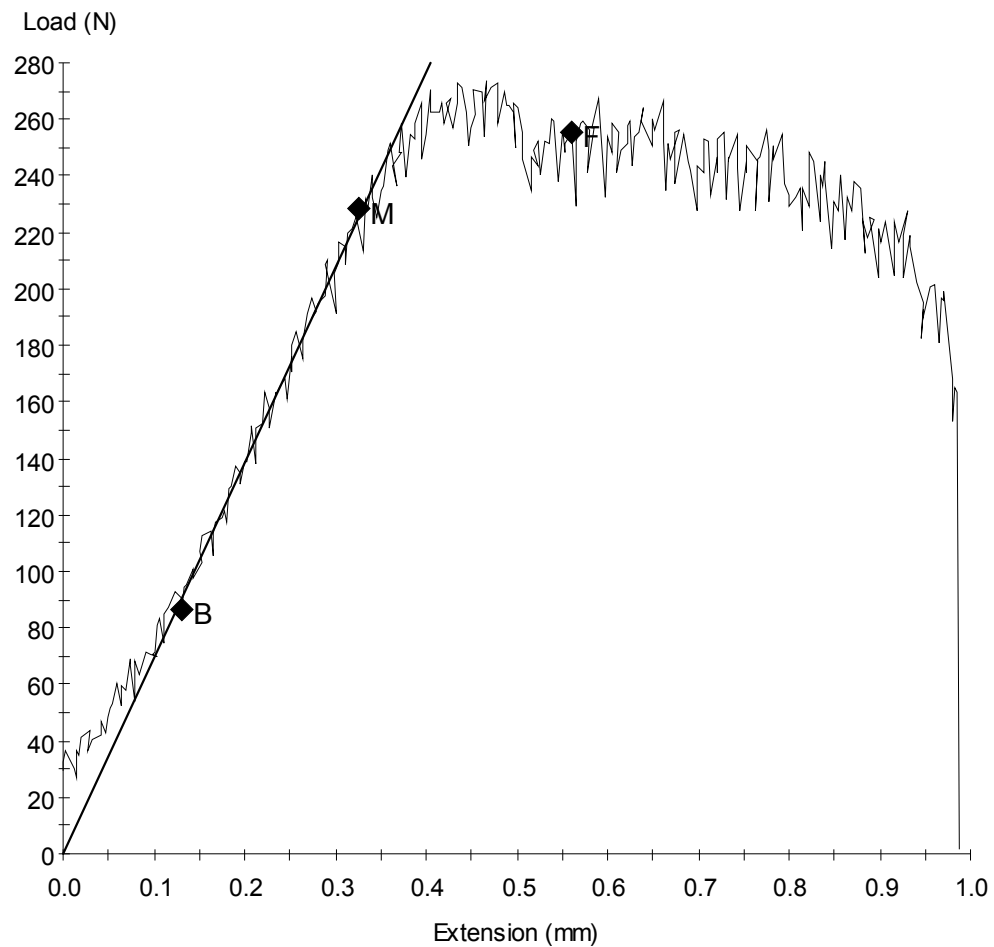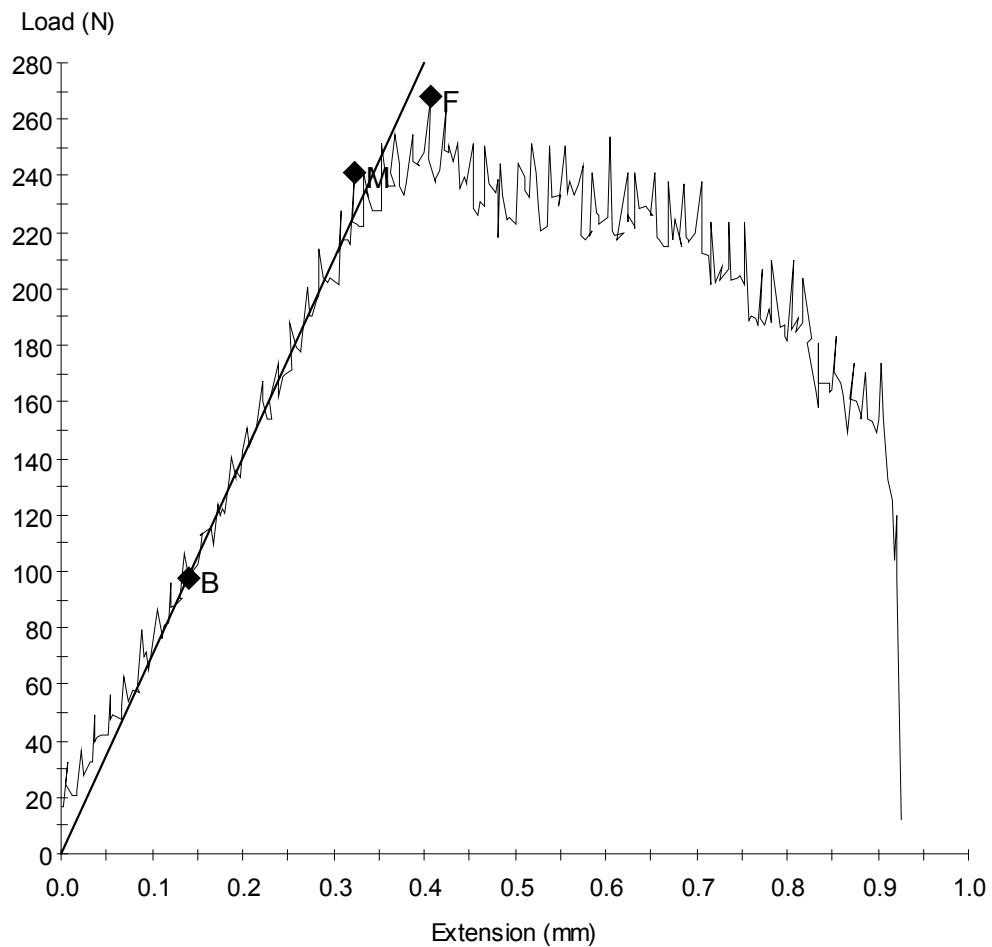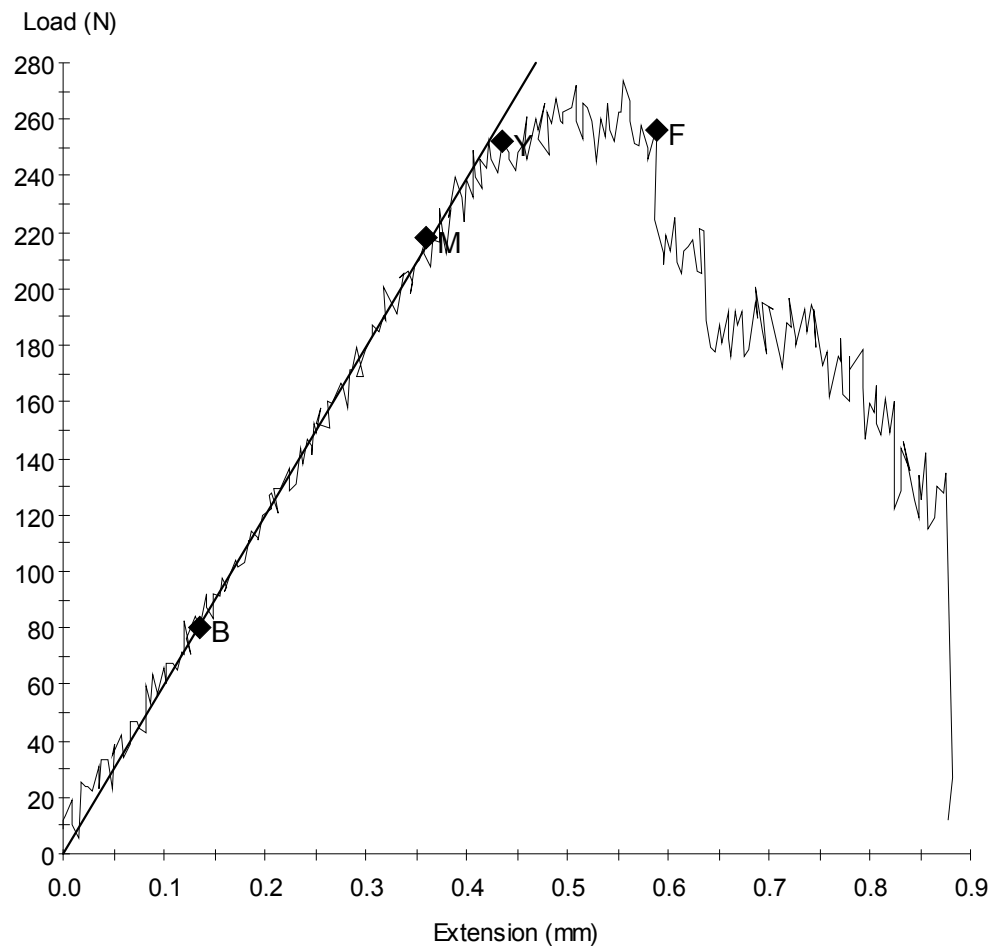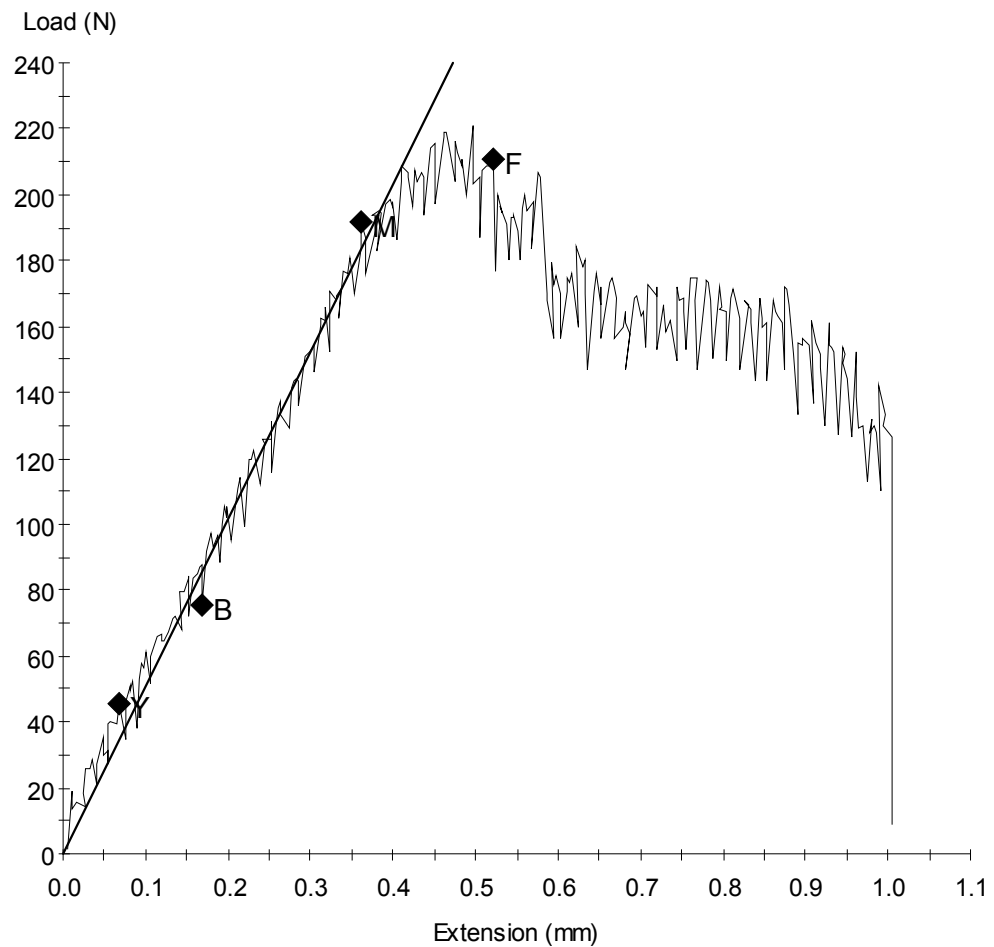Tagged: False

Specimen Results:
Name   Value   Units
Thickness   50.000 mm
Width 30.000 mm
Area   1500   mm^2
Peak Load   221   N
Peak Stress   0.15   MPa
Break Load   211   N
Break Stress   0.14   MPa
Elongation At Break   0.522   mm
Stress At Offset Yield 0.125   MPa
Load At Offset Yield 187.215   N

Test Date   : 05-Sep-06
Method   : MMT fracture toughness Test .msm

Specimen Results:

Specimen #	Thickness mm	Width mm	Area mm^2	Peak Load N	Peak Stress MPa	Break Load N	Break Stress MPa
1	50.000	30.000	1500	248	0.16	246	0.16
2	50.000	30.000	1500	248	0.16	217	0.14
3	50.000	30.000	1500	274	0.18	255	0.17
4	50.000	30.000	1500	268	0.18	268	0.18
5	50.000	30.000	1500	274	0.18	256	0.17
6	50.000	30.000	1500	221	0.15	211	0.14
Mean	**50.000**	**30.000**	**1500**	**255**	**0.17**	**242**	**0.16**
Std Dev	**0.000**	**0.000**	**0**	**21**	**0.01**	**23**	**0.02**

Specimen #	Elongation At Break mm	Stress At Offset Yield MPa	Load At Offset Yield N				
1	0.506	0.153	229.363				
2	0.738	0.138	207.615				
3	0.560	0.172	258.360				
4	0.407	0.157	235.938				
5	0.589	0.169	253.134				
6	0.522	0.125	187.215				
Mean	**0.554**	**0.152**	**228.604**				
Std Dev	**0.110**	**0.018**	**27.185**				

Load (N)

MTS 810 Testing System Data

30% by Weight of Filler

Sample ID: robert30-1.mss
Specimen Number: 1
Tagged: False
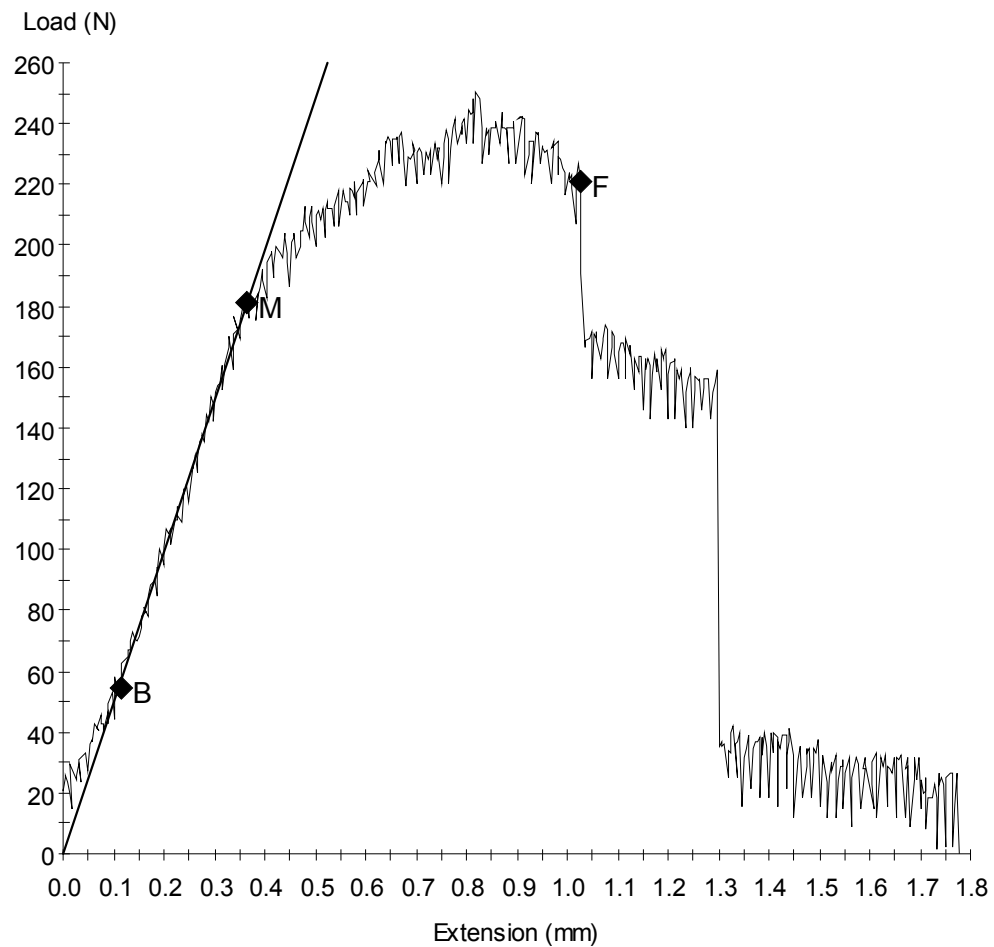
Specimen Results:
Name Value Units
Width 30.000 mm
Area 1500 mm^2
Peak Load 250 N
Peak Stress 0.17 MPa
Elongation at Peak 0.819 mm
Break Load 221 N
Break Stress 0.15 MPa
Elongation At Break 1.026 mm
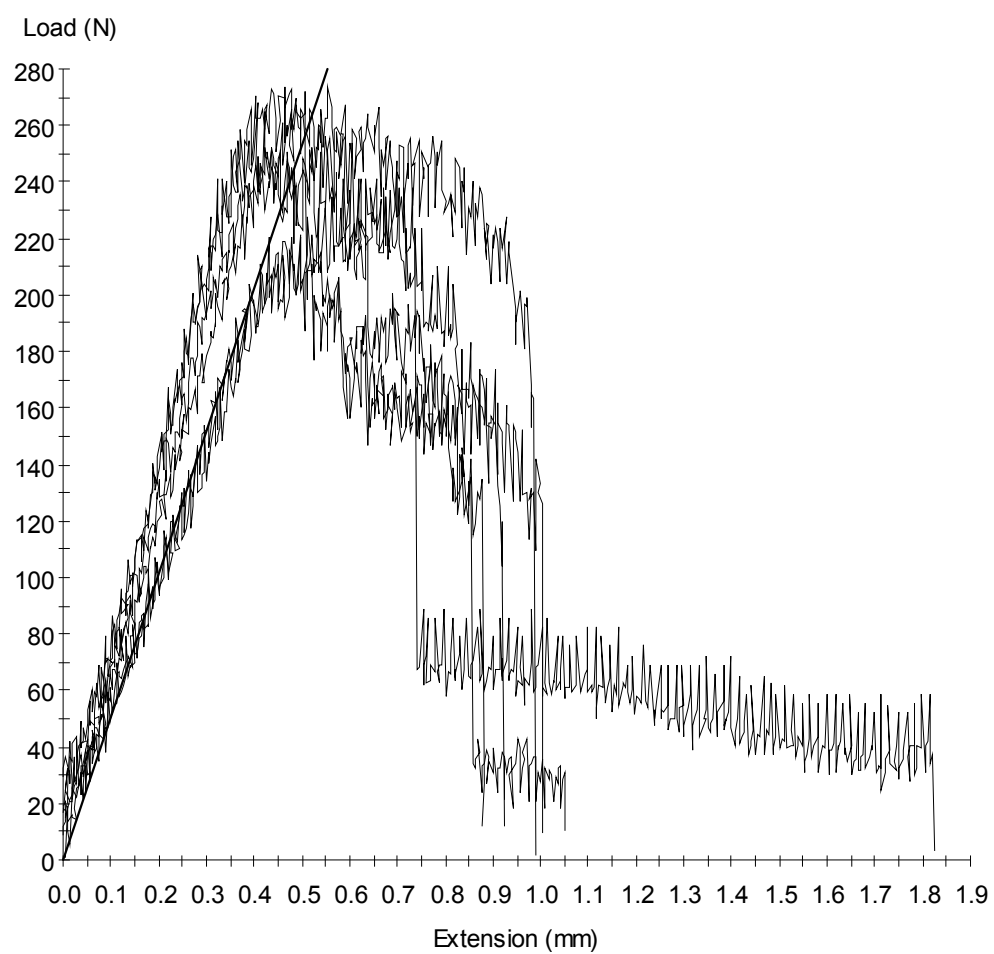Stress At Offset Yield 0.135 MPa
Load At Offset Yield 202.865 N

Sample ID: robert30-2.mss
Specimen Number: 2
Tagged: False

Specimen Results:
Name Value Units
Width 30.000 mm
Area   1500   mm^2
Peak Load   221   N
Peak Stress   0.15   MPa
Elongation at Peak   0.594   mm
Break Load   185   N
Break Stress   0.12   MPa
Elongation At Break   0.964   mm
Stress At Offset Yield 0.139   MPa
Load At Offset Yield 208.091   N

Sample ID: robert30-3.mss
Specimen Number: 3
Tagged: False

Specimen Results:
Name Value Units
Width 30.000 mm
Area   1500   mm^2
Peak Load   259   N
Peak Stress   0.17   MPa
Elongation at Peak   0.474   mm
Break Load   254   N
Break Stress   0.17   MPa
Elongation At Break 0.488   mm
Stress At Offset Yield 0.151   MPa
Load At Offset Yield 226.973   N

Sample ID: robert30-4.mss
Specimen Number: 4
Tagged: False

Specimen Results:
Name Value Units
Width 30.000 mm
Area 1500 mm^2
Peak Load 221 N
Peak Stress 0.15 MPa
Elongation at Peak 0.523 mm
Break Load 215 N
Break Stress 0.14 MPa
Elongation At Break 0.647 mm
Stress At Offset Yield 0.131 MPa
Load At Offset Yield 196.458 N

Sample ID: robert30-5.mss
Specimen Number: 5
Tagged: False

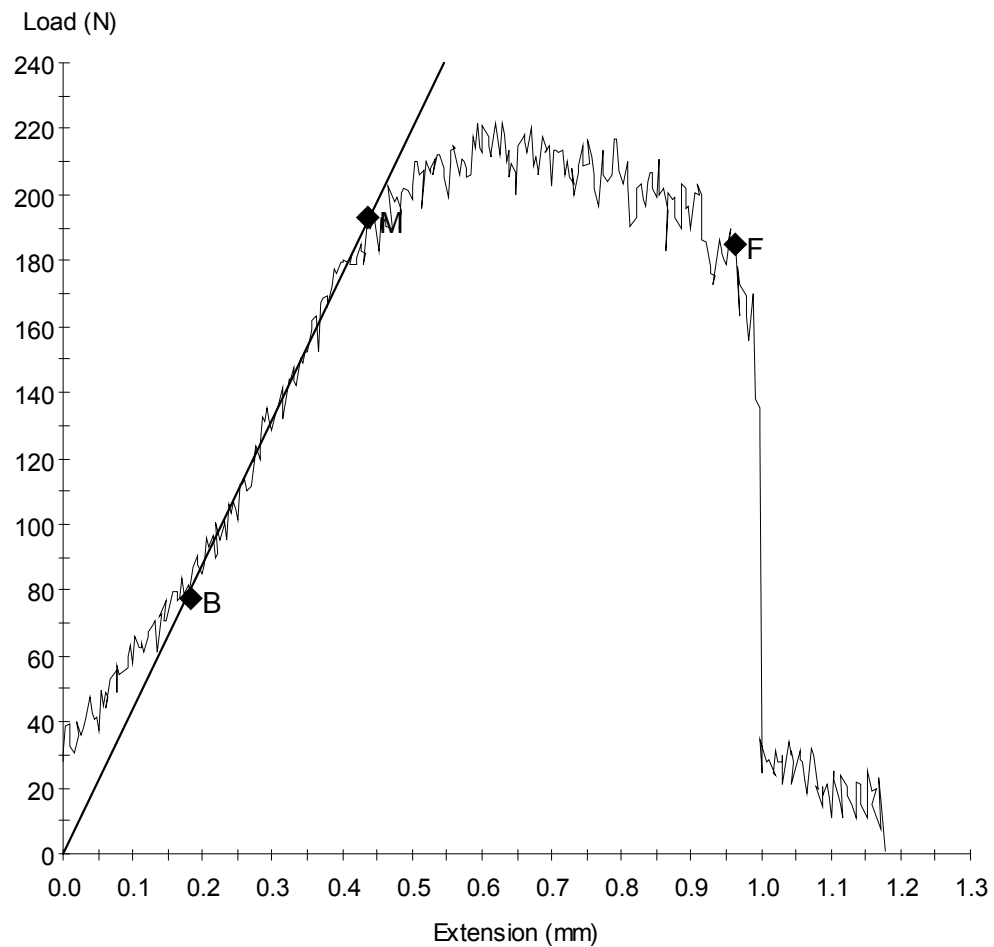

Specimen Results:
Name   Value   Units
Width 30.000 mm
Area   1500   mm^2
Peak Load   236   N
Peak Stress   0.16   MPa
Elongation at Peak   0.673   mm
Break Load   208   N
Break Stress   0.14   MPa
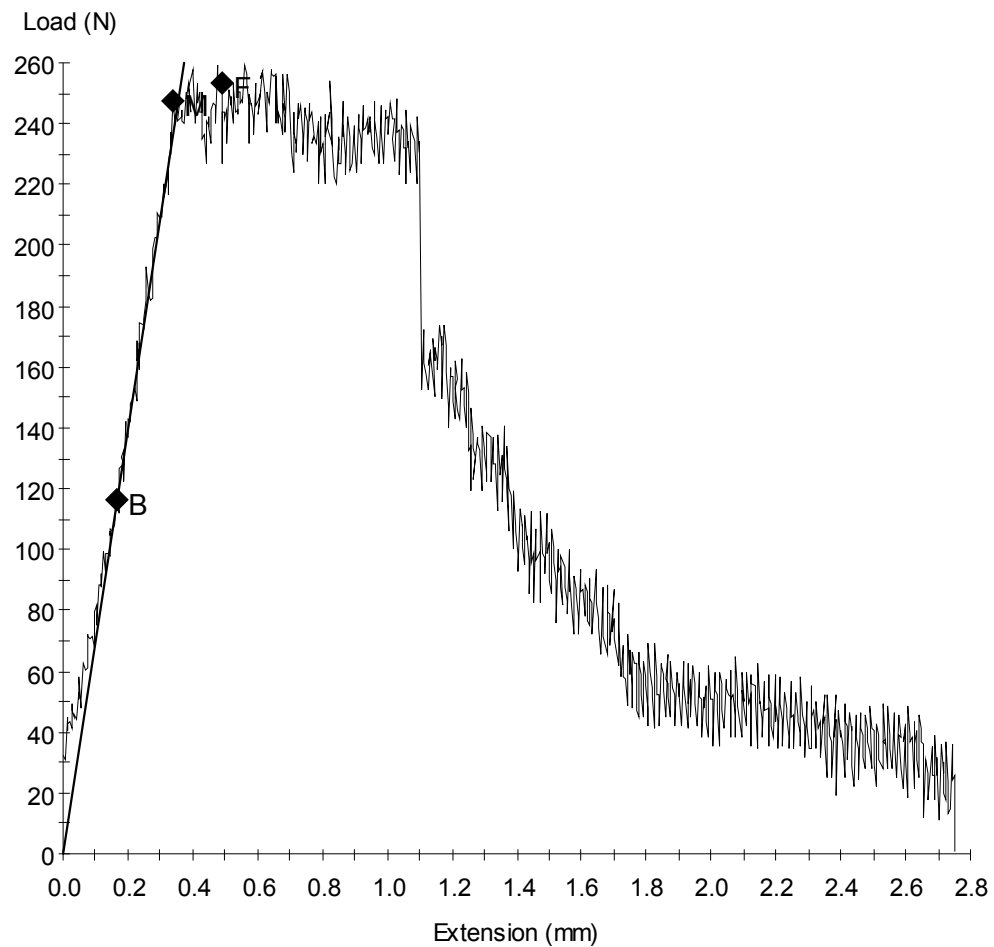Elongation At Break   0.854   mm
Stress At Offset Yield 0.134   MPa
Load At Offset Yield 201.347   N

Sample ID: robert30-6.mss
Specimen Number: 6
Tagged: False

Specimen Results:
Name Value Units
Width 30.000 mm
Area 1500 mm^2
Peak Load 258 N
Peak Stress 0.17 MPa
Elongation at Peak 0.553 mm
Break Load 199 N
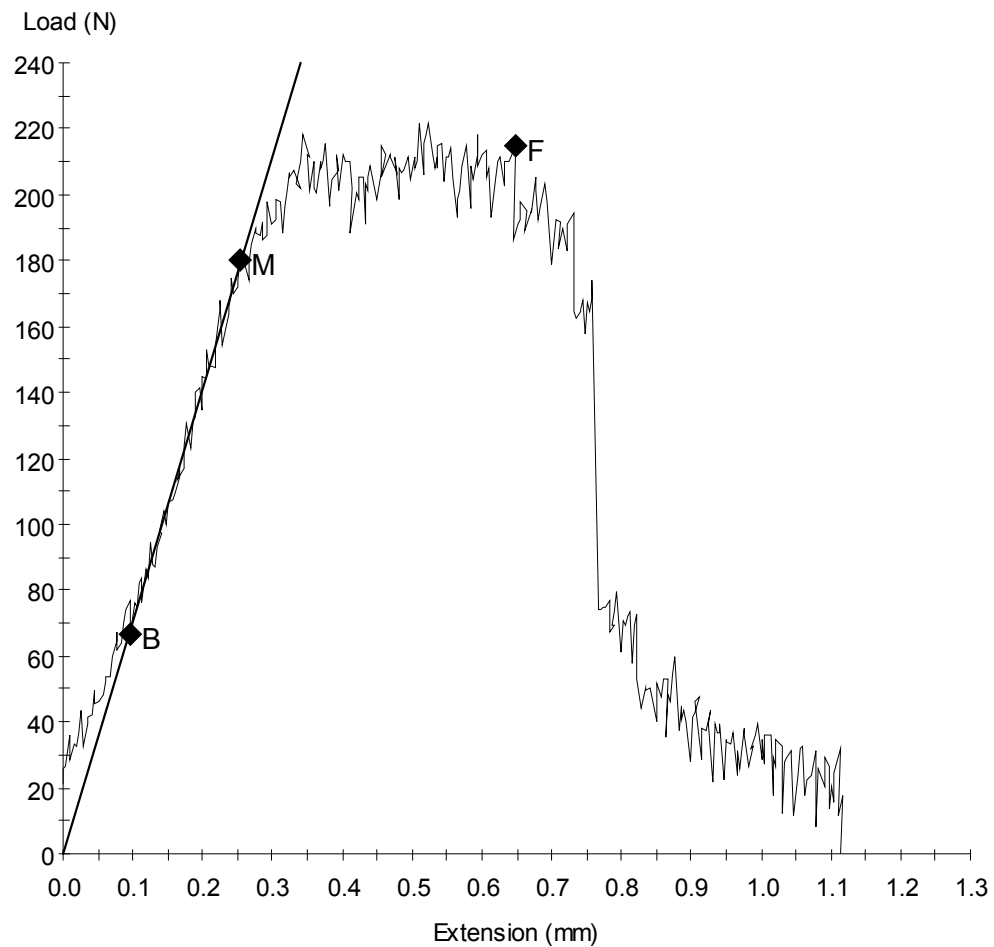Break Stress 0.13 MPa
Elongation At Break 0.800 mm
Stress At Offset Yield 0.156 MPa
Load At Offset Yield 233.379 N

Test Date   : 05-Aug-03
Method   : MMTTensile Test.msm

Specimen Results:

Specimen #	Thickness mm	Width mm	Area mm^2	Peak Load N	Peak Stress MPa	Elongation at Peak mm	Break Load N
1	50.000	30.000	1500	250	0.17	0.819	221
2	50.000	30.000	1500	221	0.15	0.594	185
3	50.000	30.000	1500	259	0.17	0.474	254
4	50.000	30.000	1500	221	0.15	0.523	215
5	50.000	30.000	1500	236	0.16	0.673	208
6	50.000	30.000	1500	258	0.17	0.553	199
Mean	**50.000**	**30.000**	**1500**	**241**	**0.16**	**0.606**	**214**
Std Dev	**0.000**	**0.000**	**0**	**17**	**0.01**	**0.124**	**23**

Specimen #	Break Stress MPa	Elongation At Break mm	Stress At Offset Yield MPa	Load At Offset Yield N			
1	0.15	1.026	0.135	202.865			
2	0.12	0.964	0.139	208.091			
3	0.17	0.488	0.151	226.973			
4	0.14	0.647	0.131	196.458			
5	0.14	0.854	0.134	201.347			
6	0.13	0.800	0.156	233.379			
Mean	**0.14**	**0.797**	**0.141**	**211.519**			
Std Dev	**0.02**	**0.201**	**0.010**	**15.058**			

MTS 810 Testing System Data

35% by Weight of Filler

Sample ID: robert35-1.mss
Specimen Number: 1
Tagged: False
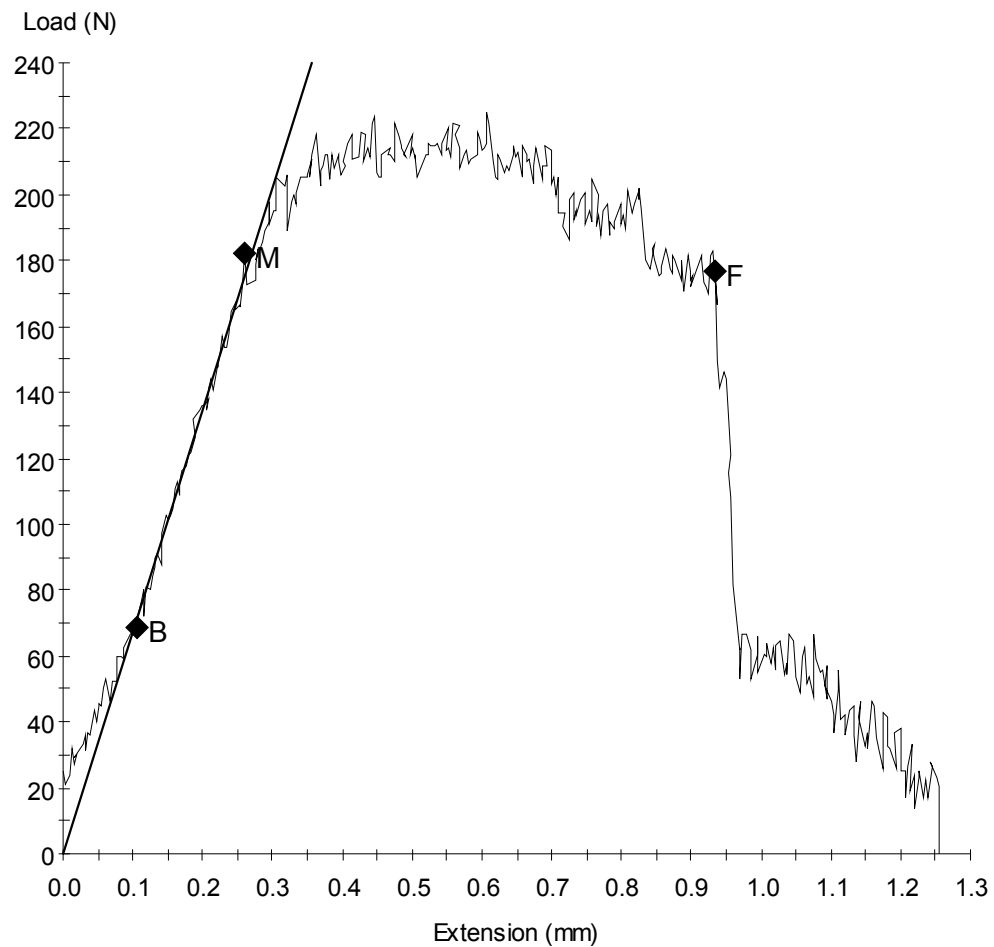
Specimen Results:
Name   Value   Units
Width 30.000 mm
Area   1500   mm^2
Peak Load   225   N
Peak Stress   0.15   MPa
Elongation at Peak   0.608   mm
Break Load   177   N
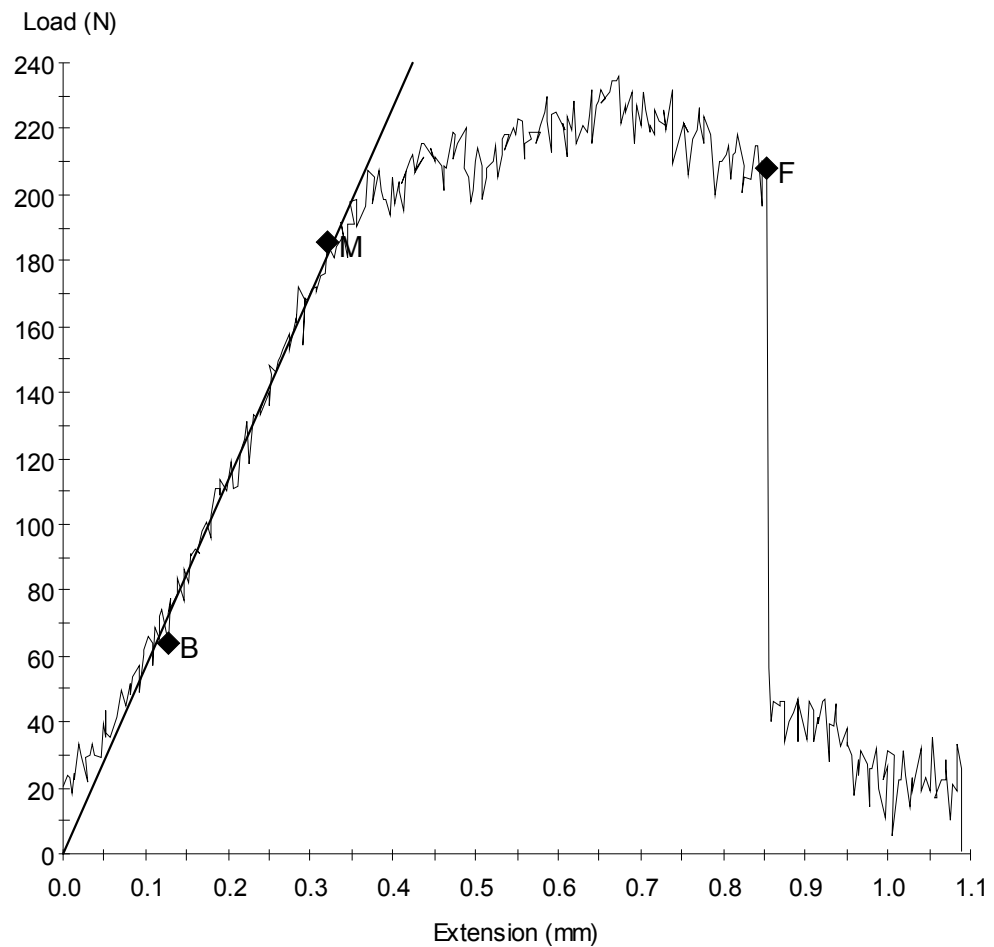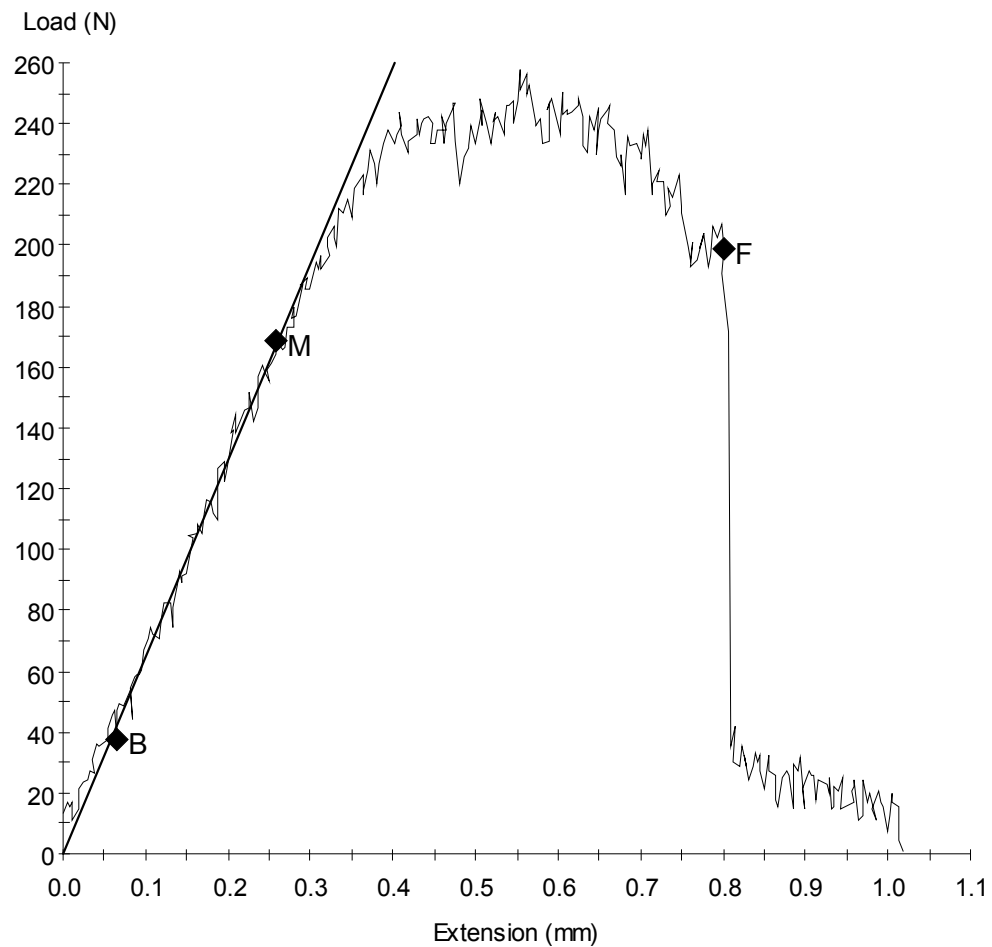Break Stress   0.12   MPa
Elongation At Break 0.936   mm
Stress At Offset Yield 0.140   MPa
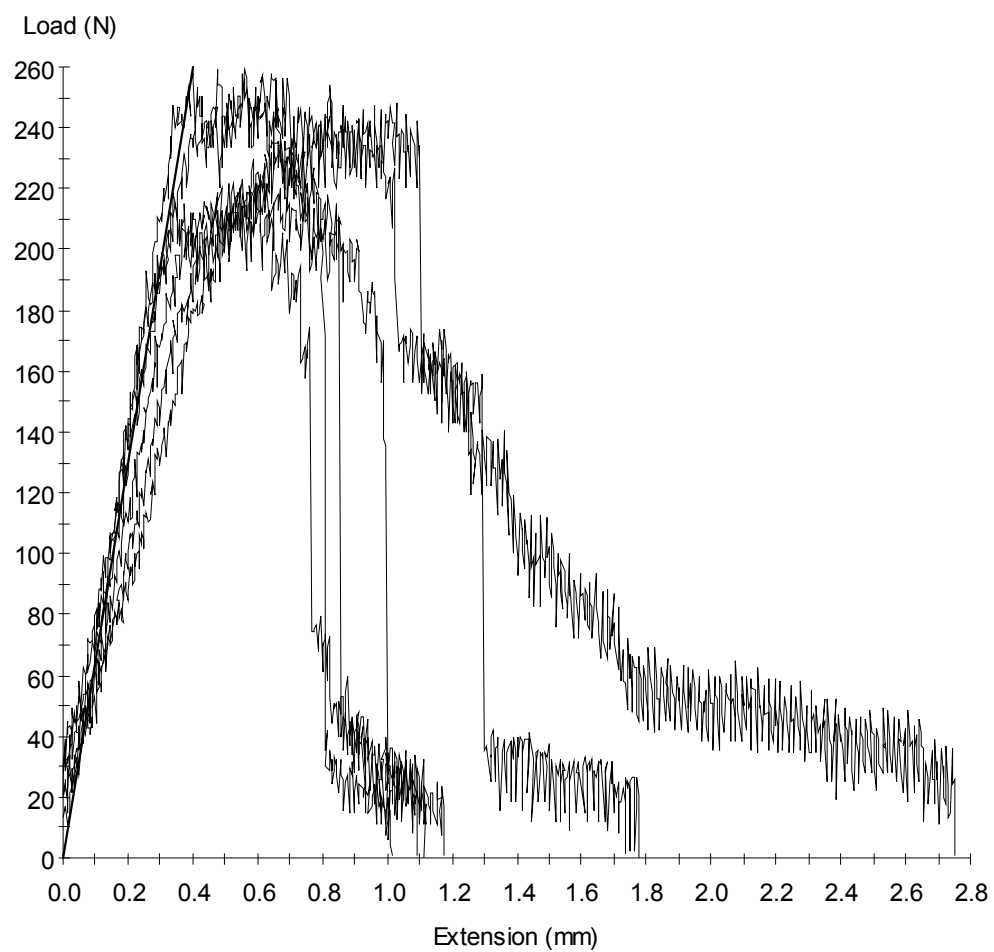Load At Offset Yield 210.774   N

Sample ID: robert35-2.mss
Specimen Number: 2
Tagged: False

Specimen Results:
Name   Value   Units
Width 30.000 mm
Area   1500   mm^2
Peak Load   223   N
Peak Stress   0.15   MPa
Elongation at Peak   0.657   mm
Break Load   187   N
Break Stress   0.12   MPa
Elongation At Break   1.026   mm
Stress At Offset Yield 0.135   MPa
Load At Offset Yield 202.190   N

Sample ID: robert35-3.mss
Specimen Number: 3
Tagged: False

Specimen Results:
Name   Value   Units
Width 30.000 mm
Area   1500   mm^2
Peak Load   218   N
Peak Stress   0.14   MPa
Elongation at Peak   0.464   mm
Break Load   176   N
Break Stress   0.12   MPa
Elongation At Break   0.960   mm
Stress At Offset Yield 0.128   MPa
Load At Offset Yield 192.749   N

Sample ID: robert35-4.mss
Specimen Number: 4
Tagged: False

Specimen Results:
Name Value Units
Width 30.000 mm
Area   1500   mm^2
Peak Load   192   N
Peak Stress   0.13   MPa
Elongation at Peak   0.943   mm
Break Load   146   N
Break Stress   0.10   MPa
Elongation At Break   1.235   mm
Stress At Offset Yield 0.108   MPa
Load At Offset Yield 162.234   N

Sample ID: robert35-5.mss
Specimen Number: 5
Tagged: False

Specimen Results:
Name   Value   Units
Width 30.000 mm
Area   1500   mm^2
Peak Load   228   N
Peak Stress   0.15   MPa
Elongation at Peak   1.191   mm
Break Load   228   N
Break Stress   0.15   MPa
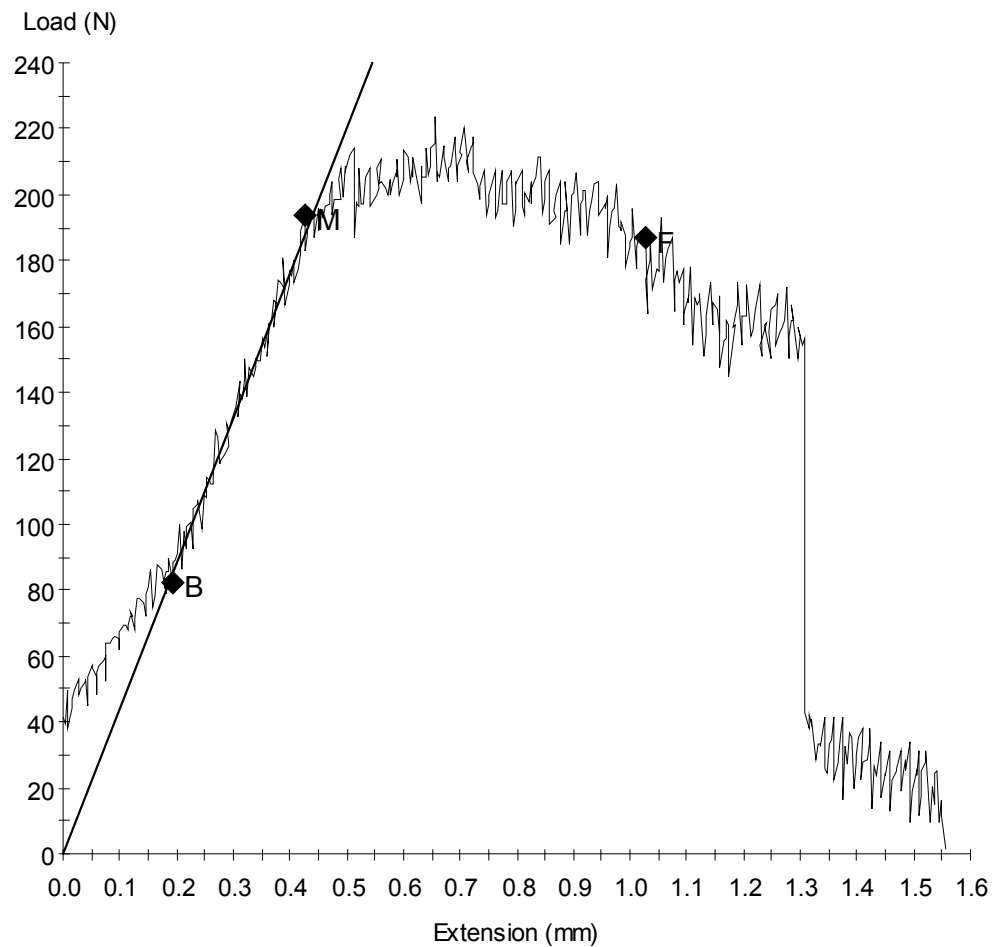Elongation At Break   1.191   mm
Stress At Offset Yield 0.122   MPa
Load At Offset Yield 182.802   N

Sample ID: robert35-6.mss
Specimen Number: 6
Tagged: False

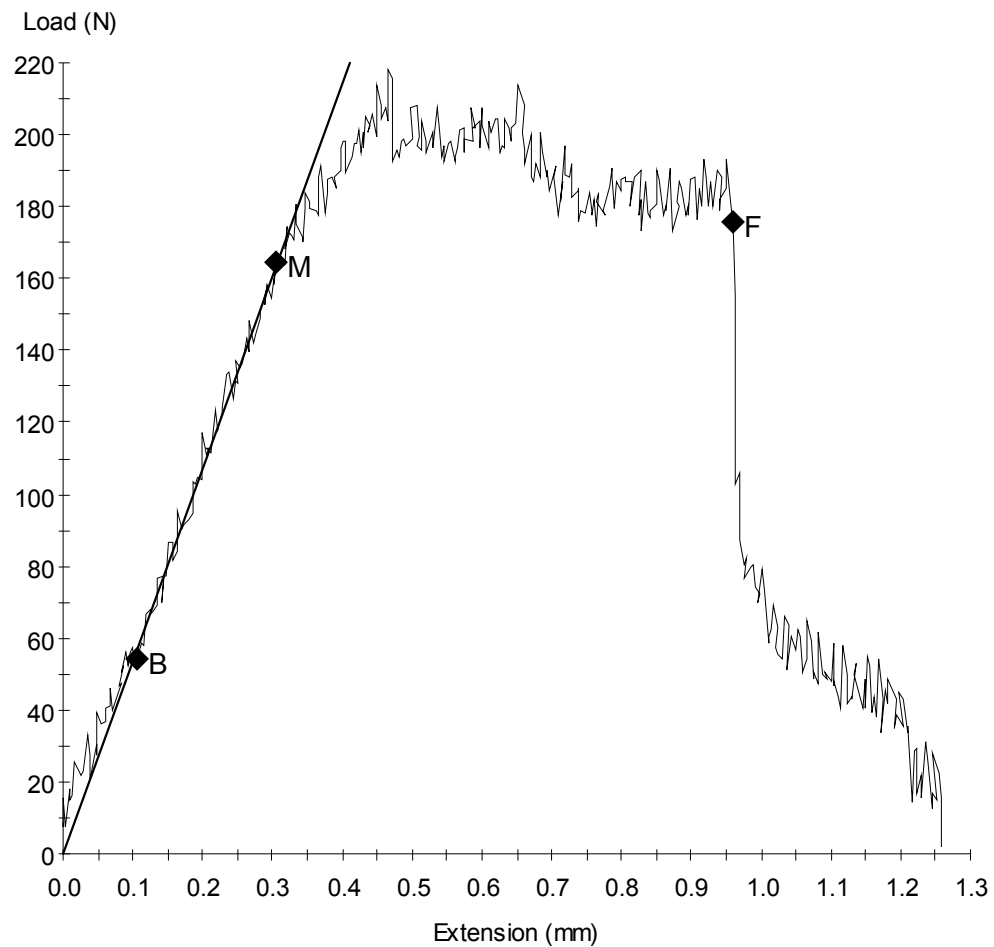**Specimen Results:**
Name   Value   Units
Width 30.000 mm
Area   1500   mm^2
Peak Load   235   N
Peak Stress   0.16   MPa
Elongation at Peak   0.496   mm
Break Load   201   N
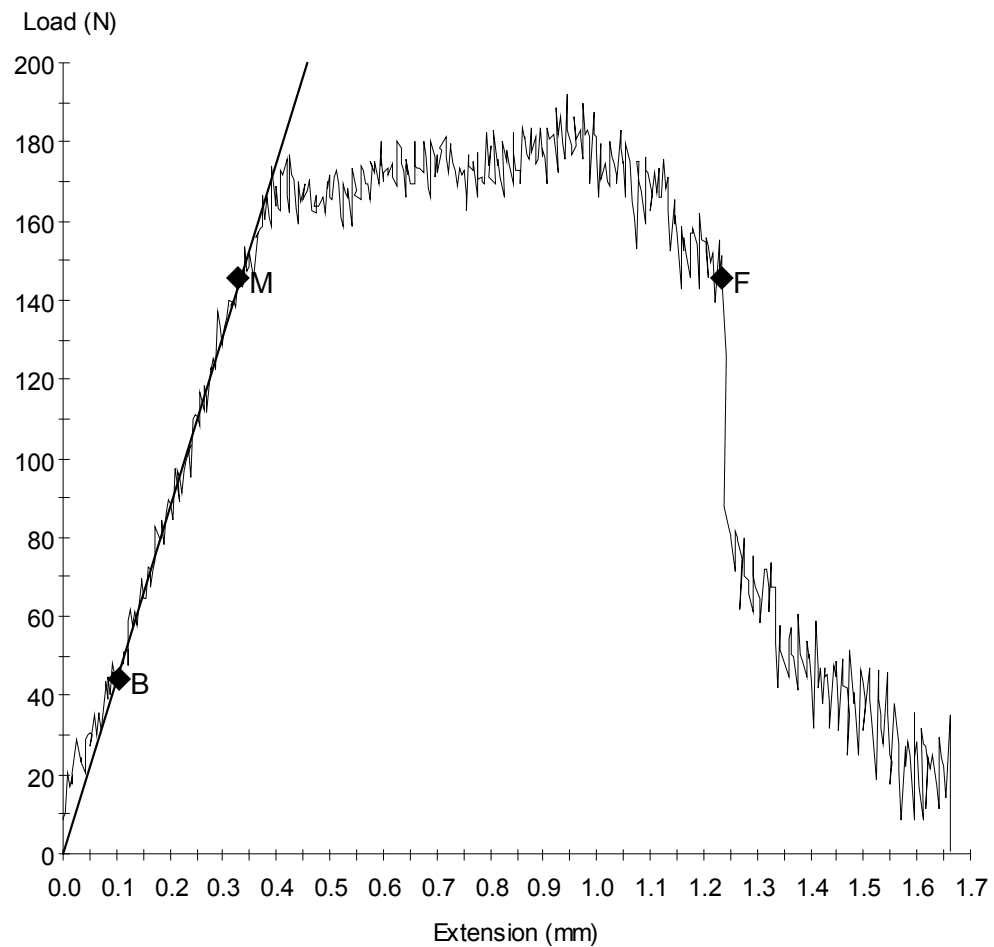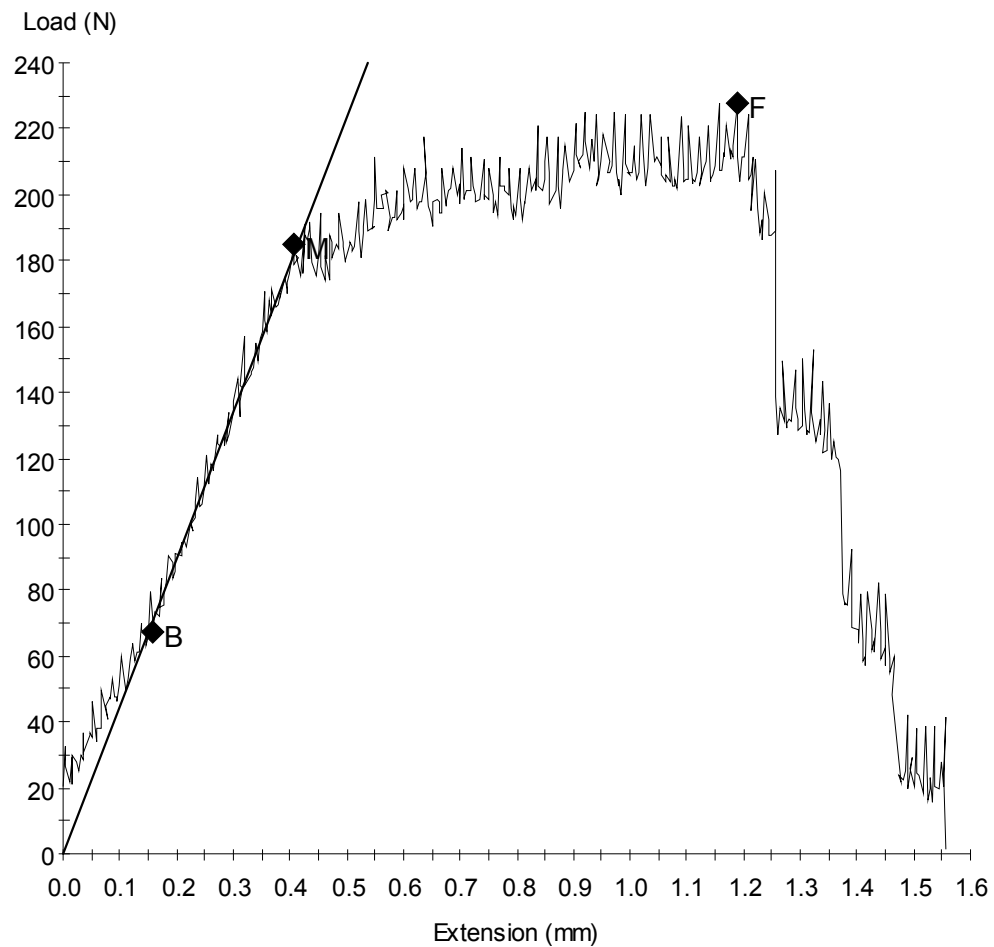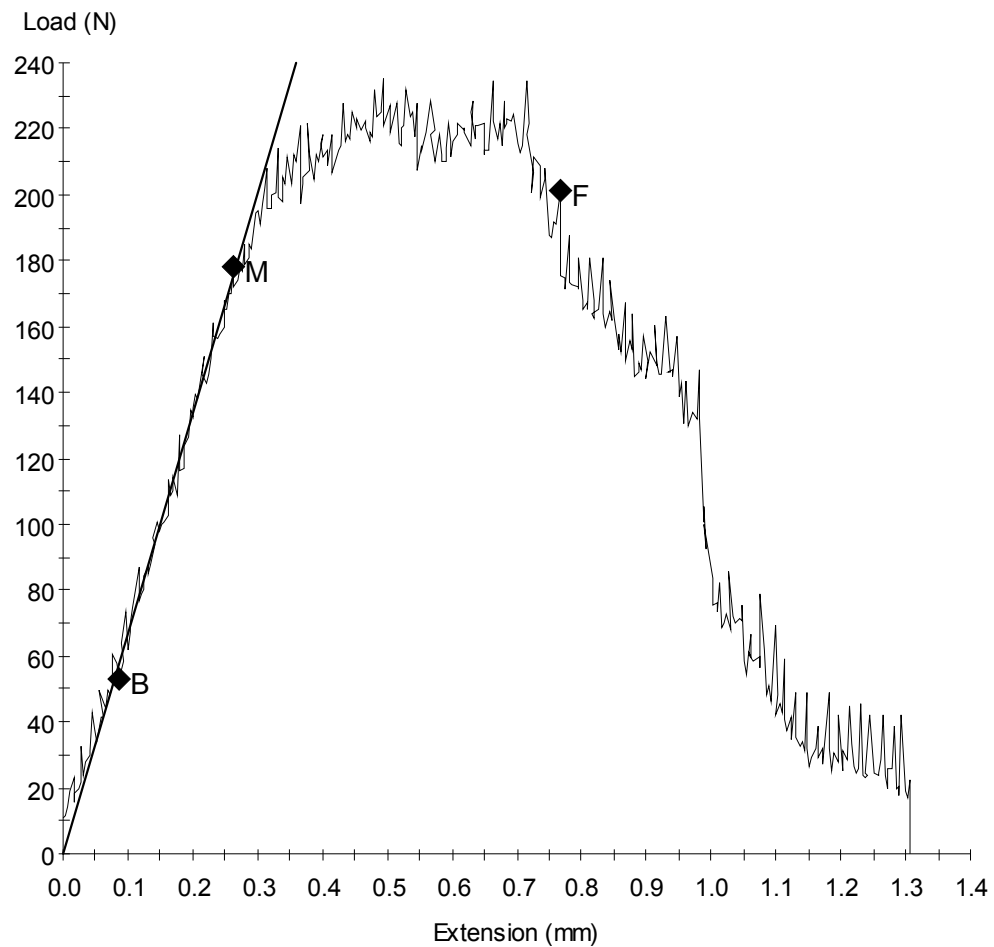Break Stress   0.13   MPa
Elongation At Break   0.768   mm
Stress At Offset Yield 0.138   MPa
Load At Offset Yield 206.911   N

Test Date   : 05-Aug-03
Method   : MMTTensile Test.msm

Specimen Results:

Specimen #	Thickness mm	Width mm	Area mm^2	Peak Load N	Peak Stress MPa	Elongation at Peak mm	Break Load N
1	50.000	30.000	1500	225	0.15	0.608	177
2	50.000	30.000	1500	223	0.15	0.657	187
3	50.000	30.000	1500	218	0.14	0.464	176
4	50.000	30.000	1500	192	0.13	0.943	146
5	50.000	30.000	1500	228	0.15	1.191	228
6	50.000	30.000	1500	235	0.16	0.496	201
Mean	**50.000**	**30.000**	**1500**	**220**	**0.15**	**0.726**	**186**
Std Dev	**0.000**	**0.000**	**0**	**15**	**0.01**	**0.284**	**27**

Specimen #	Break Stress MPa	Elongation At Break mm	Stress At Offset Yield MPa	Load At Offset Yield N			
1	0.12	0.936	0.140	210.774			
2	0.12	1.026	0.135	202.190			
3	0.12	0.960	0.128	192.749			
4	0.10	1.235	0.108	162.234			
5	0.15	1.191	0.122	182.802			
6	0.13	0.768	0.138	206.911			
Mean	**0.12**	**1.019**	**0.129**	**192.943**			
Std Dev	**0.02**	**0.173**	**0.012**	**18.135**			
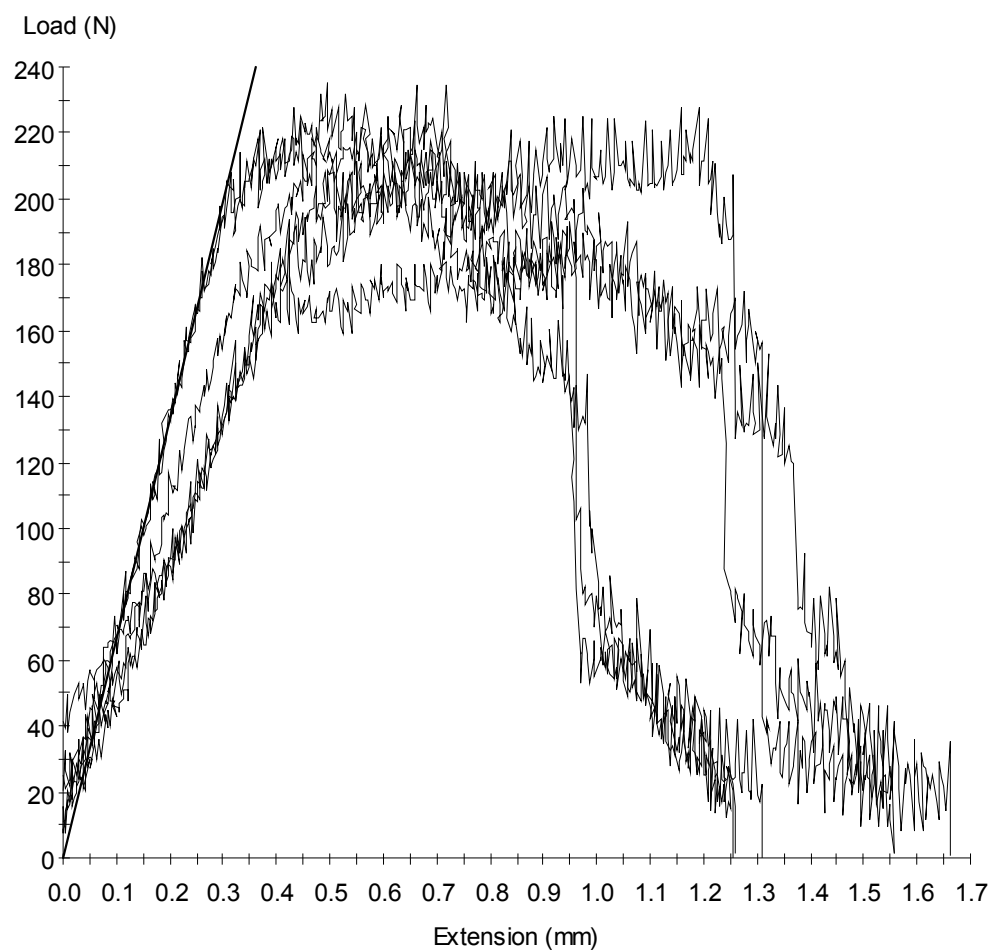
Appendix F

Specimen Measurements

After the short bar specimens had been tested certain geometrical measurements had to be made and these are tabulated on the following page for each specimen.

Table F.1: Measured values from specimens (after oven curing)

Percentage by weight of filler	Specimen Number	W	H	a_0	a_1
15	1	72.9	43.7	23.5	70.9
	2	73.4	43.9	23.61	70.9
	3	72.9	43.5	23.16	68.9
	4	73.36	43.7	23.5	70.9
	5	72.54	43.9	22.98	70.17
	6	72.76	43.71	23.77	68.5
20	1	73.2	43.8	22.7	70.9
	2	72.9	43.81	23.45	70.9
	3	72.8	43.6	23.39	70.9
	4	72.84	43.8	23.3	69.06
	5	73.32	43.7	23.32	70.9
	6	73.2	43.9	22.9	70.9
25	1	72.72	43.9	23.55	69.58
	2	72.6	43.75	23.1	70.9
	3	73.1	43.85	23.38	70.9
	4	73.2	43.85	22.9	69.55
	5	73	43.91	23.2	69.9
	6	72.9	43.98	23.5	70.45
30	1	74	43.76	23.18	70.97
	2	73.3	43.85	22.85	70.3
	3	73.4	43.8	22.71	70.97
	4	73.25	44.05	23.45	68.6
	5	73.9	43.8	22.85	69.74
	6	72.67	43.95	22.3	69.5
35	1	73.1	43.99	22.9	67
	2	73.4	43.6	23.61	66.8
	3	73.25	43.84	23.14	68
	4	73.43	43.75	23.58	67.8
	5	73.2	43.6	23.31	71
	6	73.1	43.62	22.72	69.1

Appendix G

Fracture Toughness Results

Following the procedure in chapter 8 the fracture toughness for each specimen tested was calculated. The results are tabulated on the following page and the mean and standard deviations are also calculated and included.

Table G.1: Fracture Toughness Calculations

Percentage by weight of filler	Specimen Number	Peak Load $F_{\max}$ (N)	Y_m^*	W (mm)	$K_{ICSB}^{\#}$ $\left(MPa\sqrt{m}\right)$	Average (Std. Dev.)
15	1	228	16.295	72.9	8.703()	10.495 (2.297)
	2	283	16.221	73.4	10.716	
	3	298	15.908	72.9	11.104	
	4	332	16.163	73.36	12.530	
	5	345	15.996	72.54	12.959	
	6	182	16.298	72.76	6.955	
20	1	356	15.700	73.2	13.066	12.502 (0.440)
	2	315	16.262	72.9	11.999	
	3	314	16.253	72.8	11.963	
	4	341	16.024	72.84	12.805	
	5	336	16.060	73.32	12.604	
	6	340	15.824	73.2	12.577	
25	1	248	16.264	72.72	9.460	9.619 (0.711)
	2	248	16.120	72.6	9.384	
	3	274	16.159	73.1	10.357	
	4	268	15.716	73.2	9.846	
	5	274	15.986	73	10.253	
	6	221	16.255	72.9	8.415	
30	1	250	15.794	74	9.180	8.816 (0.595)
	2	221	15.719	73.3	8.115	
	3	259	15.660	73.4	9.468	
	4	221	15.962	73.25	8.244	
	5	236	15.521	73.9	8.522	
	6	258	15.478	72.67	9.369	
35	1	225	15.530	73.1	8.174	8.122 (0.533)
	2	223	15.863	73.4	8.258	
	3	218	15.722	73.25	8.009	
	4	192	15.925	73.43	7.136	
	5	228	16.096	73.2	8.579	
	6	235	15.598	73.1	8.574	

$^{\#}$ K_{ICSB} is calculated using equation (5.1), where B is equal to 50mm by design following the procedure set out in Section 8.1 Results and Discussion